LOCAL BOILING PRESSURE DROP FOR FORCED

CIRCULATION OF WATER

By

GERALD EUGENE TANGER

Bachelor of Science
South Dakota School of Mines and Technology
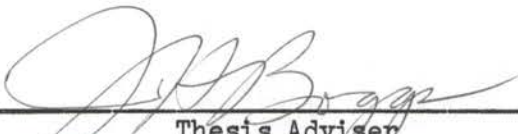Rapid City, South Dakota
1950

Master of Science
South Dakota School of Mines and Technology
Rapid City, South Dakota
1951

Submitted to the Faculty of the Graduate School of
the Oklahoma State University
in partial fulfillment of the requirements
for the degree of
DOCTOR OF PHILOSOPHY
May, 1959

LOCAL BOILING PRESSURE DROP FOR FORCED

CIRCULATION OF WATER

Thesis Approved:

_____
Thesis Adviser

_____
R. N. Maddox

_____

_____
O. H. Hamilton

_____
Dean of the Graduate School

ii

ACKNOWLEDGMENT

into the community — a spirit which aided to encourage completion of the task.

Finally, the writer expresses his deep conviction that this project would certainly have failed without the patience, understanding, and fortitude of his wife, Shirley. This thesis is dedicated to her.

TABLE OF CONTENTS

LIST OF TABLES

LIST OF FIGURES

LIST OF FIGURES (Continued)

LIST OF PLATES

CHAPTER I

INTRODUCTION

The increasing interest in the study of liquid flow with high heat
flux to the liquid has been stimulated by the importance of such flow
in nuclear reactors and high-pressure boilers. Water is of particular
importance for these applications because it has desirable thermodynamic
properties. For forced circulation of water through any heat exchange
apparatus, both heat-transfer and pressure-drop determinations are of
importance. Heat transfer to water flowing through a heated tube, both
for nonboiling and boiling of the water, has been studied extensively.
(1), (2), (3), (4), (5). Pressure drop for such systems has received
less attention than heat transfer, but a knowledge of pressure drop is
important because it is essential to a complete understanding of the
fluid flow system.

Pressure drop for liquid flowing in a tube without heat transfer
can be predicted by the Fanning Friction Factor Equation. When heat is
being added to the fluid the determination of pressure drop is complicated
since the properties of the fluid change with temperature. Some results
and correlations of pressure drop with heat transfer to water without
boiling have been presented by Kreith and Summerfield (4) and Rohsenow
and Clark (5). Because increased heat transfer rates occur during
boiling, boiling has been used extensively when a high heat flux is
desired.

1

The determination of pressure drop during boiling is further compli-
cated by the effect of vapor formation on the pressure drop. Net boiling
or two-phase pressure drop for water has been studied by Weiss (6) and
Leppert (7). Local or surface boiling as a form of nucleate boiling is
of particular importance at this time since little is known about its
characteristics. Only one correlation equation for local boiling pressure
drop data of water has been reported. (8). The present study was concerned
with the determination of pressure drop during local boiling and during
heat transfer with no boiling.

Local boiling occurs when a subcooled liquid is brought into contact
with a surface whose temperature is above the saturation temperature of the
liquid. Boiling occurs at the solid-liquid interface and the vapor formed
is absorbed in the subcooled liquid. The two purposes of this investigation
were to make experimental measurements of the pressure drop for forced
circulation of distilled water with nonboiling and with local boiling in
a horizontal heated tube and to correlate the experimental data with the
variables of heat flux, subcooling, mass velocity and absolute pressure.
These correlations were then compared with existing correlations which
have been proposed by other investigators.

The test section was a type AISI 304 welded stainless steel tube,
0.399 inch inside diameter by 0.502 inch outside diameter with a heated
length of 4.667 feet. The range of variables covered in the investi-
gation was:

System Pressure:	50 to 250 psia
Heat Flux:	100,000 to 300,000 Btu/ft^{2}hr
Mass Velocity:	194 to 347 lb/ft^{2}sec

CHAPTER II

LITERATURE SURVEY

Few data for local boiling pressure drop have been reported in the literature. Since heat transfer and pressure drop must be considered together for boiling, other studies relating to the present problem will be discussed in this chapter. Heat transfer and pressure drop studies in the net boiling region also will be considered.

Reynolds (8) presents the only data on local boiling pressure drop for which a correlation equation has been determined. His experiments covered the following range of variables for flow of water in a horizontal heated tube:

System Pressure: 45 to 99.5 psia

Mass Velocity: 343 to 652 lb/ft^2 sec

Heat Flux: 130,000 to 300,000 Btu/ft^2 hr

Reynolds' equation is

$$\Delta P_{L.B.} = \left(\frac{dP}{dL}\right)_o \frac{G'\, D C_p (\Delta t_{sub})_o}{4a\, q''}\ \sinh\left(\frac{4Z\, q''\, L}{G'\, D\, C_p (\Delta t_{sub})_o}\right), \quad (II\text{-}I)$$

where

$\Delta P_{L.B.}$ = local boiling pressure drop, in. of H_2O;

$(dP/dL)_o$ = isothermal liquid pressure gradient at average bulk

            temperature, in. of H_2O/ft;

G' = mass velocity of fluid through tube, lb/ft^2 sec;

3

D = inside diameter of the tube, ft;

C_p = specific heat of water, Btu/lb °F;

$(\Delta t_{sub})_o$ = subcooling at point where local boiling starts,

$(t_{sat} - t_b)$, °F;

a = parameter related to heat flux (q'') by equation,

$(a = 4.6 \times 10^{-6} q'' + 1.2)$;

q'' = rate of heat flux, Btu/ft^2 hr;

Z = reciprocal of the boiling length, ft^{-1}; and

L = distance from the point where local boiling starts to

any point in question (along the length of local boiling),

up to the point where net boiling starts $\left[(\Delta t_{sub}) = 0 \right]$, ft.

Reynolds' data showed a deviation of ± 20 per cent from his correlation

equation.

Jens and Lottes (1) present a discussion of heat transfer and pressure drop data for water gathered by research teams at the University of California at Los Angeles, Purdue University, and Massachusetts Institute of Technology, but no correlation for local boiling pressure drop was given. The UCLA data showed a deviation of ± 50 per cent from Reynolds' correlation equation. For heat fluxes above 500,000 Btu/ft^{2}hr, the UCLA data did not agree with the correlation.

The method for correlating pressure drop which was reported in the literature, was to find the ratio of the pressure gradient for the data with respect to a reference pressure gradient. Martinelli and Nelson (9) used either the pressure gradient for liquid or the pressure gradient for vapor flow as a reference gradient. Leppert (7) and Reynolds (8) used the isothermal pressure gradient of the liquid at saturation temperature which occurred at the start of boiling. One of the reasons for using this

particular pressure gradient was because it could be calculated easily. It will be shown by the writer why the nonboiling constant heat flux pressure gradient was used to correlate the present data. An excellent discussion on correlating two-phase pressure drop is given by Isbin, Moen, Wickey, Mosher, and Larson (10) and Isbin, Moen, and Mosher (11).

The analysis of the data is based upon a determination of the local boiling length which involves specifying where local boiling begins. Two methods of calculation have been presented for determining the inception of local boiling. Jens and Lottes (1) from their analysis of UCLA, Purdue, and MIT data conclude that the difference between wall temperature and saturation temperature may be computed from

$$\Delta t_{sat} = \frac{60 \left(\dfrac{q''}{10^6} \right)^{\frac{1}{4}}}{e^{p/900}} , \qquad (II-2)$$

where

Δt_{sat} = wall superheat, $^{\circ}F$;

q'' = heat flux, $Btu/ft^2 hr$; and

p = system pressure, psia.

Local boiling starts at the position along the tube where the difference in wall and saturation temperature is equal to Δt_{sat}.

The start of local boiling can also be predicted from a plot of outside wall temperature to distance along the heated length of the test section. The test section temperature remains constant at all stations downstream from the point of local boiling. Once the start of local boiling has been determined, the local boiling length may be found graphically as will be shown in Chapter IV.

A method of calculation for determining the extent of local boiling was presented by Weiss (6). In this method use was made of the equation for Δt_{sat}. (1). The equations Weiss used are as follows:

$$q'' = h\left[(t_{sat} + \Delta t_{sat}) - t_b\right], \qquad (II-3)$$

where

$\qquad q'' = $ heat flux, Btu/ft^2hr;

$\qquad h = $ film coefficient, Btu/ft^2hr^oF;

$\qquad t_{sat} = $ saturation temperature at the given pressure, ^oF;

$\qquad \Delta t_{sat} = $ temperature of the wall above saturation temperature, ^oF; and

$\qquad t_b = $ bulk temperature, ^oF.

$$q = W\, C_p\, \Delta t_b\, 3600, \qquad (II-4)$$

where

$\qquad q = $ heat, Btu/hr;

$\qquad W = $ flow rate, lb/min;

$\qquad C_p = $ specific heat at constant pressure, Btu/lb^oF; and

$\qquad \Delta t_b = $ bulk temperature increase, ^oF.

$$q''A_s = (\rho\, A\, V)C_p\, (t_b - t_i)\, 3600, \qquad (II-5)$$

where

$\qquad A_s = $ surface area $= \pi\, y\, D$, ft^2;

$\qquad \rho = $ fluid density, lb/ft^3;

$\qquad A = $ tube cross sectional area, ft^2;

$\qquad V = $ fluid velocity, ft/sec;

$\qquad t_i = $ inlet temperature, ^oF; and

$\qquad y = $ variable length of the tube not in local boiling, ft.

Equation (II-5) may be substituted into Equation (II-3) to obtain

$$q'' = h \left[t_{sat} + \Delta t_{sat} - \frac{4y \ q''}{D \ G \ C_p \ 3600} - t_i \right], \qquad \text{(II-6)}$$

where

G = mass velocity = ρV, $lb/ft^2 sec$.

Equation (II-6) may be solved for y to give

$$y = \frac{D \rho C_p \times 3600}{4q''} \left[t_{sat} + \Delta t_{sat} - \left(\frac{q''}{h} + t_i \right) \right], \qquad \text{(II-7)}$$

where the heat transfer film coefficient (h) is a variable which depends upon the local temperature. Equation (II-7) must be solved by trial and error since both y and h are variables.

Another expression for Δt_{sat} has been given by McAdams, Addoms, and Kennel (2) as

$$\Delta t_{sat} = C' \ (q'')^{0.26} , \qquad \text{(II-8)}$$

where

$C' = 0.189$ for 0.30 cubic centimeters of air per liter,

or

$C' = 0.074$ for 0.06 cubic centimeters of air per liter.

Combining this equation with the forced convection equation, McAdams obtained

$$\Delta t_{sat,tr} = \left[\frac{0.026 \ \Delta t_{tr} \ K}{C' \ D} \left(\frac{D \ G}{\mu} \right)^{0.8} \right.$$

$$\left. \left(\frac{C_p \mu}{K} \right)^{.33} \left(\frac{\mu}{\mu_w} \right)^{0.14} \right]^{0.259} , \qquad \text{(II-9)}$$

where

Δt_{sat},tr = difference between wall temperature and saturation

temperature at start of local boiling, °F;

Δt_{tr} = difference in bulk temperature from inlet to point

of local boiling, °F;

μ = dynamic viscosity, lb/ft hr.

Pressure plateaus noted by Reynolds (8), Figure 1, were also observed

in the present study. Closely related to pressure drop is the mechanism

of bubble formation and absorption in the main stream of the fluid. Attempts

have been made to study bubble formation and motion by means of high–speed

photography in order to clarify the local boiling phenomenon. An excellent

photographic study of local boiling has been reported by Gunther (12).

An important variable which affects bubble motion is the subcooling

of the liquid. For subcooling greater than 100°F, Gunther concluded that

surface bubbles do not detach from the heated surface but grow and collapse

as they are swept along the wall of the heated surface. An analytical

method for predicting local boiling pressure drop was not available in the

literature.

Rohsenow and Clark (13) drew conclusions about bubble motion from an

analysis of heat transfer data. They found that heat transfer by bubble

motion into the fluid accounted for a negligible part of the heat transfer

which was observed. Increased heat transfer was explained on the basis of

increased turbulence of the boundary layer caused by agitation of the fluid

as bubbles were formed and then collapsed. Zuber (14) considered further

the disturbance of the boundary layer by moving vapor bubbles. The ideas

which have been advanced here will be used later to discuss qualitatively

some of the observed pressure drop results.
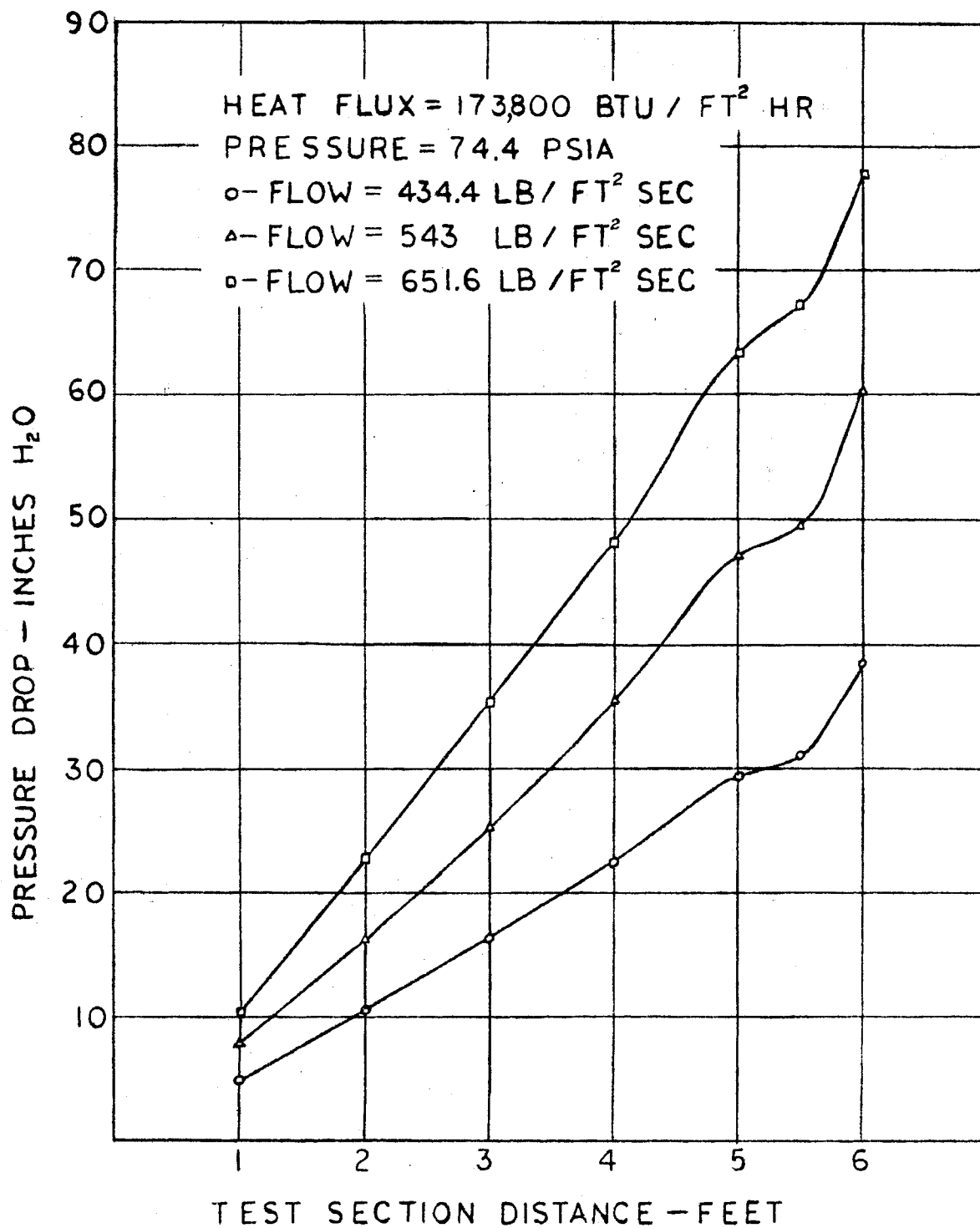
Figure 1. Typical Pressure Profiles, from Reynolds (8)

In the tube upstream of the point at which local boiling started, Buchberg, Romie, Lipkis, and Greenfield (15) found that the frictional pressure drop for a 0.174 inch vertical heated tube could be correlated by:

$$\Delta P_F = \left(0.164 \; \frac{\ell}{D^{1.175}} \; \frac{G^{1.825}}{2g_c} \right) \left(\frac{\mu^{0.175}}{\rho} \right), \qquad (II\text{-}10)$$

where

ℓ = tube length, ft;

D = tube diameter, ft; and

g_c = gravitational constant, ft/sec^2.

Maximum deviation from the correlation equation was $\pm$ 4 per cent. The first term in parenthesis in the equation was found to be constant for a given mass velocity.

Nonboiling pressure drop data for water may be correlated in terms of friction factors and fluid viscosities at bulk and wall temperatures. Kreith and Summerfield (4) give the equation for friction factor ratio as

$$\frac{C_F \; (\text{heat transfer})}{C_F \; (\text{isothermal})} = \left(\frac{\mu_w}{\mu_b} \right)^{0.13}, \qquad (II\text{-}11)$$

where

C_F = friction factor.

Rohsenow and Clark (5) give for the nonboiling region

$$\frac{f \, (\text{isothermal})}{f_f} = \left(\frac{\mu_b}{\mu_w} \right)^{0.14}, \qquad (II\text{-}12)$$

where

f(isothermal) = friction factor with no heat transfer, and

f_f = pressure drop coefficient for friction drop.

and

$$\frac{f(isothermal)}{f_{f,M}} = \left(\frac{\mu_b}{\mu_w}\right)^{0.60} , \qquad (II-13)$$

where

$f_{f,M}$ = pressure drop coefficient for friction drop and momentum change.

The resulting change in pressure for a horizontal tube becomes

$$\Delta P_{f,M} = 4 f_{f,M} \frac{G^2}{2g_c D} \int_0^L \frac{dx}{\rho} . \qquad (II-14)$$

A method based on the Colburn Equation (16) for forced convection heat transfer will be presented in Chapter V of this thesis.

CHAPTER III

EXPERIMENTAL APPARATUS

A heat transfer loop for the forced circulation of water was constructed to study local boiling pressure drop. The apparatus design was similar in principle to one used by Mumm (3), Leppert (7), and Reynolds (8). Several changes in design were made to overcome objections cited by these authors for their apparatus as well as to make construction simpler. Basic changes were made as follows:

1. Pump and drive system; a Moyno pump was used with a variable speed drive.

2. The power available for the preheater was increased by 50 per cent.

3. A compact water-cooled condenser was used.

4. A special test-section was designed for the study.

5. Provision was made to take heat-transfer and pressure-drop data simultaneously.

6. The exhaust manifold was made more compact.

7. A bypass control valve was mounted on the control panel for ease of operation.

Component Parts

The principal component of the experimental apparatus was the test section which is shown in Figure 2. Two views of the test section

Figure 2.   Test Section

(uninsulated and insulated) are seen in Plates I and II. The test section was fabricated of AISI type 304 stainless steel welded tubing with a 0.502 inch outside diameter and a 0.399 inch inside diameter. The tube was especially selected for its straightness and uniformity of inside diameter and wall thickness. Static pressure taps of 0.125 inch outside diameter stainless steel tubing were silver soldered to the test section wall in a careful manner. Holes were then drilled through the tube wall and deburred on the inside wall of the test section. Power lugs were clamped to the tube at 19.2 inches from the inlet flange and 8.8 inches from the exit flange. Six voltage taps were attached to the test section, one at each power lug and four spaced at intervals of 12 inches starting from the outlet power lug. Iron-constantan 30-gage thermocouple wires were spot welded to the test section wall every 3 inches and wrapped with glass tape. See Plate I. Twenty-two thermocouples were attached in this manner. Before usable data were taken a 2 inch layer of fiber glass insulation was applied to the test section between the inlet and outlet flanges. Aluminum foil was wrapped around the insulation in order to reduce radiative heat loss. See Plate II. Five thermocouples were placed in the insulation to permit an estimation of heat loss through the insulation. The bulk temperature of the water at the inlet and exit of the test section was measured by means of Minneapolis-Honeywell "Megopak" type iron-constantan thermocouples.

Electrical energy was supplied to the test section by three Lincoln 400 "Fleetwelder Special" transformers connected in parallel. National Electrical Manufacturers Association code output rating of each transformer was 400 amps at 40 volts. The transformers were positioned remotely from the control panel. The complete installation is shown in Plate III.

PLATE I. UNINSULATED TEST SECTION
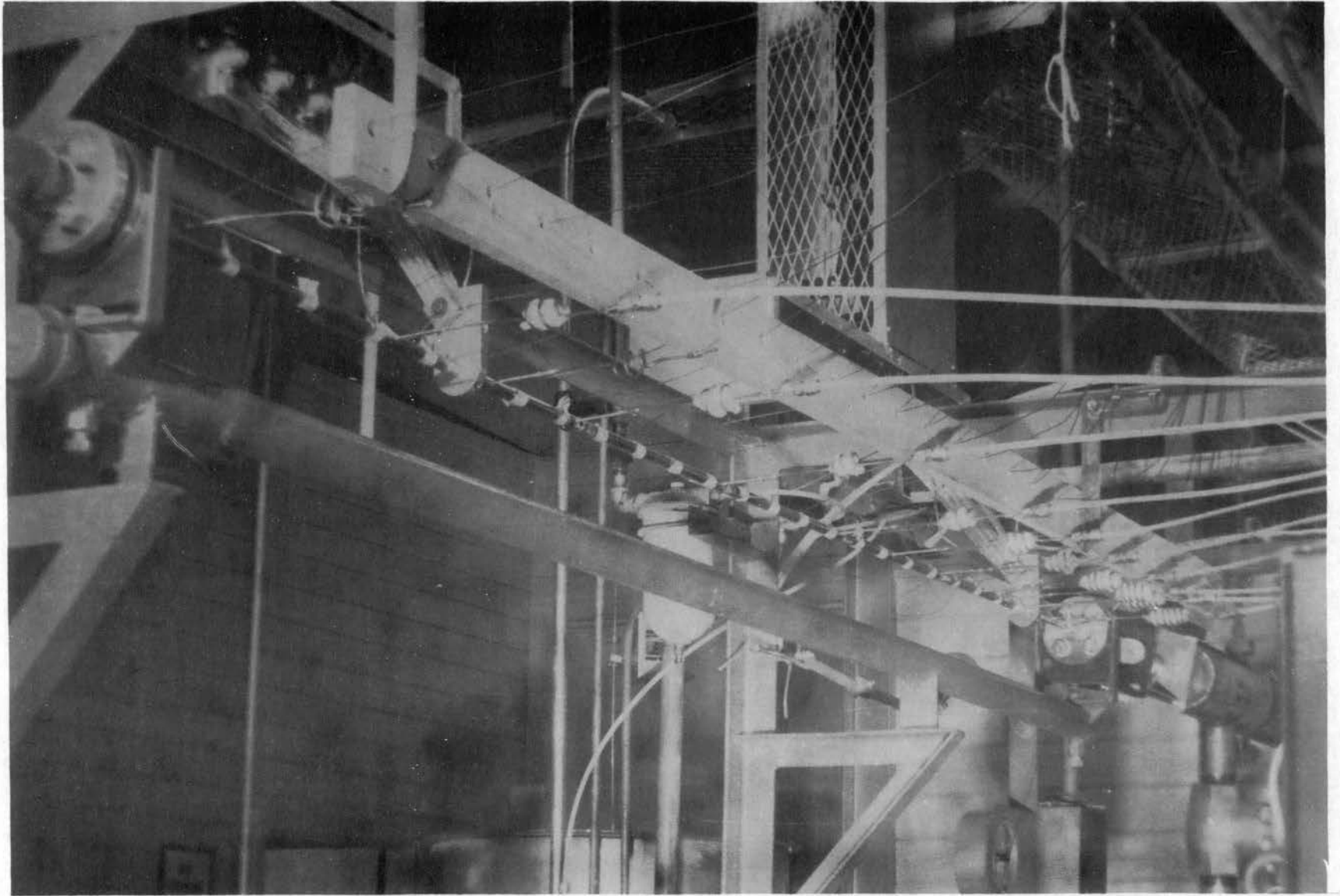
PLATE II.   INSULATED TEST SECTION

PLATE III. INSTALLATION OF THE MAIN TRANSFORMERS
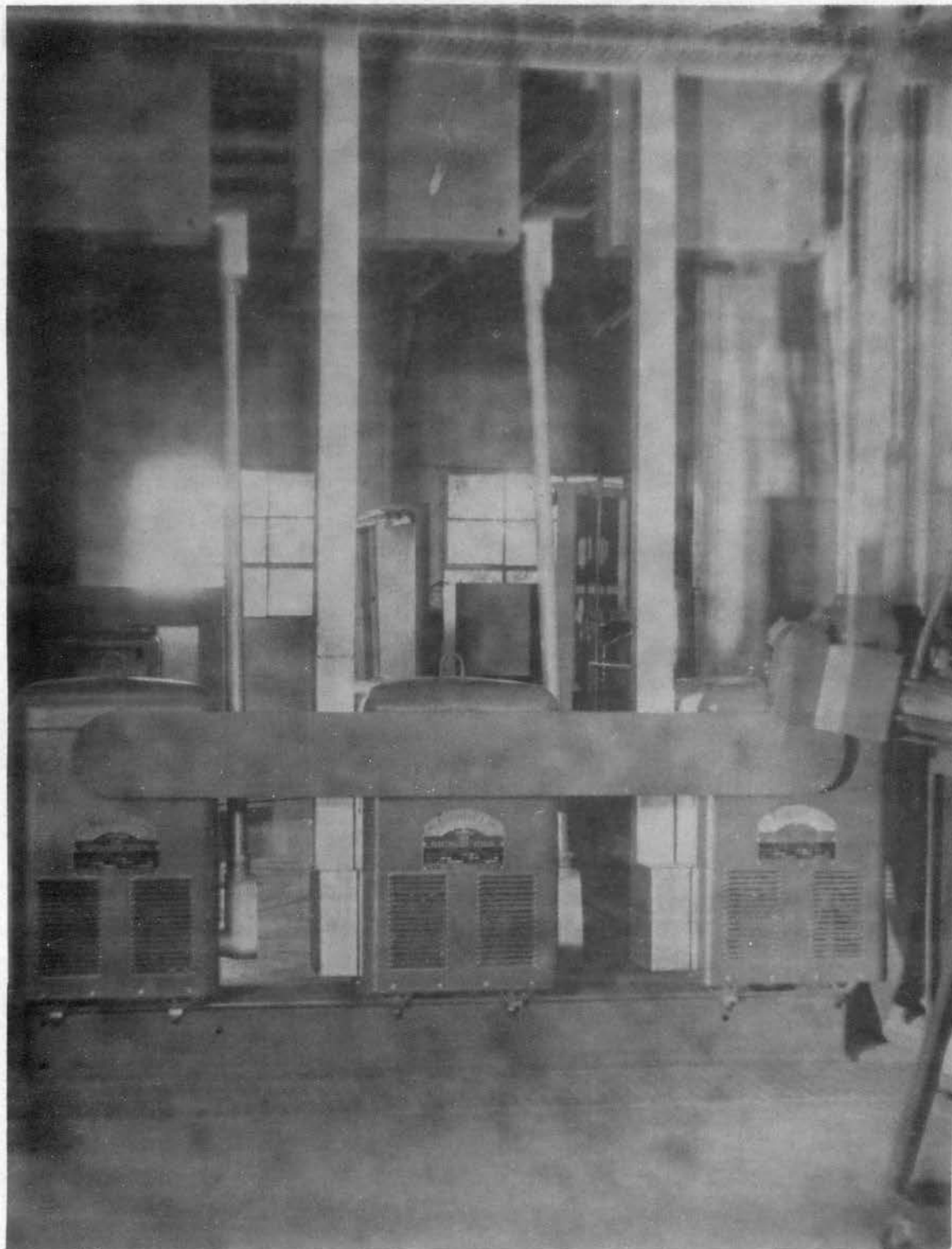
Main components of the loop were supply tank, main pump, pump drive, auxiliary pumps, metering network, flow control system, preheater, exhaust manifold, condenser, holdup tank, and ion exchanger. Important features of several components of the loop will be discussed in the next paragraphs.

Piping and fittings which came in contact with the water were stainless steel type 304 or non-ferrous metal. The two auxiliary pumps had cast iron housings. An examination of the auxiliary pumps after a months contact with water showed only a trace of rust. An ion exchanger was included in the system to remove iron ions which might alter heat transfer characteristics and hydraulic flow resistance. Rohm and Haas "Amberlite" resin was used as recommended by Rohsenow and Clark (5). The complete facility is shown in Figure 3.

The main pump was a stainless steel Robbins and Myers "Moyno" Pump, Frame 6M, type SSQ, which was a six-stage progressing-cavity type pump. Pump capacity was 0.26 gallon per 100 rpm. The pump drive unit was a U. S. Varidrive Syncrogear Motor with a speed range of 366 to 5000 rpm. Pulley diameters were chosen to reduce pump speed to 0.620 times that of the driver speed. The resulting pump speed range is approximately 250 to 3000 rpm or a variable capacity of 0.65 gallon per minute to 7.80 gallons per minute. Flow rates of from 10 to 18 pounds per minute were considered in this investigation.

The two auxiliary pumps, one for the ion exchanger and the other for the fluid transfer from holdup tank to supply tank were identical. They were Yoemans Brothers centrifugal pumps driven by 1/3 horsepower rating, single phase, 115-230 volt, totally enclosed General Electric motors.

WATER
TEMPERATURE
THERMOCOUPLES

SIGHT
GLASS

PRESSURE
RELIEF
VALVE

PRESSURE
RELIEF
VALVE

POWER
SUPPLY

TEST
SECTION

EXHAUST HEADER

WATER
TEMPERATURE
THERMOCOUPLE

FLOW
ORIFICES

FLOW
CONTROL
VALVE

CONDENSER

WATER
SUPPLY
TANK

ION
EXCHANGER

HEAT
EXCHANGER

PREHEATER

TO
MANOMETER

HOLDUP
TANK

HOLDUP
TANK
PUMP

ION
EXCH.
PUMP

DIFFERENTIAL
PRESSURE
TRANSMITTER

CIRCULATING
PUMP

WATER TEMP.
THERMOCOUPLE

COOLING
WATER SUPPLY

DRAIN

Figure 3. Schematic Diagram of Test Facility

19

The metering network consisted of two parallel paths of 1 inch schedule 40 stainless steel pipe with a sharp-edged orifice plate installed in each path. Appropriate valving made it possible to use either orifice plate. The orifice plates were supplied by the Daniel Orifice Fitting Company and were 0.353 inch and 0.453 inch in diameter. Flange pressure taps were connected to a Meriam, Model 30, flow manometer with a 60 inch scale graduated in inches and tenths of inches. Meriam No. 3 red manometer fluid with a specific gravity of 2.95 was used. Only the 0.353 inch orifice plate was used in this investigation. It was calibrated in place by means of a tank and scales. Manometer readings were taken in the interval of 3.9 to 12.8 inches of red fluid which were the limits of flow rate investigated. The orifice calibration results are shown in Appendix F.

The pneumatic flow control system was not used because it was found that adequate flow control was achieved with the Moyno pump and associated drive system. System pressure pulses of ± 0.5 pound were noted only at flow rates less than 1 gallon per minute. One gallon per minute was the minimum flow rate considered. At flow rates of 4 gallons per minute and larger, a slow change of flow rate was noted which caused an additional error in flow of ± 1 per cent above the error introduced by orifice calibration. The change of flow increased for flows greater than 4 gallons per minute. Flow rates above 2.5 gallons per minute were not used.

Preheating of the water was accomplished with a heating system of six Cromalox MT-201, 240 volt, 10,000 watt, two-element heaters. Six of the single heaters were connected through individual switches to the power bus bars and six were connected by individual switches to a

remotely operated 45 KW Powerstat variable transformer supplied by the Superior Electric Company. The preheater construction and heating element location are shown in Figure 4.

Pressure control was obtained by throttling the water from an exhaust manifold. A 3/4 inch stainless steel needle valve provided the main system pressure control. Pressure downstream from the throttle valve was somewhat above atmospheric pressure. Cooling was accomplished by a water-cooled, Ross type BCF-501-2 two-pass heat exchanger. The cooling tubes were fabricated of admiralty metal and the exchanger body was brass. System pressure was measured by a Heise calibrated gage, 0-750 pounds per square inch range, 16 inch diameter dial. Differential pressure along the test section was measured with five Meriam Model 30 flow manometers.

Temperature was measured with the following instruments:

1. Brown 48-point Electronik Precision Indicator, type J, 0-1200°F.

2. Brown Multipoint Electronik strip Chart Recorder, type J, 0-600°F, 10 record.

A calibration curve was prepared for the temperature measuring system and is presented in Appendix G.

Preheater power was indicated by Simpson Panel Meters, 2 per cent accuracy, connected as shown in Figure 5. All instruments and all controls were mounted on the panel board shown in Plate IV and identified in Figure 6. The interlock controls and other safety features of the loop will be discussed in the Operation section of this chapter.

TO
ELECTRICAL
SWITCHBOX

OUTLET

HEATER   LOCATION

POWERSTAT SWITCHING   ORDER: 1W, 2W, 3W, 4W, 5W, 6W.
DIRECT-CONNECTED SWITCHING   ORDER: 1R, 2R, 3R, 4R, 5R, 6R.

BAFFLE   LOCATION

INLET
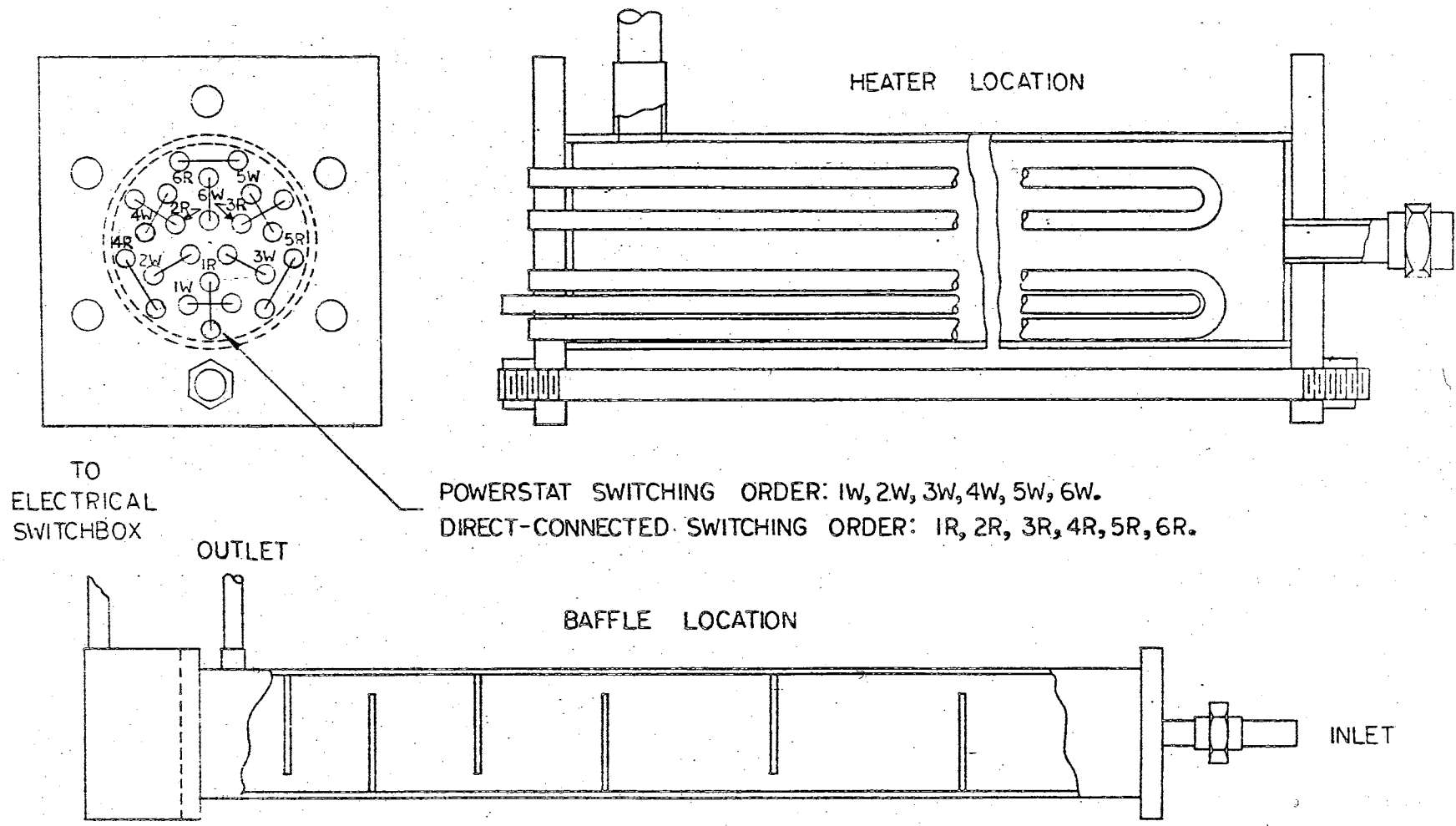
Figure 4.   Preheater Construction

TEST SECTION

VOLT

POWERSTAT

DIRECT CONNECTED

AMPS

VOLTS

AMPS

VOLTS

AMPS

TO INSTRUMENT
TRANSFORMER

TO VOLTMETER
TAPS

TO INSTRUMENT
TRANSFORMER

TO VOLTMETER
TAPS

MAIN CURRENT
TRANSFORMER
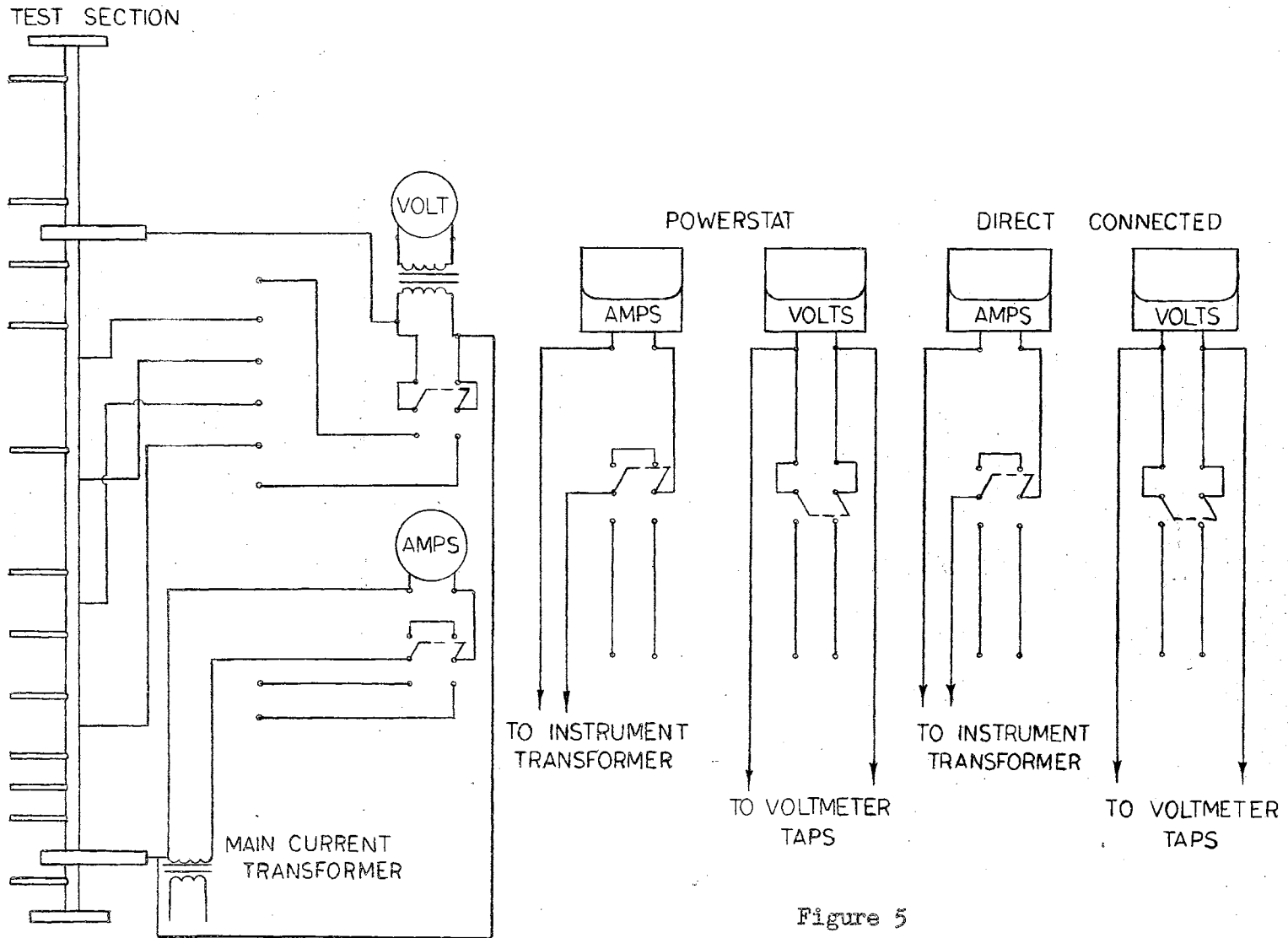
Figure 5

Preheater Electrical Metering Circuits

PLATE IV. CONTROL PANEL BOARD
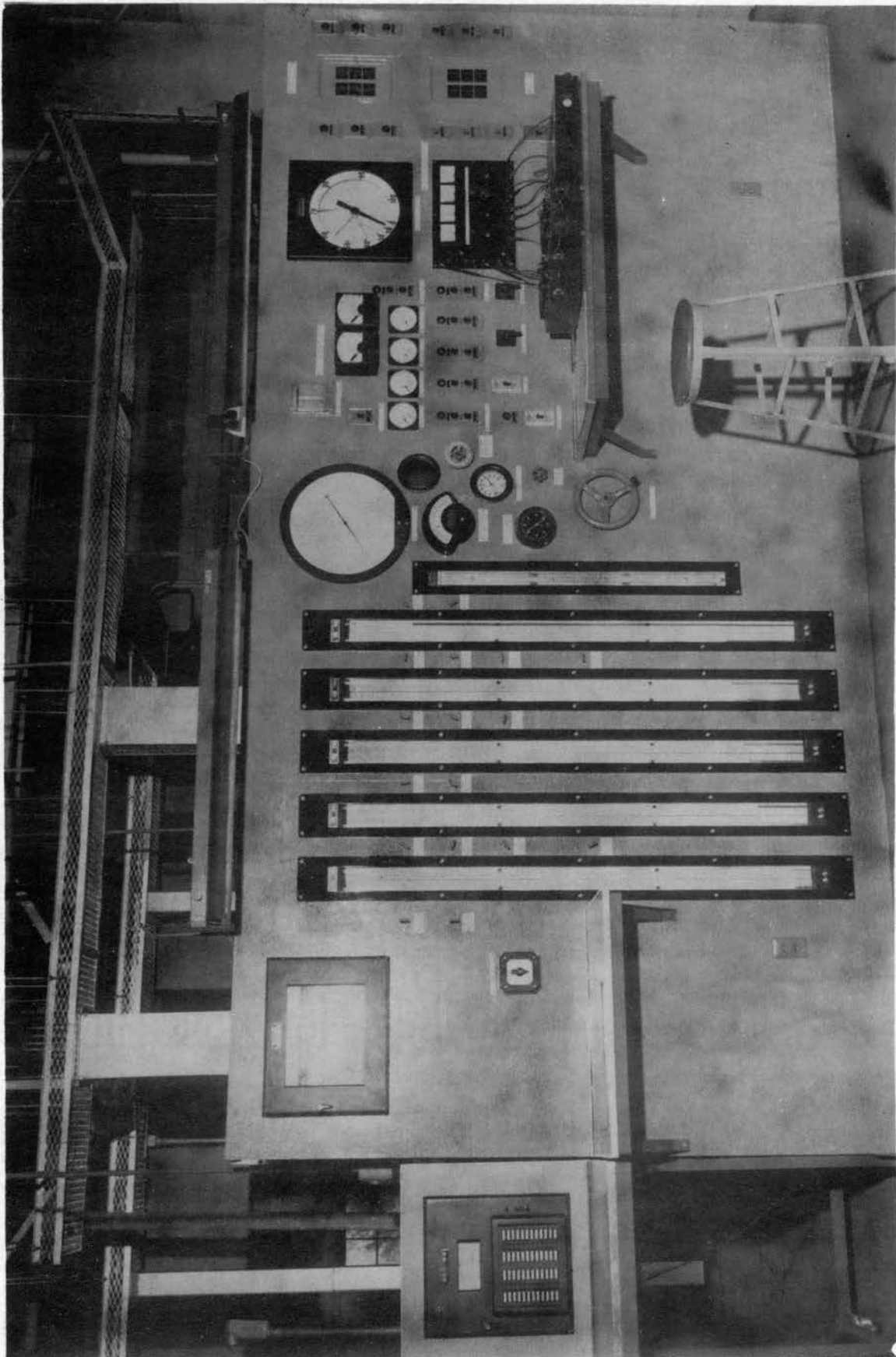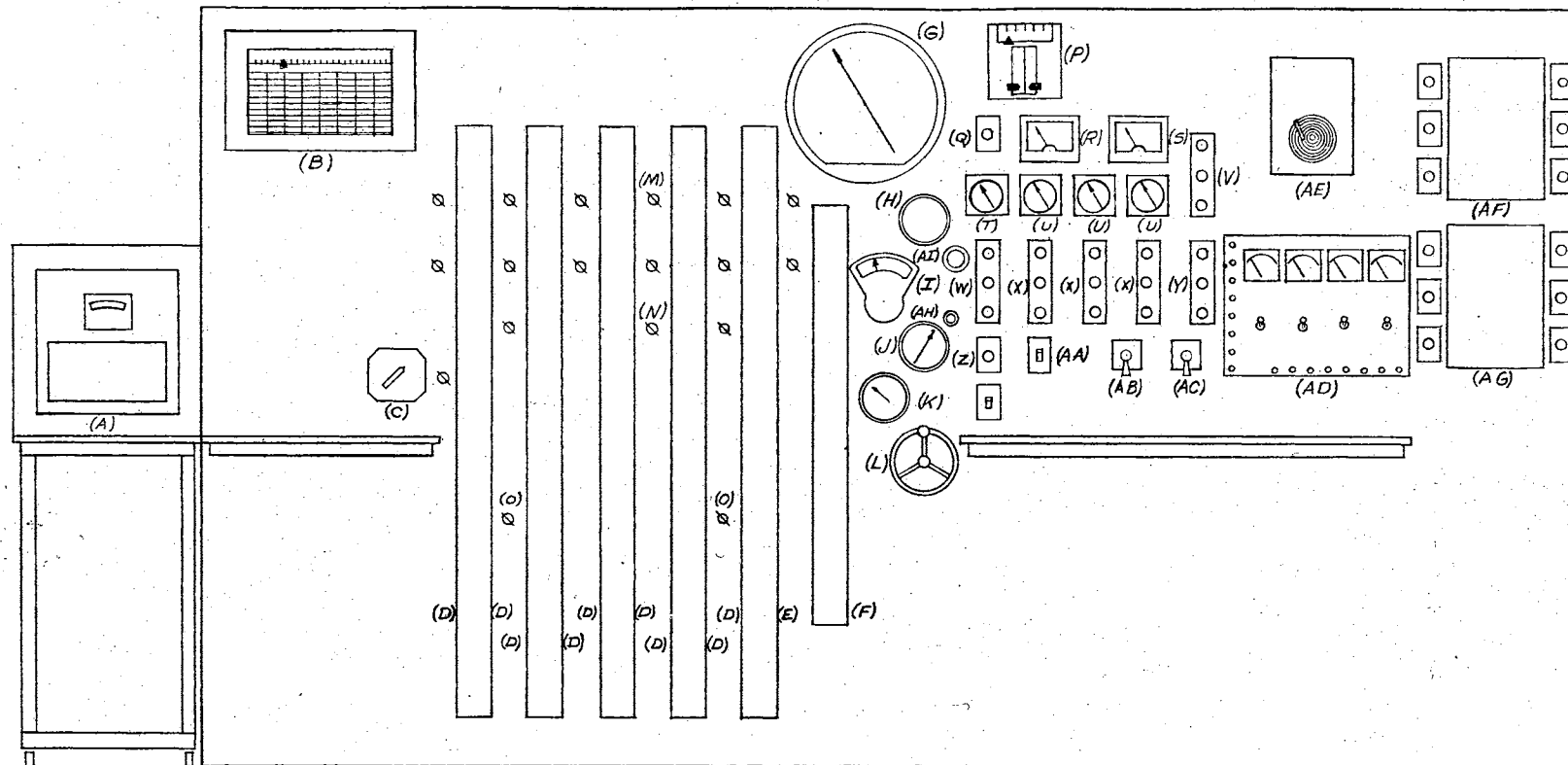
(A) 48 POINT TEMPERATURE INDICATOR
(B) TEMPERATURE RECORDER
(C) THERMOCOUPLE SELECTOR SWITCH
(D) PRESSURE DROP MANOMETERS
(E) FLOW MANOMETER
(F) 36 INCH MANOMETER
(G) PRECISION PRESSURE GAGE
(H) OBSERVATION PORT
(I) VARIDRIVE SPEED INDICATOR
(J) SYSTEM PRESSURE
(K) HOLDUP TANK TEMPERATURE INDICATOR
(L) VARIDRIVE SPEED ADJUSTMENT
(M) MANOMETER VALVES

(N) MANOMETER BYPASS VALVES
(O) MANOMETER REFERENCE VALVES
(P) CONTROL SYSTEM PRESSURE INDICATOR
(Q) PANIC SWITCH
(R) TEST SECTION VOLTMETER
(S) TEST SECTION WATTMETER
(T) TOTAL CURRENT AMMETER
(U) INDIVIDUAL TRANSFORMER AMMETER
(V) DIRECT CONNECTED PREHEATER
(W) MAIN PUMP SWITCH
(X) TRANSFORMER POWER SWITCH
(Y) POWERSTAT SWITCH
(Z) TRANSFER PUMP SWITCH

(AA) ION PUMP SWITCH
(AB) POWER TRANSFORMER DRIVE SWITCH
(AC) POWERSTAT POSITION SWITCH
(AD) PREHEATER INSTRUMENT PANEL
(AE) TEST SECTION CURRENT RECORDER
(AF) PREHEATER JUNCTION BOX
(AG) POWERSTAT JUNCTION BOX
(AH) BYPASS VALVE
(AI) THROTTLE VALVE

Figure 6. Control Panel Board

Instrumentation

Power to the test section was measured with a single-phase General Electric P-3 wattmeter with a range of 0-200/400 watts and an accuracy of 0.2 per cent of full scale. Voltage drop along the test section was measured with a General Electric P-3 voltmeter with a range of 0-15/30 volts and an accuracy of 0.2 per cent of full scale. General Electric JKR-2 current transformers with ratios of 5:500 and 5:1500 were used to supply current to the ammeters. Either transformer could be switched into the circuit depending upon the range of power to be measured. A precise determination of preheater power was not required as preheating was used only to obtain a given inlet bulk temperature.

Pressure measurements were of paramount importance and special care was taken to see that all pressure measurements were reliable. Reference pressures were taken at pressure tap zero and pressure tap four, Figure 7. The precision gage could be connected to pressure tap zero or nine. The difference in pressure as read on the gage could be checked against the manometer readings. Uncertainty in all pressure readings was reduced materially by the excellent main pump characteristics as noted previously.

The drive pump was chosen because of its smooth positive-displacement pumping action. Pump characteristic curves, Figure 8, show that flow rate is almost independent of system pressure. Pumping rate could be accurately controlled by varying pump speed. Low flow rate could be obtained at higher pump speed than normal by use of a bypass needle valve. Part of the pump discharge could be shunted directly to the holdup tank.
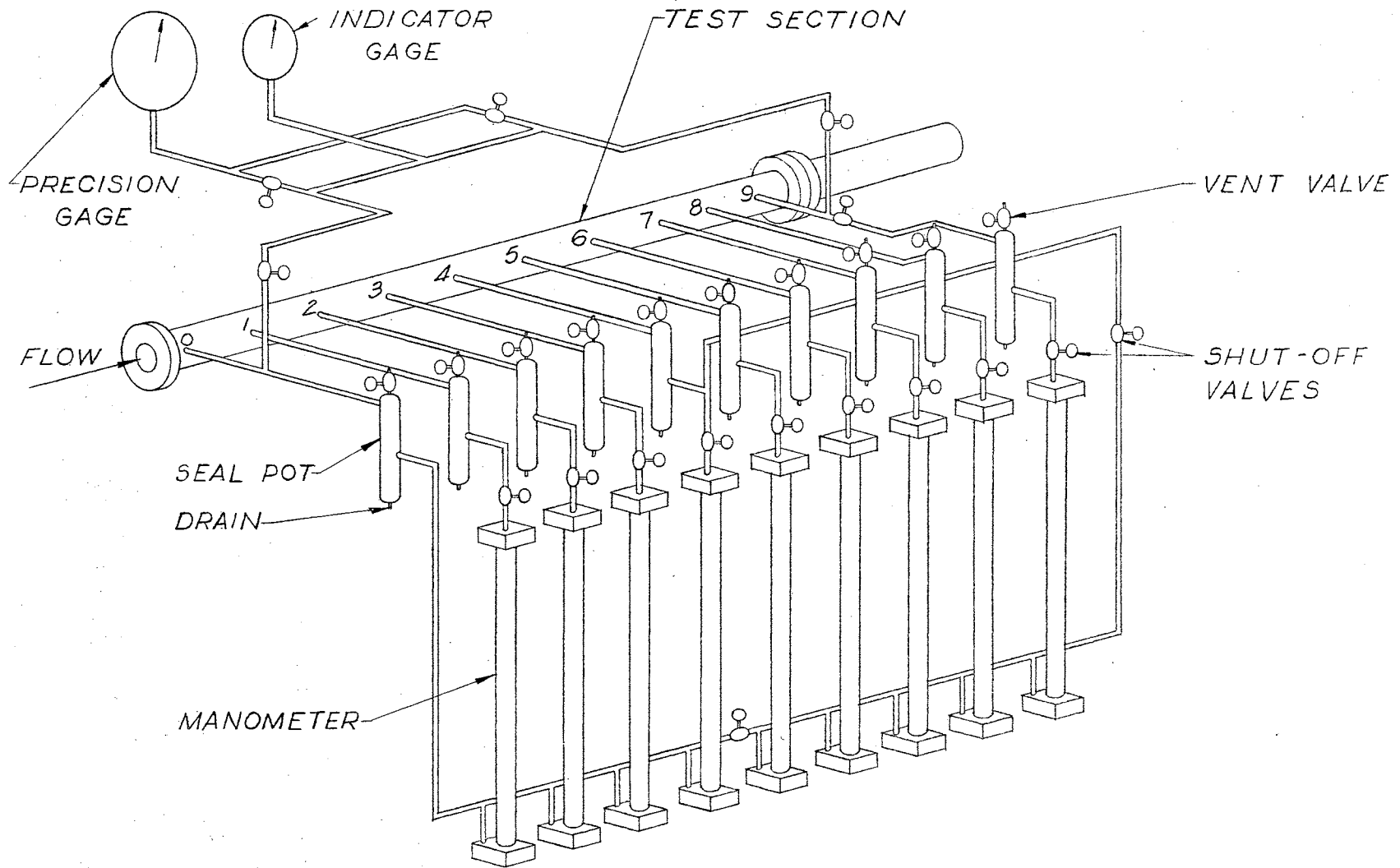
Figure 7. Pressure Measurement System
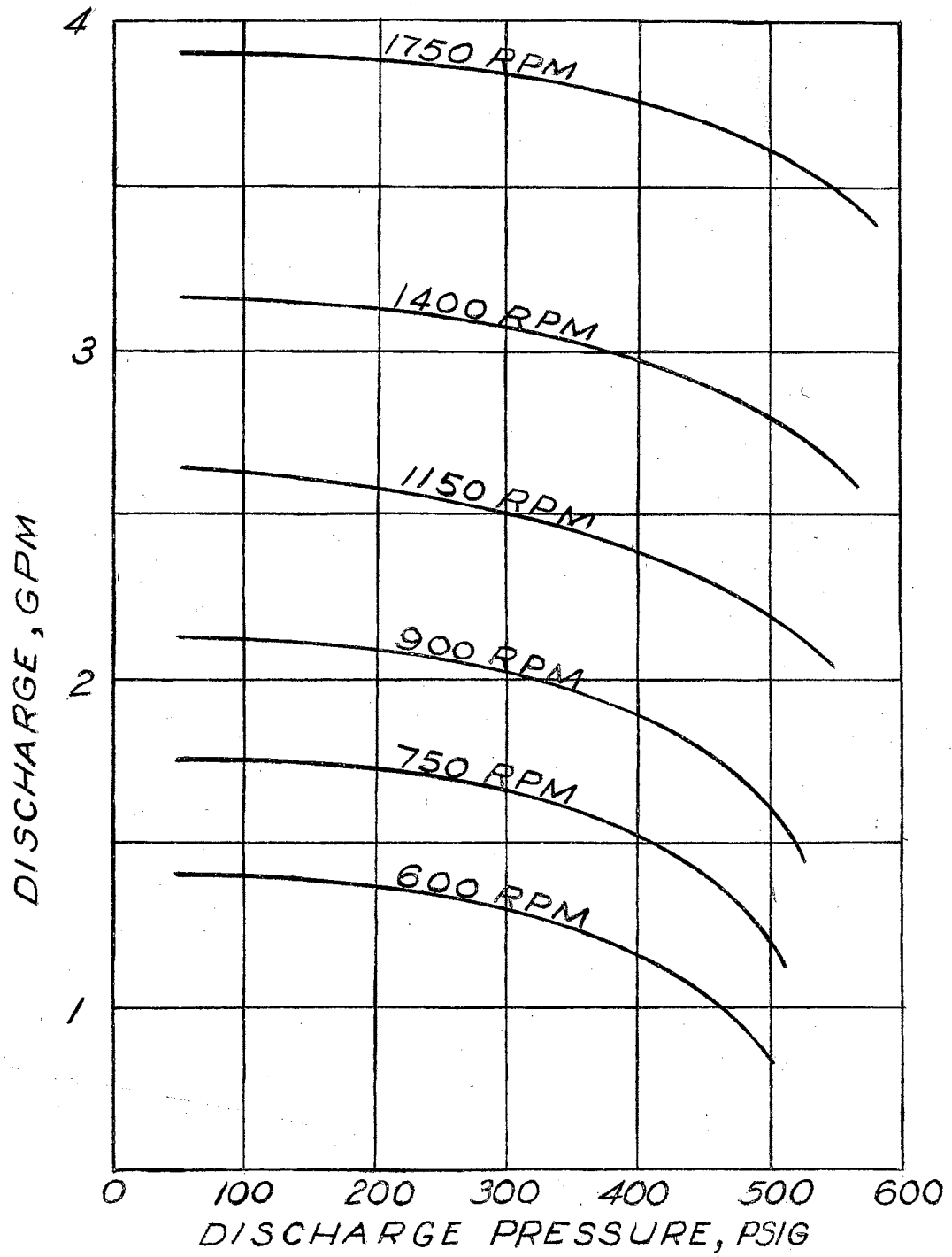
Figure 8

Pump Performance for 6-stage Moyno Pump

Operation

Operation of the fluid flow system involved the use of rather large amounts of electrical energy and high operating pressures. Especially, when the system was operated near saturation temperature or in the local boiling region of water, any failure of the flow network could result in injury to operating personnel or damage to equipment. Special precautions were taken in the design of electrical circuits to prevent continued heating if the main pump should fail or if water to the condenser should not be available. The auxiliary pump circuits are shown in Figure 9 and the main pump drive circuit is shown in Figure 10. The main pump Varidrive was provided with two operating ranges which were interlocked with a drive control circuit to prevent speed range change during operation. Visual check on pump drive circuit and speed of driver was provided on the control panel.

In case of emergency, two "panic" buttons were provided which shut down operation of the system. These buttons were located near the panel view port and at the test section end of the panel.

The preheater elements were divided into two banks of heaters so that six elements were connected to one circuit and six were connected to a second circuit, Figure 11. The position of heating elements in the preheater was shown in Figure 4. Preheater elements are switched into the circuit according to the numbering order shown for the purpose of maintaining as uniform heating as possible. Any desired setting of preheat could be obtained by connections of combinations of direct-switched and Powerstat-connected heaters. The voltage for the heaters connected through the Powerstat could be varied continuously for any number of heaters one through six. Front and back views
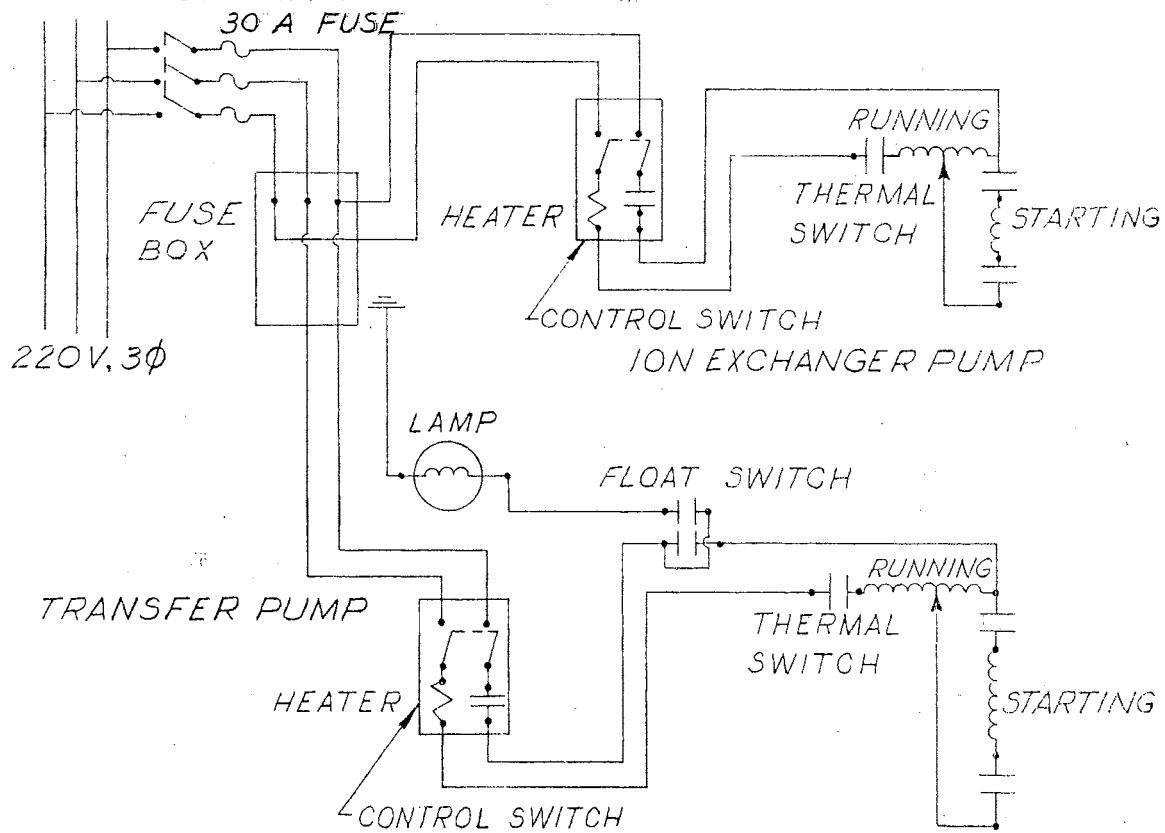
Figure 9. Auxiliary Pump Circuits
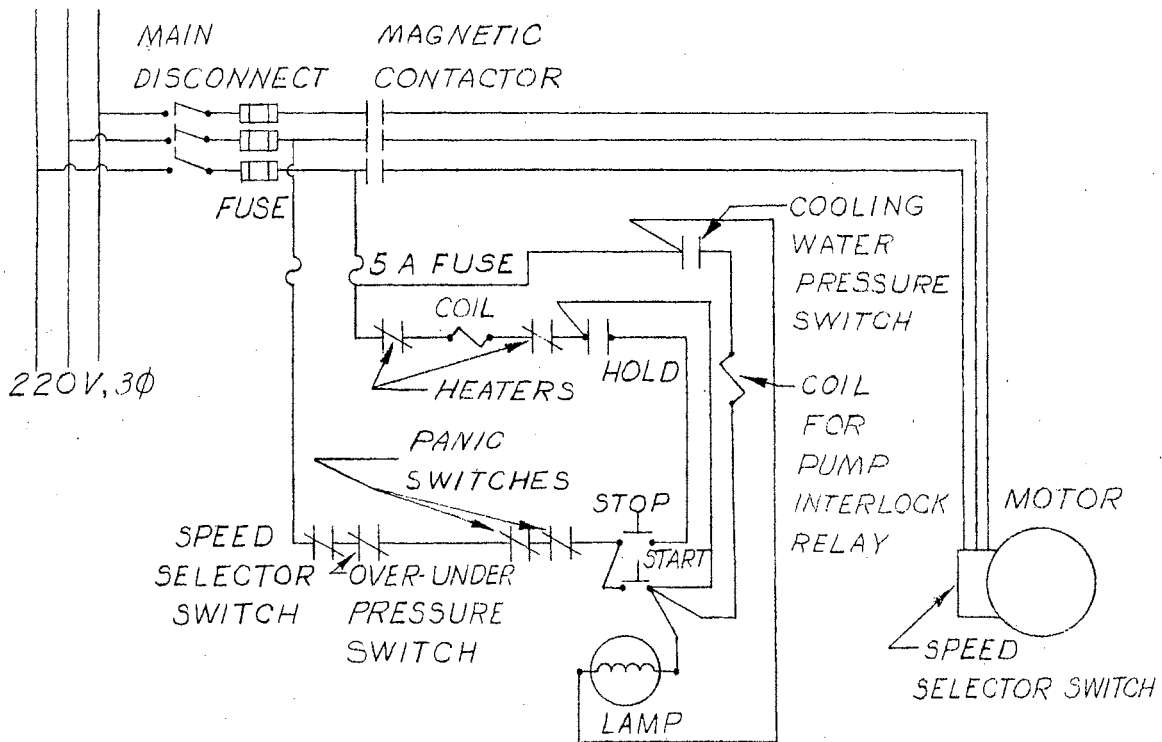
Figure 10. Main Pump Drive Circuit
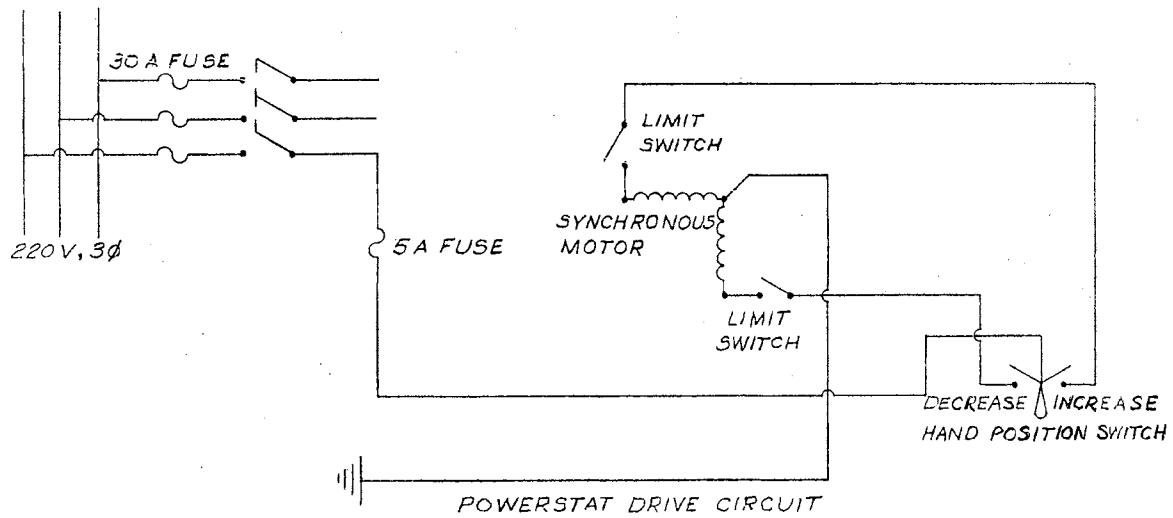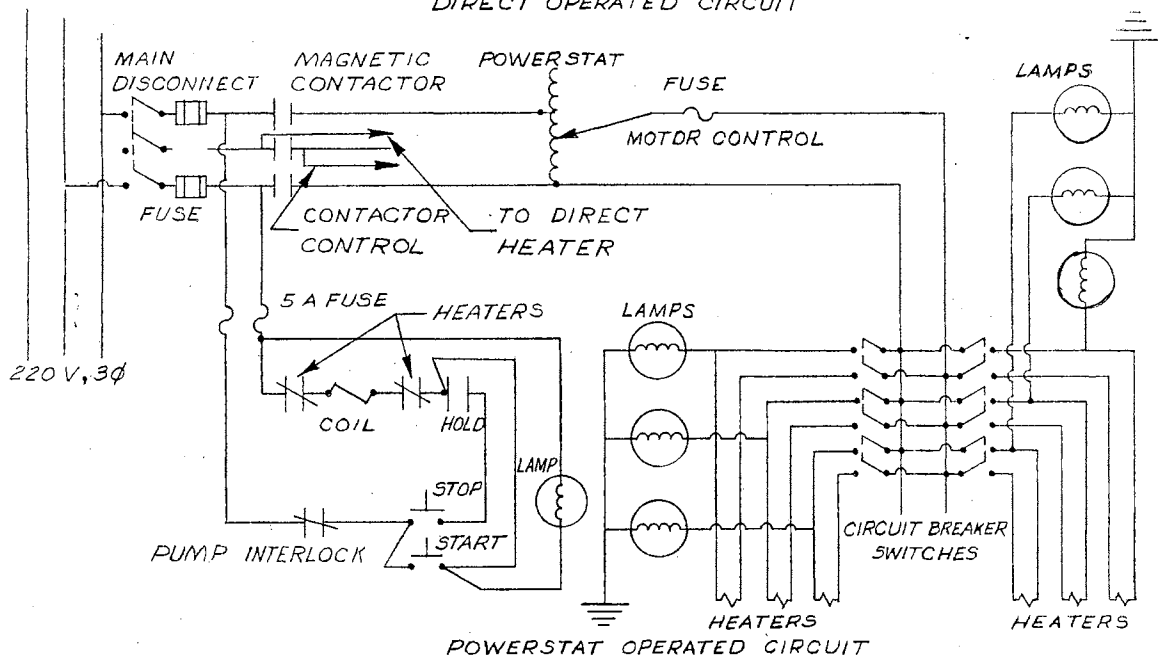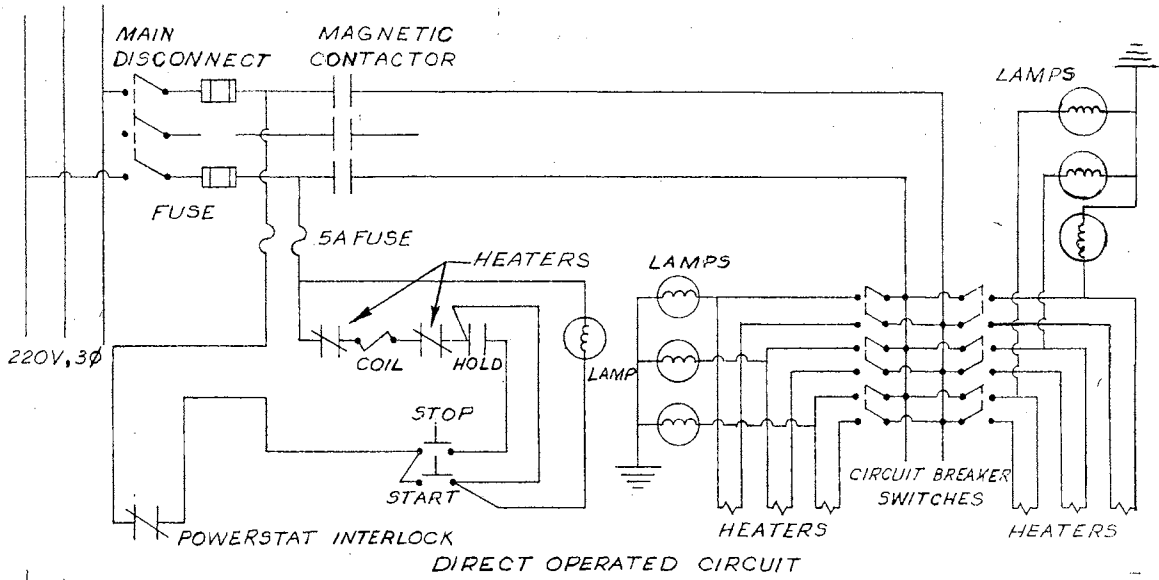
Figure 11. Preheater Electrical Circuits

of the instrumentation section may be seen in Plates V and VI. A clear view of the exhaust manifold discussed earlier, may also be seen in Plate VI.

PLATE V. INSTRUMENTATION SECTION OF CONTROL PANEL BOARD
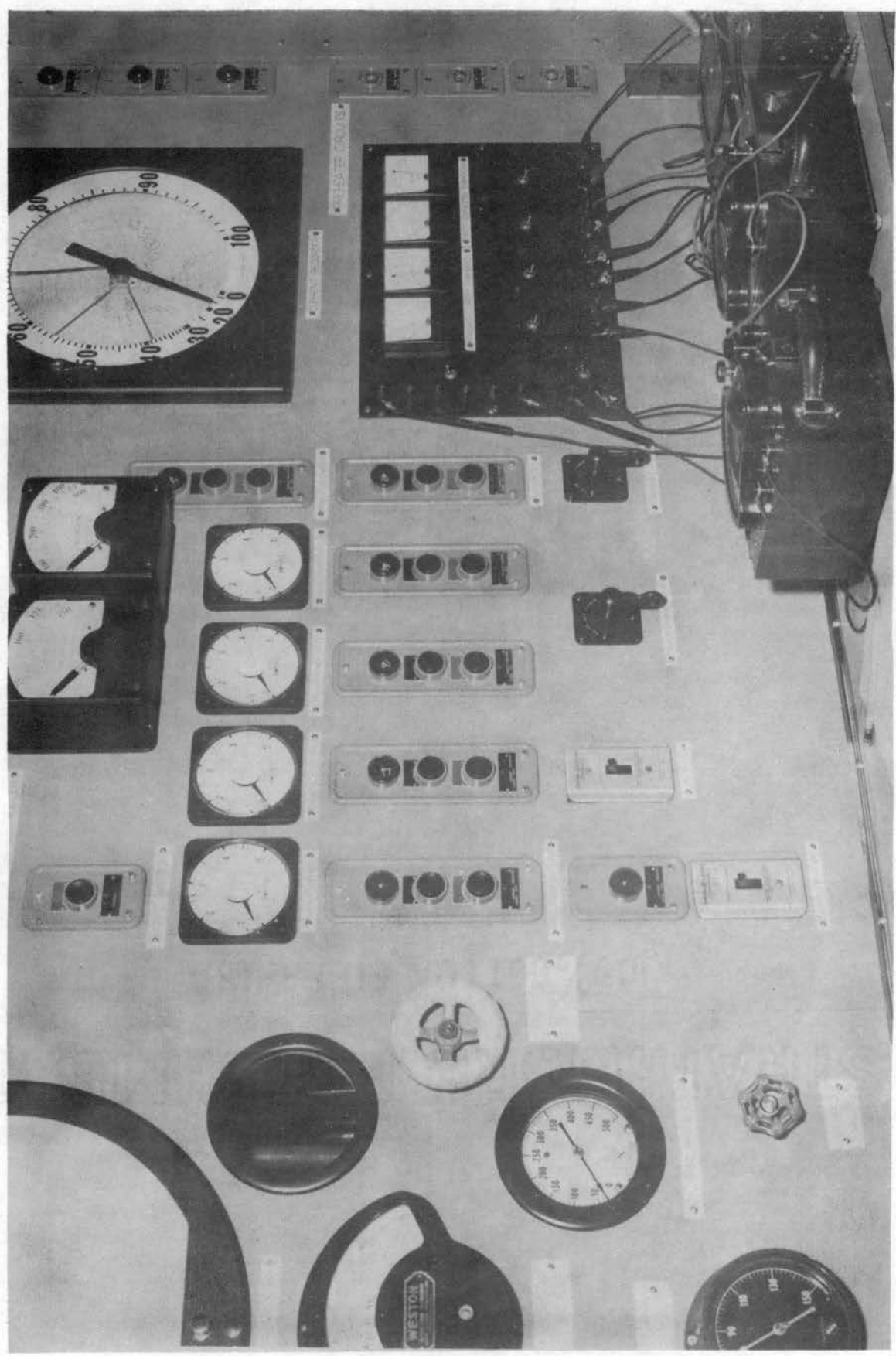
PLATE VI. BACK VIEW OF CONTROL PANEL BOARD AND EXHAUST MANIFOLD
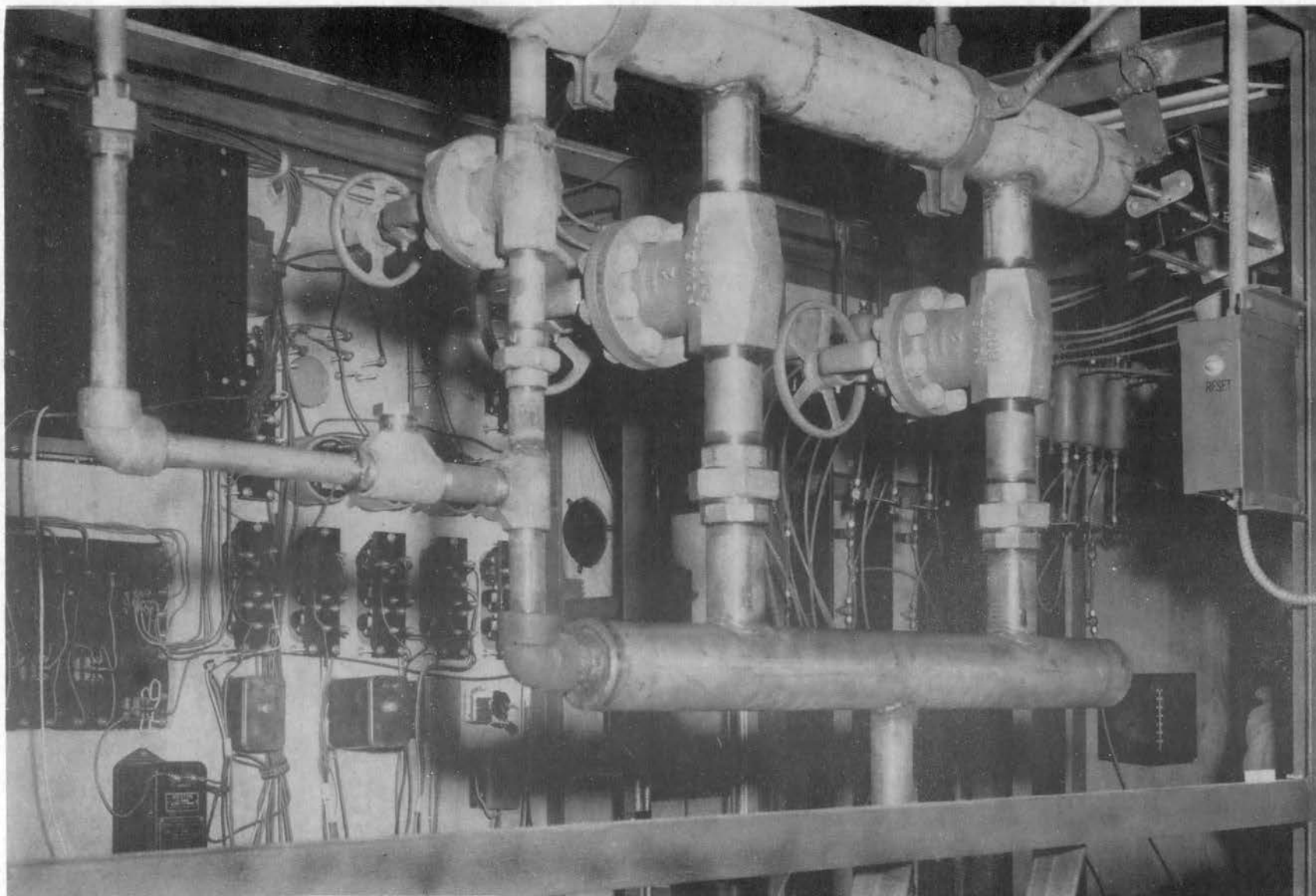
CHAPTER IV

ANALYSIS OF LOCAL BOILING PRESSURE DROP

Logically, the analysis of the data may be divided into two areas:
(1) the local boiling region; and (2) the nonboiling region. As discussed
previously, the start of local boiling must be determined in order to
analyze the local boiling pressure drop data. Two methods were used in
the present case.

The first method used to determine the start of local boiling consist-
ed of finding the position along the tube where the inside wall tempera-
ture t_w, satisfied the equation,

$$t_w = t_{sat} + \Delta t_{sat} .$$ (IV-I)

The quantity, Δt_{sat}, may be evaluated from Equation (II-2) and the
saturation temperature may be found from Figure 30 for the system pres-
sure. (1). Due to the variation of bulk temperature and heat transfer
film coefficient, the outside wall temperature and therefore inside
wall temperature varied along the length of the tube. The temperature
difference across the tube wall must be computed. Temperature distri-
bution through the wall of an electrically heated tube is represented
by the differential equation,

$$\frac{d^2t}{dr^2} + \left[\frac{1}{r} + \frac{K_1(dt)}{K(dr)} \right] \frac{dt}{dr} + \frac{E^2}{JKR} = 0 .$$ (IV-2)

35

A Taylor series solution of Equation (IV-2) for the temperature difference between inside and outside wall for an adiabatic outside wall has been given by Kreith and Summerfield (4) as

$$\Delta t = t_o - t_w$$

$$= \frac{m}{K_o \rho_o} \left[\overline{(\Delta x)}^2 + \frac{1}{3r_o} \overline{(\Delta x)}^3 \right.$$

$$+ \overline{(\Delta x)}^4 \left\{ \frac{m(3\alpha + 4\alpha\beta t_o + \beta)}{6(1 + \beta t_o)^2(1 + \alpha t_o)^2} \right.$$

$$\left. + \frac{1}{4r_o^2} \right\} + \cdots \left. \right] , \qquad (IV-3)$$

where

$$m = \frac{3.413 \, I^2 \rho^2}{2\pi^2(r_o^2 - r_i^2)^2} ,$$

K_o = thermal conductivity of tube at outside wall temperature, Btu/ft hr°F;

ρ_o = density at outside wall temperature, lb/ft^3;

Δx = wall thickness, ft;

r_o = outside radius, ft;

r_i = inside radius, ft;

ρ_m = mean density, lb/ft^3;

α = temperature coefficient of electrical resistivity, °F^{-1}; and

β = temperature coefficient of thermal conductivity, °F^{-1}.

Variation of electrical resistivity of AISI stainless steel type 304 used in this investigation is shown in Figure 33 and thermal conductivity is shown in Figure 34. On substituting the various constants into

Equation (IV-3), Equation (IV-4) is obtained. Thus,

$$\Delta t = 1.03216m$$

$$+ 2.9370 \times 10^{-10}m^2 \left[\frac{2.377 \times 10^{-3} + 1.282}{(1 + 5.17 \times 10^{-4}t_o)^2} \right.$$

$$\left. \frac{\times 10^{-2} t_o}{(1 + 6.2 \times 10^{-4}t_o)^2} \right] , \qquad\qquad (IV-4)$$

where

$$m = 6.6604 \times 10^6 \, \rho_m^2 \, I^2 ,$$

and

$$\rho_m = 2.265 \times 10^{-6} (1 + 0.00062t) ,$$

for

$$\Delta t < 0.4 \text{ F} \qquad\qquad t = t_o$$

$$\Delta t > 0.4 \text{ F} \qquad\qquad t = t_o - \tfrac{1}{2}\Delta t.$$

The Kreith and Summerfield equation was programmed for an IBM 650 digital computer and the results of the solution are plotted in Figure 32 for variation of temperature difference with outside wall temperature for different values of current.

The second method used to determine the start of local boiling consisted of examination of the pressure curves. If the shape of the pressure curve in the nonboiling region could be determined, then local boiling started where the pressure curve changed its shape. For the range of variables considered in the present investigation, the pressure variations in the nonboiling region were without exception represented by straight lines. The start of local boiling from the pressure curves could be determined within ± 1.5 inches and this point was then checked

with the temperature determination method. For many runs the temperature determination method did not prove to be reliable because the two lines, saturation temperature and wall temperature minus Δt_{sat}, were approximately parallel so that the intersection was not well defined. Both methods of determining the start of local boiling were used.

Pressure drop data for each run were plotted with distance along the test section and the start of local boiling was determined. The pressure profile was then divided into 1.5 inch increments beginning with local boiling point and the slope of the curve was measured at the beginning of each increment. In all cases the slope at the beginning of local boiling was equal to the slope of the curve at the end of the nonboiling region. The ratio (R) of the pressure curve slope in the boiling region to that at the beginning of boiling was plotted as the ordinate vs. a dimensionless distance (L/L_B) as abscissa.

Basis of the ratio (L/L_B) is the local boiling length; i.e., the length of tube where local boiling occurs if the tube is imagined extended until net boiling starts. Local boiling length may be solved for graphically (Figure 12), or may be computed according to the formula which may be derived using the geometrical relationships of Figure 12; thus,

$$L_B = \frac{\Delta t_{sub}\ G\ A_c\ C_p\ L_{T.S.}}{q''\ A_t\ 3600}, \tag{IV-5}$$

where

$L_{T.S.}$ = length of test section, ft.

Outside wall temperatures were measured in the experimental investigation and were then used to solve for inside wall temperatures. From measured pressure the corresponding saturation temperature (t_{sat})
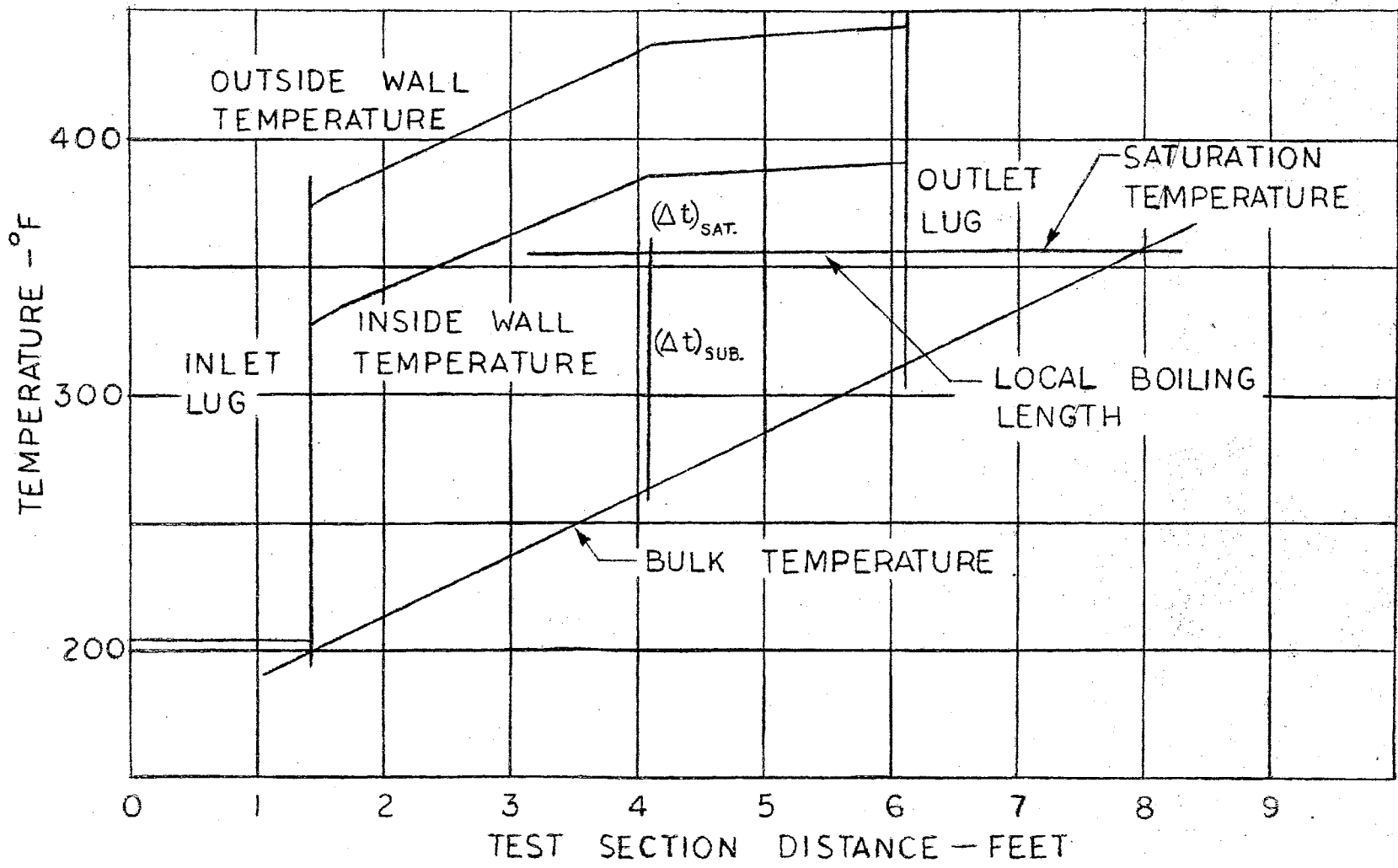
Figure 12. Method for Determination of Local Boiling Length

can be found from Figure 30. The bulk temperature at any point can be computed from the measured inlet temperature of the test section and from the heat added to the fluid up to the point considered. With the values of bulk fluid temperature and saturation temperature known, the amount of the subcooling of the fluid, Δt_{sub}, can be computed. Temperature difference between wall temperature and bulk fluid temperature is:

$$\Delta t = \Delta t_{sat} + \Delta t_{sub} . \tag{IV-6}$$

The Δt may be used to compute heat transfer film coefficients. The Δt_{sat} and Δt_{sub} may be used in the correlation equation for pressure drop and also in a determination of the position where local boiling starts.

Several assumptions were examined before the data were analyzed. These are as follows:

1. The heat flux is constant along the tube length.

2. The specific heat is equal to 1.0.

3. The heat loss through the insulation is negligible.

4. The axial heat conduction along the tube is negligible.

5. The heat loss from the lugs is negligible.

In order to check the validity of the assumptions, several measurements were made. If the voltage drop along the tube is constant and axial heat flow is negligible, then assumption 1 is correct. Several voltage profiles are shown in Figure 13. The straight lines validate the assumption.

In range of temperatures considered (100-500°F) specific heat may written as:

$$C_p = 1.04000 - 0.081021 \times 10^{-2}t + 0.051167 \times 10^{-4}t^2$$
$$- 0.012388 \times 10^{-6}t^3 + 0.0013148 \times 10^{-8}t^4 , \tag{IV-7}$$
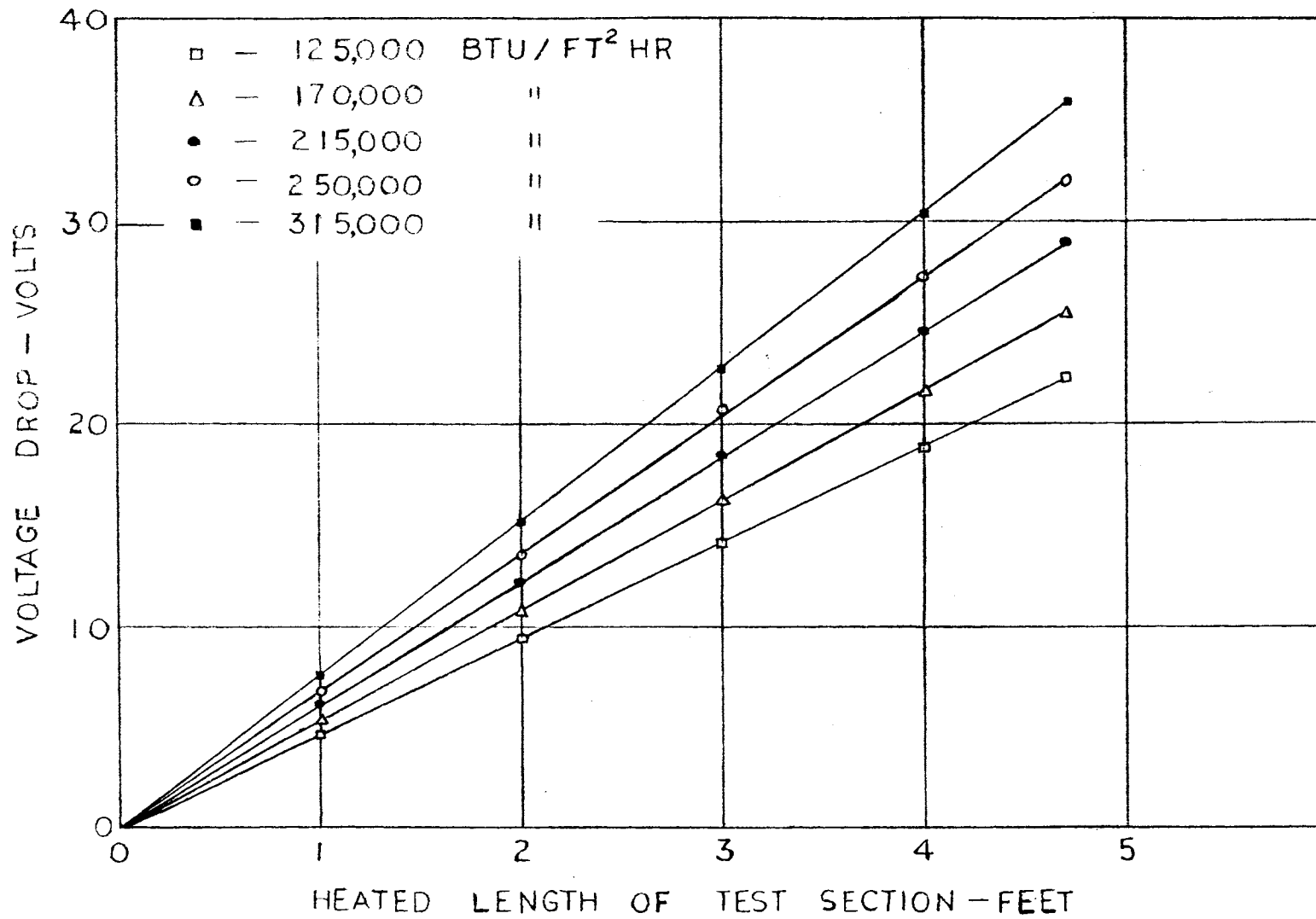
Figure 13. Voltage Drop Along Test Section

where

t = temperature, ^{O}F.

Evaluation of the integral, $\int_{t_1}^{t_2} C_p \, dt$, gives the change in enthalpy:

$$h_2 - h_1 = \int_{t_1}^{t_2} C_p \, dt = 1.04000 \, (t_2 - t_1) - 0.040511$$

$$x \, 10^{-2} \, (t_2{}^2 - t_1{}^2) + 0.017056 \times 10^{-4} \, (t_2{}^3 - t_1{}^3)$$

$$- 0.003097 \times 10^{-6} \, (t_2{}^4 - t_1{}^4) + 0.002630$$

$$x \, 10^{-8} \, (t_2{}^5 - t_1{}^5) \tag{IV-8}$$

Taking $t_1 = 100^O$F and $t_2 = 300^O$F as representative temperature limits, the enthalpy change calculated from Equation (IV-8) is 201.52 Btu compared with an enthalpy change of 200 Btu when a specific heat of 1.0 is used. The error is less than one per cent; thus the assumption is justified.

The most extreme condition for heat loss through the insulation occurs when the heat flux is low and wall temperature of the tube is high; i.e., for lowest water flow at highest inlet temperature. For this condition the heat loss may be computed as:

$$q_{(loss)} = \frac{KA \, \Delta t}{r_o \ln\left(r_o/r_i\right)} = \frac{0.04 \times 0.5 \times 300}{1.9 \times 1/12 \, \ln\left(\dfrac{1.90}{0.25}\right)} = 18.68 \text{ Btu/hr}$$

The heat loss for a heat flux of 100,000 Btu/ft^{2}hr is 0.04 per cent and is negligible.

Heat conduction along the tube would be greatest for minimum flow and maximum flux since this condition produces the greatest axial wall temperature gradient. Considering a temperature difference of 400°F for 1 foot of the tube, the axial heat flow may be calculated as:

$$q_{(axial)} \;=\; K\,A\,\frac{\Delta t}{\Delta x} \;=\; \frac{10(\pi)(.5) \times (.050) \times (400)}{(144) \times (1)} \;=\; 2.18 \text{ Btu/hr}$$

The axial heat conduction is small, so the assumption may be accepted.

Heat loss from the copper lugs will be of much greater value than axial heat conduction and must be considered carefully. The most severe condition will occur at the downstream lug. Considering heat conduction along the lug for a maximum temperature difference of 200°F, the computation will be:

$$q_{(loss)} \;=\; K\,A\,\frac{\Delta t}{\Delta x} \;=\; \frac{210 \times 1 \times 200}{12 \times 3} \;=\; 1051 \text{ Btu/hr}$$

which is about 2 per cent of the heat transferred to the water. No effect on the outside wall temperatures at the exit lug was observed. The calculated heat flux was corrected for heat loss through the power lugs.

CHAPTER V

CALCULATION OF NONBOILING PRESSURE DROP

Since the pressure profiles in the nonboiling region are straight
lines, as mentioned previously, the pressure gradient for the same run
in the nonboiling region was used as the reference pressure gradient for
that run. The writer believes that this pressure gradient most precisely
reflects the effect of local boiling on the pressure gradient. One of
the requirements for the reference pressure gradient is that it be calcu-
lable. This proved to be the case. The method used to calculate the non-
boiling pressure gradient is developed in this chapter.

Nonboiling pressure drop was solved with heat flux, q''; mass veloc-
ity, G; and inlet temperature, t_i as input data. Information on out-
side wall temperature was not used for this solution. The static pressure
change for a horizontal tube, is composed of two components: (1) frictional
drop and (2) momentum drop. Pressure drop (dP) is expressed as

$$-dP = \frac{dF}{v} + \frac{VdV}{vg} .$$ \hfill (V-1)

Equation (V-1) may be integrated to obtain the pressure drop between two
successive points of the tube as

$$-\Delta P = \frac{L}{2g_c D} G^2 f_{av} v_{av} + \frac{G^2}{g_c} (v_2 - v_1) ,$$ \hfill (V-2)

where

L = length between points 1 and 2, ft; and

$G = \rho_{av} \; v_{av} = \rho_i \; v_i$, lb/ft^{2}sec.

As long as no net amount of vapor forms in the test section, v_1 and v_2 can be evaluated from tables of properties at the respective pressure and temperature of the fluid. Although no net amount of vapor is formed for local boiling conditions, there is an effective change in the average density of the fluid. The property values of saturated water are given in Appendix B.

The Blasius equation for turbulent flow through a smooth tube for the range of Reynolds numbers (10,000-50,000) considered in this solution may be written as

$$f = 0.316 \; (Re)^{\frac{1}{4}} \; ,$$

where

Re = Reynolds number = $\dfrac{GD}{\mu}$, dimensionless.

The Blasius equation will be used in the form,

$$f = \frac{0.316}{(GD)^{\frac{1}{4}}} \; (\mu)^{\frac{1}{4}} \; , \tag{V-3}$$

In order to find the temperature at which the friction factor should be evaluated, several temperatures ranging in value from those of the bulk fluid temperature to the wall temperature, were tried. Wall temperatures gave the better results.

The tube was divided into several equal length segments, Figure 14, and Equation (V-2) was solved for each segment. Temperature difference between bulk and wall temperature was used to find the wall temperature. The change in bulk temperature may be computed from the equation,

$$\Delta t_b \cong \frac{3413 \, q'' \, A_t \, n\ell}{C_p L \, G \, A_c \times 3600} \quad , \tag{V-4}$$

where

A_t = surface area, ft^2

$n\ell$ = distance from inlet to point to be computed, ft;

L = total length, ft;

N = total number of intervals,

n = number of intervals between the point being considered and the beginning of the heated section;

A_c = cross-section area, ft^2; and

C_p = specific heat assumed to be 1, $Btu/lb°F$.

Start of Heater Section
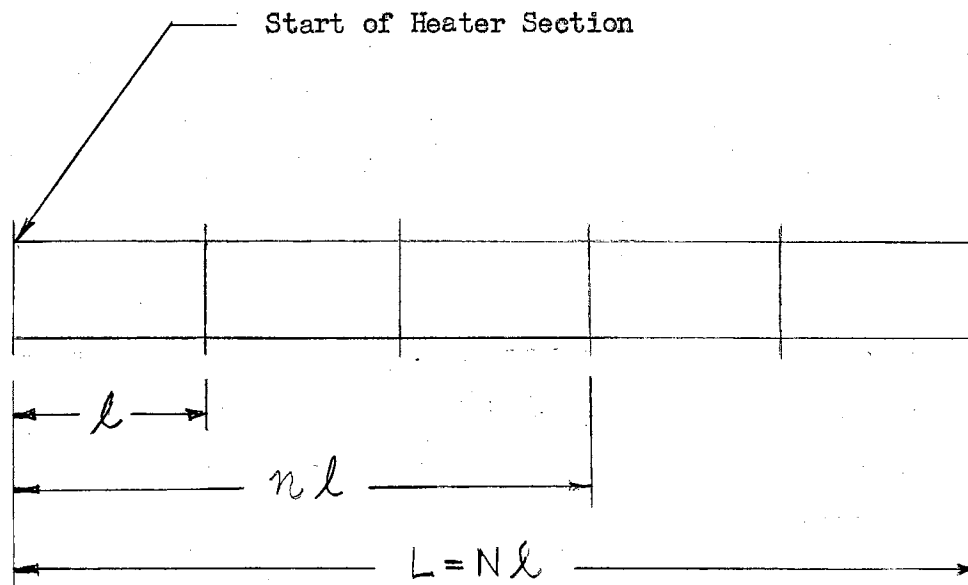
Figure 14

Illustration of Test Section Segments

The temperature difference across the film may be computed from the Colburn Equation (16) for heat transfer film coefficient,

$$\frac{hd}{K} = 0.023 \ (Re)^{0.8} \ (Pr)^{0.4} \quad , \tag{V-5}$$

where

  h = heat transfer film coefficient, $Btu/ft^2 hr\,^\circ F$;

  K = thermal conductivity of water, $Btu/ft\ hr\,^\circ F$;

  Pr = Prandtl number, dimensionless;

and the heat transfer equation,

$$q'' = h\,\Delta t_f \ , \tag{V-6}$$

where

  Δt_f = temperature difference across the film, $^\circ F$.

Equations (V-5) and (V-6) may be combined to obtain

$$\Delta t_f \quad = \quad \frac{D\ q''}{0.023\ K(Re)^{0.8}\ (Pr)^{0.4}} \ . \tag{V-7}$$

Inside wall temperature at any point may now be found as

$$t_w = t_1 + \Delta t_b + \Delta t_f \quad . \tag{V-8}$$

After all the property values and friction factors were evaluated at each tube segment end point, f_{av} and v_{av} for each tube segment were computed from

$$f_{av} = \frac{f_1 + f_2}{2} \qquad \text{and} \tag{V-9}$$

$$v_{av} = \frac{v_1 + v_2}{2} \ . \tag{V-10}$$

The computed quantities are substituted into

$$\Delta P_{1-2} = \frac{L}{2g_c\ D}\ G^2\ f_{av}\ v_{av} + \frac{G^2}{g_c}\ (v_2 - v_1)\ . \qquad (V-11)$$

Finally the pressure gradient is computed as

$$\frac{\Delta P}{\Delta \ell} = \frac{P_1 - P_4}{\ell_1 - \ell_4}\ . \qquad (V-12)$$

In order to study the solution and permit a selection of the proper temperature for the computation of friction factors, the problem was programmed for an IBM 650 digital computer. For the manual solution the property values of water may be read from appropriate graphs or tables but for the computer solution they must be put in a form which is suitable for the computer. The following fourth order polynomials for the computer solution were found by using a least squares curve fitting procedure for the temperature range 100-500°F. For the dynamic viscosity (μ), lb/ft hr:

$$\mu = 3.900745 - 3.331342 \times 10^{-2}T$$
$$+ 1.255388 \times 10^{-4}T^2 - 0.219447 \times 10^{-6}T^3$$
$$+ 0.0144995 \times 10^{-8}T^4 \qquad (V-13)$$

For the Prandtl number (Pr), dimensionless:

$$Pr = 11.383069 - 10.347279 \times 10^{-2}T$$
$$+ 4.051182 \times 10^{-4}T^2 - 0.725569 \times 10^{-6}T^3$$
$$+ 0.049070 \times 10^{-8}T^4 \qquad (V-14)$$

For specific volume (v), ft^3/lb:

$$v = 0.016138 - 0.0003637 \times 10^{-2}T$$
$$+ 0.0004358 \times 10^{-4}T^2 - 0.0000831 \times 10^{-6}T^3$$
$$+ 0.000009 \times 10^{-8}T^4 \qquad (V-15)$$

For thermal conductivity (K), Btu/ft hr°F:

$$K = 0.291745 + 0.103754 \times 10^{-2}T$$

$$- 0.035696 \times 10^{-4}T^2 + 0.005363 \times 10^{-6}T^3$$

$$- 0.000383 \times 10^{-8}T^4 \tag{V-16}$$

The standard error of estimate of the least squares fit was:

0.936911×10^{-2}	(μ)
0.333633×10^{-1}	(Pr)
0.108169×10^{-4}	(v)
0.537662×10^{-3}	(K)

Maximum error of the computed pressure gradient from experimental values was ± 5 per cent. Many of the pressure gradients in the nonboiling region were found to be the same as measured. Examples of computed and measured profiles are shown in Figure 15.
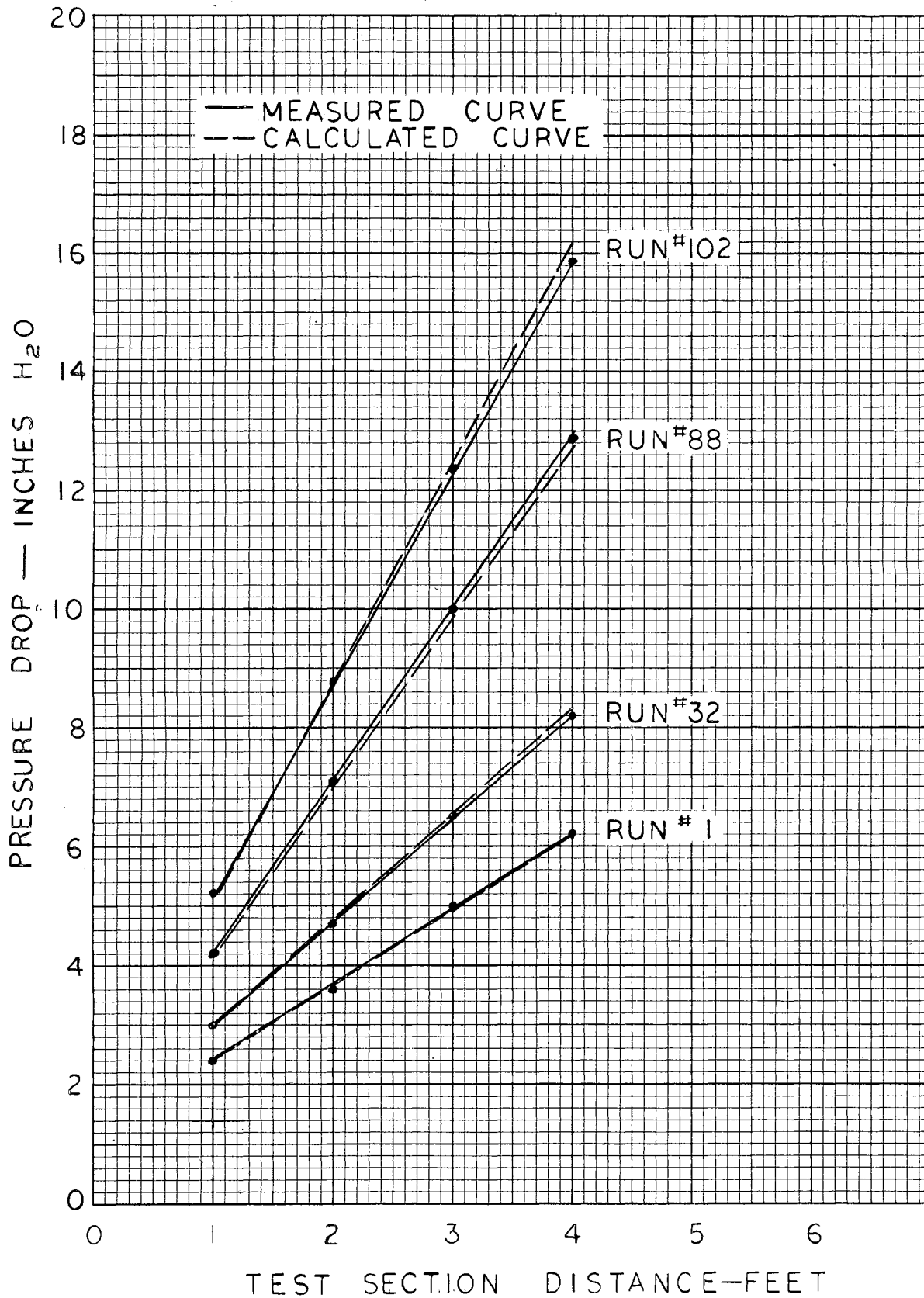
Figure 15. Calculated and Experimental Nonboiling Pressure Drop

CHAPTER VI

EXPERIMENTAL RESULTS AND DATA CORRELATION

In order to check the experimental pressure measurements, isothermal runs were made. The pressure profiles for these data should be straight lines as shown by the equation,

$$\frac{dP}{dL} = \frac{f \, G^2}{2 \, D \, g_c \, \rho}.$$ (VI-1)

The straight lines, Figure 16, were verified for each series of runs. Results of the isothermal runs may be used to show that the friction factor, f, approached that for a smooth tube. Figure 17 is a plot of friction factor for various Reynolds numbers. The curve is compared with friction factors for smooth tubes reported by Moody (17). The data are higher than the Moody results by 2 per cent at a Reynolds number of 30,000. The test section was assumed to be a smooth tube for the calculation presented in Chapter V.

The local boiling data were plotted with the pressure gradient ratio (R), as the ordinate and the length ratio (L/L_B) as the abscissa. A representative plot is shown in Figure 18. For individual runs the variables of pressure, flow rate, and length ratio were considered.

The Effect of Pressure

A careful study of the pressure gradient curves indicated that a pressure effect was present. The pressure effect was small. This fact

51

CURVE	RUN NO.
A	5
B	4
C	3
D	2
E	1
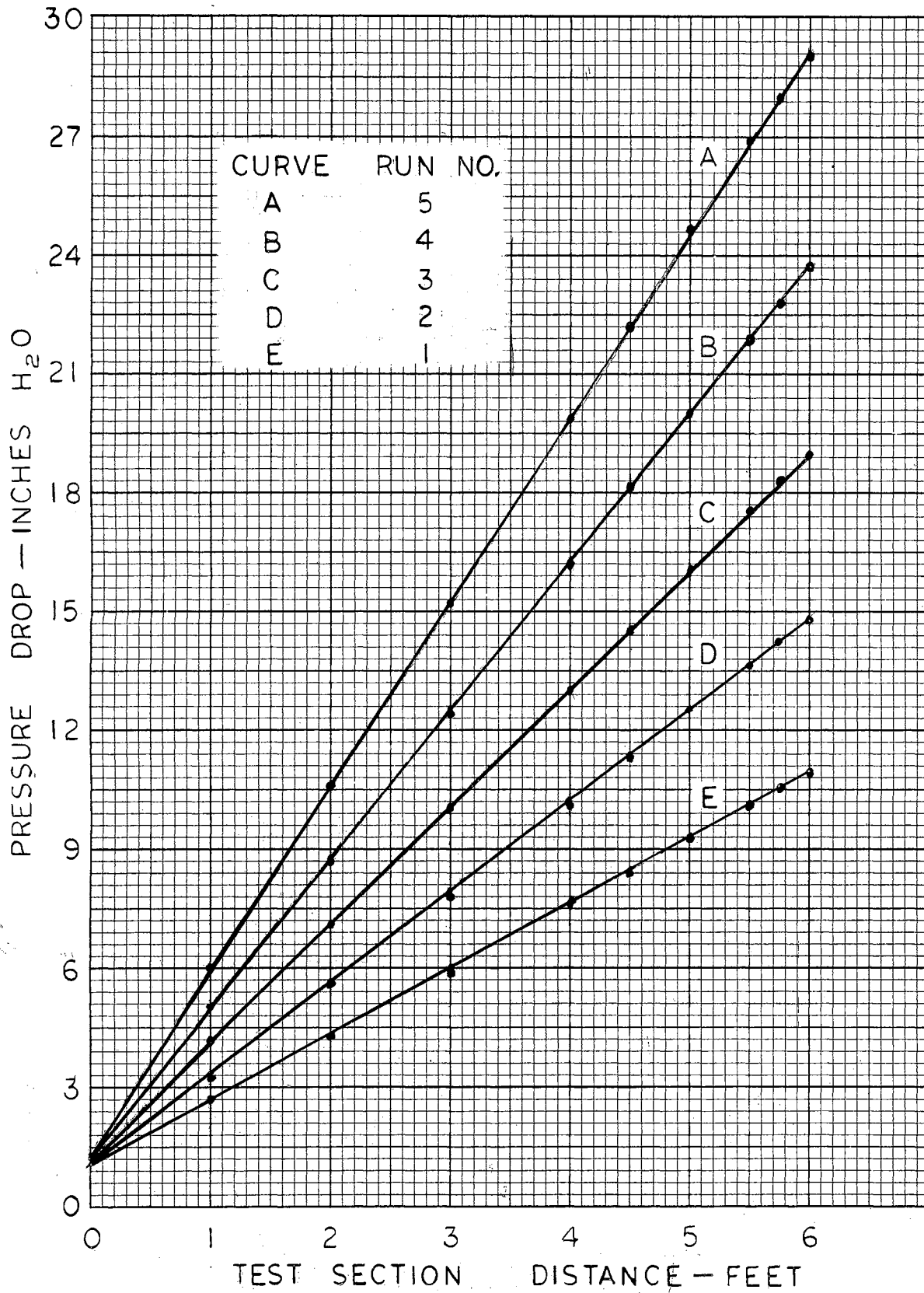
Figure 16. Isothermal Pressure Profiles
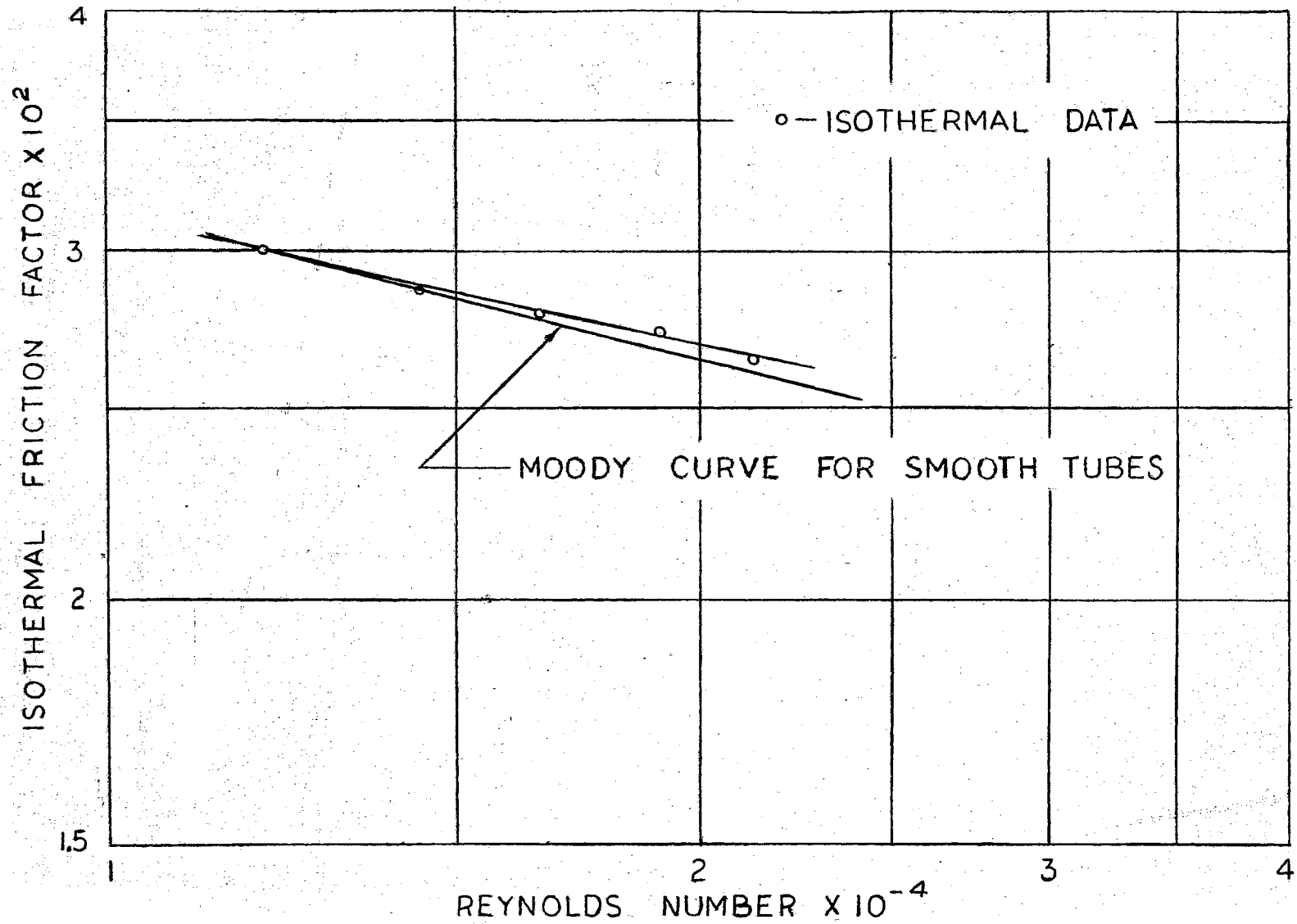
Figure 17.   Deviation of Isothermal Friction Factor from the Moody Smooth Tube Curve
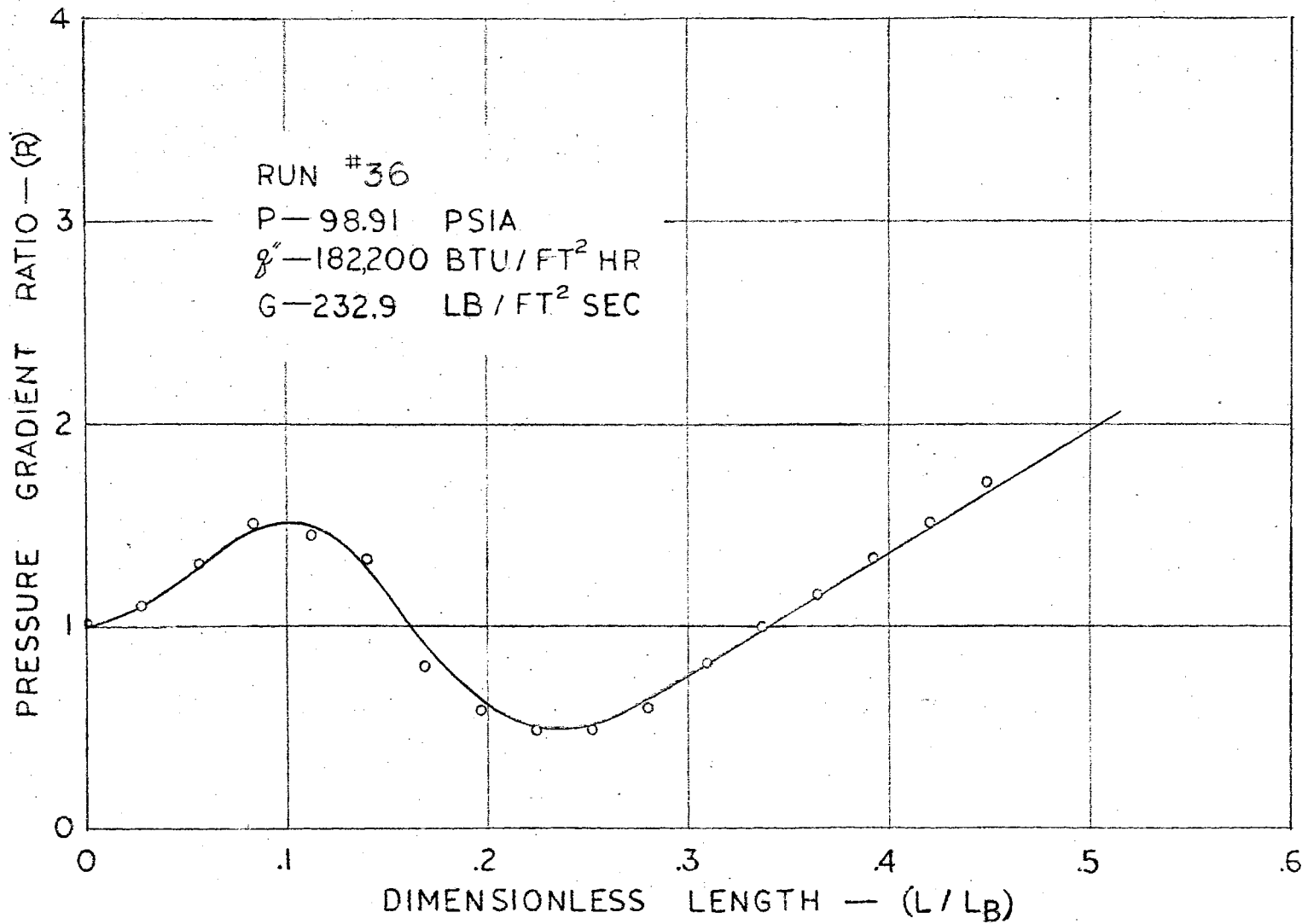
Figure 18. Typical Experimental Pressure Gradient Ratio Curve

confirms Reynolds' (1) assumption that the data for local boiling in a limited pressure range are independent of pressure. As reported by Buchberg, Romie, Lipkis and Greenfield (13) the pressure gradient ratio is larger at lower pressure.

In an effort to account for the effect of pressure, (R - 1) was multiplied by

$$e^{K(P/P_o - 1)} , \qquad\qquad (VI\text{-}2)$$

where

P = absolute pressure at the start of local boiling, psia;

P_o = 200 psia, reference pressure;

$K = 0.2$; and

R = pressure gradient ratio.

The value of the multiplying factor for various pressures is shown in Figure 19. Because of data scatter, the values of K and P_o could not be determined precisely. Additional detailed data on the effect of pressure will certainly clarify the values of the constants to be used for other data. The effect of the pressure multiplier was to increase (R - 1) for pressures higher than P_o and to decrease (R - 1) for pressures lower than P_o.

The Effect of Flow Rate

As has been noted by other investigators the pressure gradient ratio was independent of flow rate. (7), (8). The variation of R with L/L_B for various flow rates after correcting the data for the pressure is shown in Figure 20. As was expected, the predominate variable is the heat flux.
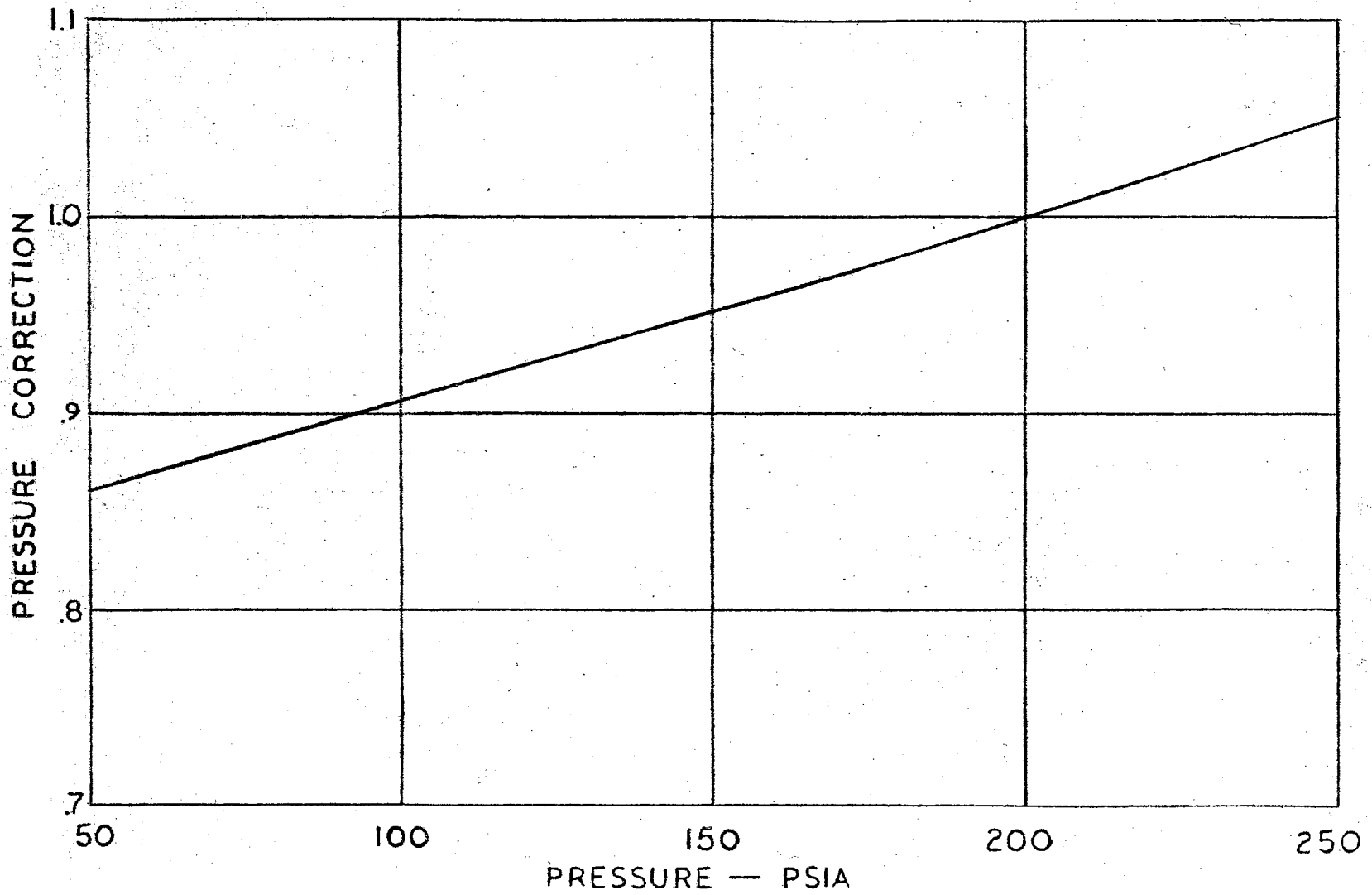
Figure 19. Pressure Correction Multiplier
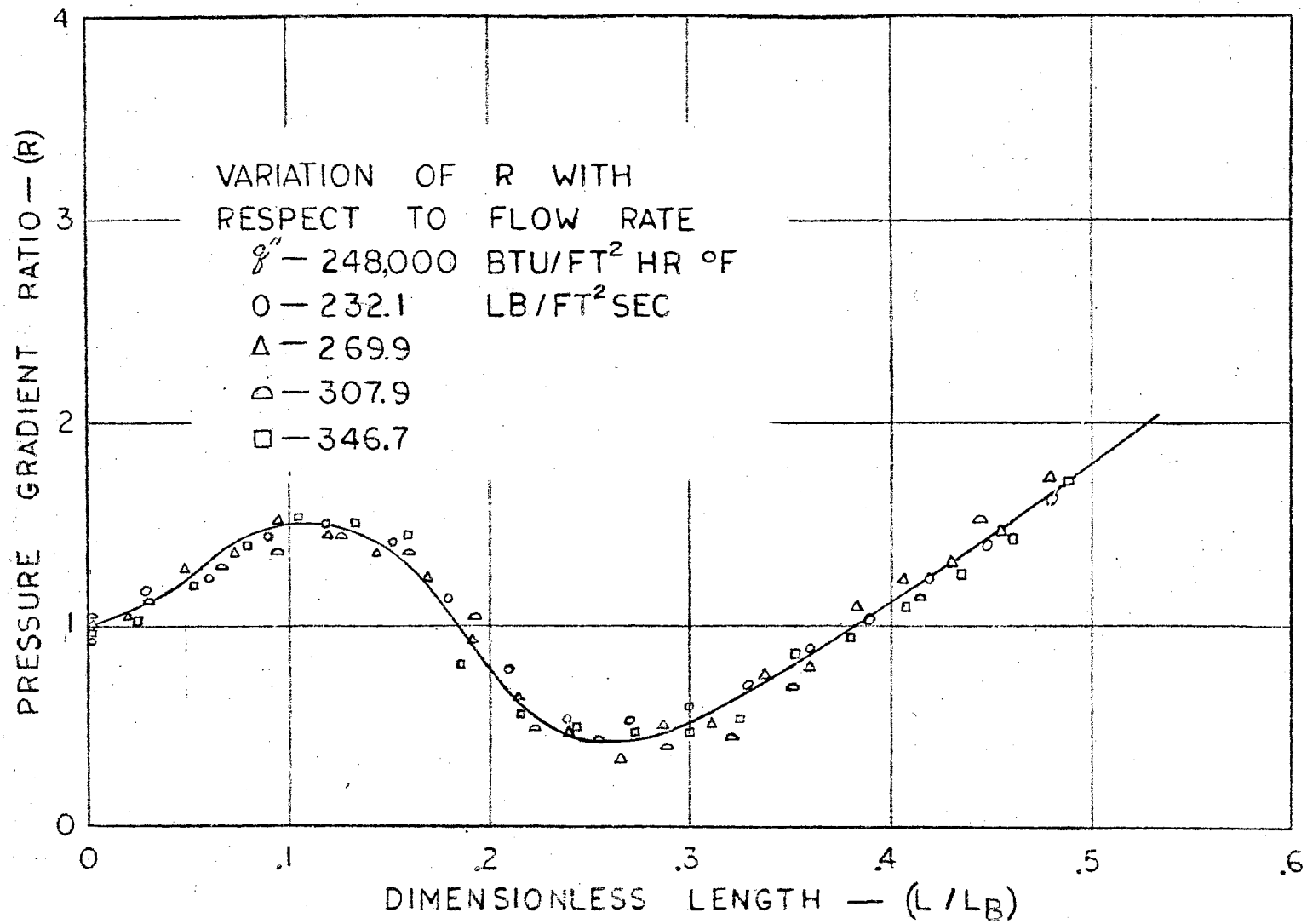
Figure 20. Variation of Pressure Gradient Ratio Showing Effect of Flow Rate

The Effect of Heat Flux

It was difficult to obtain the same heat flux for different flow rates and pressures; therefore, a range of heat fluxes $\pm$ 1.0 per cent of a given heat flux was considered as the same heat flux. For example, if a heat flux of 157,000 Btu/ft^2hr was being considered, then all runs in the range of $\pm$ 1500 Btu/ft^2hr of 157,000 Btu/ft^2hr were used together. Even though the value of the heat flux measurement is more accurate than this (approximately $\pm$ 0.5 per cent), errors in the pressure drop data would not permit more accurate analysis of the data. The composite data are plotted in Figure 21. Using this graph the correlation equation was found to be

$$\left(\frac{dP}{dL}\right)_{L.B.} = \left(\frac{dP}{dL}\right)_{N.B.} \left[1 + \left\{ e^{0.2(1 - P/200)} \right\} \right.$$

$$\left\{ \frac{q''}{q''_o} - 2 \right\} \left\{ 0.04332 + 2.50586 \ (L/L_B) \right.$$

$$\left. \left. - 21.81864 \ (L/L_B)^2 + 37.21943 \ (L/L_B)^3 \right\} \right] \quad (VI-2)$$

where

q''_o = constant heat flux, 40,000 Btu/ft^2hr; and

$$\left(\frac{dP}{dL}\right)_{N.B.} = \text{nonboiling pressure gradient, in. of } H_2O/in.$$

The isothermal data are tabulated in Table I and the nonisothermal data are tabulated in Table II.
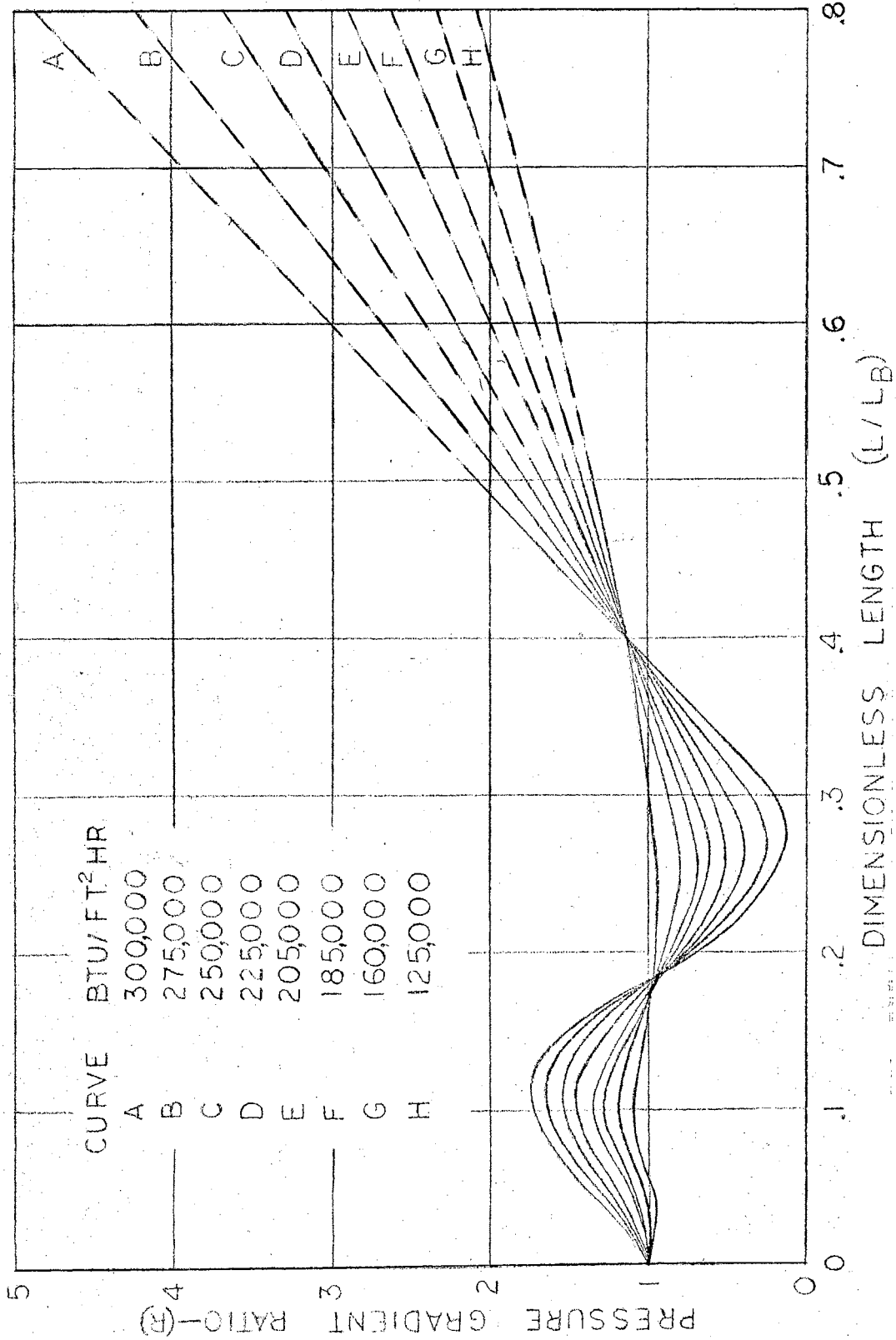
Figure 21. Graph of Local Boiling Pressure Gradient Ratio

TABLE I

ISOTHERMAL TEST DATA

Run No.	P Pressure psia	G Velocity lb/(ft^2)(sec)	q" Heat Flux Btu/ft^{2}hr	Water Temp °F In-let	Out-let	Pressure Drop [a] in. H$_2$O								
						1	2	3	4	5	6	7	8	9
1	49.5	194.3	0	85	85	2.69	4.27	5.87	7.61	8.40	9.24	10.14	10.53	10.93
2	49.5	232.9	0	85	85	3.22	5.58	7.80	10.14	11.31	12.50	13.65	14.24	14.76
3	49.5	270.3	0	85	85	4.19	7.12	10.06	13.08	14.64	16.15	17.67	18.35	19.07
4	49.5	307.9	0	85	85	5.03	8.70	12.42	16.19	18.12	19.91	21.86	22.62	23.71
5	49.5	346.7	0	85	85	6.05	10.59	15.22	19.89	22.21	24.71	26.87	28.04	29.09

a. All pressure drop data were measured with respect to (0) pressure tap.

TABLE II

NONISOTHERMAL TEST DATA

Run No.	P Pressure psia	G Velocity $lb/(ft^2)$ (sec)	q" Heat Flux $Btu/ft^2\,hr$	Water Temp °F Inlet	Outlet	Start of local boiling in. [a]	Pressure Drop in. H_2O [b]								
							1	2	3	4	5	6	7	8	9
1	48.98	194.3	64,300	196.0	247.9	48.0	2.36	3.55	4.86	6.12	6.57	7.18	7.72	8.25	8.76
2	48.97	194.3	78,800	176.4	240.0	54.0	2.48	3.61	4.89	6.10	6.70	7.08	7.78	8.39	8.99
3	48.97	194.3	149,200	81.1	201.6	52.0	2.67	3.71	4.86	5.99	6.67	7.29	7.76	8.17	8.78
4	98.99	194.3	85,800	225.0	290.7	51.0	2.38	3.51	4.82	6.03	6.55	7.02	7.59	7.64	8.01
5	98.99	194.3	103,600	205.0	285.2	49.0	2.36	3.51	4.74	5.93	6.65	7.02	7.53	7.86	8.23
6	98.99	194.3	118,100	180.5	272.3	51.1	2.42	3.55	4.80	5.99	6.63	7.14	7.61	7.80	8.60
7	98.98	194.3	156,700	150.0	272.8	51.0	2.46	3.57	4.80	5.97	6.94	7.12	7.55	8.35	9.20
8	98.98	194.3	187,000	109.5	256.6	51.0	2.57	3.63	4.82	5.99	6.92	7.16	7.57	8.35	9.36
9	98.98	194.3	207,300	86.0	249.5	51.0	2.67	3.67	4.80	5.89	6.75	7.06	7.57	8.21	9.56
10	148.99	194.3	91,200	256.0	325.7	48.0	2.36	3.45	4.66	5.87	6.42	6.79	7.35	7.47	7.69

TABLE II (Continued)

Run No.	P Pressure psia	G Velocity lb/(ft^2)(sec)	q" Heat Flux Btu/ft^{2}hr	Water Temp $^\circ$F In-let	Out-let	Start [a] of local boil-ing in.	Pressure Drop [b] in. H$_2$O								
							1	2	3	4	5	6	7	8	9
11	149.99	194.3	114,000	222.00	310.4	49.5	2.36	3.51	4.66	5.89	6.57	6.92	7.41	7.59	7.96
12	148.99	194.3	146,800	188.5	303.4	49.5	2.40	3.51	4.68	5.89	6.77	7.02	7.39	7.55	8.00
13	148.99	194.3	174,100	159.0	295.9	49.0	2.42	3.51	4.66	5.83	6.65	6.92	7.35	7.64	8.37
14	148.98	194.3	203,100	129.0	289.3	49.2	2.48	3.59	4.70	5.81	4.80	7.04	7.47	7.94	8.68
15	148.99	194.3	219,800	86.2	263.5	48.0	2.65	3.69	4.72	5.85	6.63	7.00	7.43	7.80	8.60
16	198.99	194.3	99,500	272.9	353.2	49.0	2.34	3.51	4.70	5.83	6.32	6.86	7.49	7.64	8.15
17	198.99	194.3	125,600	235.3	336.7	49.5	2.34	3.49	4.68	5.89	6.44	6.84	7.41	7.61	7.94
18	198.99	194.3	150,500	206.5	328.0	48.0	2.34	3.47	4.68	5.85	6.57	6.83	7.31	7.78	8.35
19	198.99	194.3	186,600	166.4	316.9	48.5	2.44	3.51	4.66	5.85	6.63	6.86	7.35	7.45	8.39
20	198.99	194.3	204,800	133.3	298.6	49.5	2.50	3.51	4.64	5.79	6.59	6.75	7.31	7.58	7.96
21	198.99	194.3	250,900	101.2	303.6	49.0	2.54	3.51	4.52	5.65	6.88	6.79	7.25	7.64	8.31
22	198.99	194.3	263,700	84.2	297.0	49.5	2.63	3.57	5.62	5.69	6.53	6.84	7.23	7.62	8.21
23	249.04	193.8	85,400	295.4	364.7	63.0	2.36	3.55	4.82	6.05	6.63	7.23	7.82	8.05	7.98
24	249.04	193.8	147,200	235.4	354.8	62.0	2.34	3.51	4.70	5.85	6.47	7.00	7.48	7.70	8.03

TABLE II (Continued)

Run No.	P Pressure psia	G Velocity lb/(ft²) (sec)	q" Heat Flux Btu/ ft²hr	Water Temp °F Inlet	Outlet	Start of local boiling in.[a]	Pressure Drop[b] in. H_2O								
							1	2	3	4	5	6	7	8	9
25	249.04	193.8	164,600	219.6	353.1	61.0	2.34	3.51	4.66	5.85	6.42	6.99	7.41	7.59	8.01
26	249.04	193.8	196,900	182.6	342.3	52.0	2.40	3.55	4.70	5.91	6.55	7.14	7.51	7.76	8.06
27	249.04	193.8	228,800	146.9	332.5	49.9	2.40	3.51	4.66	5.77	6.44	7.00	7.29	7.66	8.35
28	48.93	232.9	82,900	195.5	251.4	49.5	2.96	4.66	6.38	8.05	8.78	9.57	10.34	11.00	11.52
29	48.90	232.9	87,100	177.9	226.6	51.0	3.08	4.82	6.59	8.27	9.01	9.89	10.61	11.39	12.15
30	48.89	232.9	142,900	126.8	223.2	51.0	3.18	4.82	6.47	8.15	8.99	9.91	10.49	11.08	11.54
31	48.80	232.9	186,600	85.2	210.9	48.0	3.33	4.93	6.40	8.05	9.07	9.67	10.37	11.12	11.99
32	98.92	232.9	103,500	220.4	290.2	51.7	2.93	4.58	6.38	8.00	8.76	9.44	10.20	10.61	11.13
33	98.90	232.9	142,900	166.4	262.8	50.1	3.04	4.66	6.44	8.03	8.93	9.59	10.31	10.82	11.43
34	98.91	232.9	145,000	176.4	274.2	49.0	3.00	4.64	6.42	8.00	8.99	9.59	10.30	10.71	11.33
35	98.90	232.9	163,600	156.4	266.7	49.9	3.04	4.68	6.44	8.11	9.05	9.83	10.41	10.96	11.76
36	98.91	232.9	182,200	137.3	260.2	49.5	3.06	4.62	6.32	7.96	9.10	9.59	10.10	10.76	11.52
37	98.90	232.9	208,300	106.2	246.7	49.3	3.26	4.72	6.38	7.96	8.99	9.67	10.10	10.78	11.74
38	98.90	232.9	230,700	86.2	24.18	49.3	3.33	4.82	6.40	8.00	9.15	9.79	10.12	10.88	11.86

TABLE II (Continued)

Run No.	P Pressure psia	G Velocity lb/(ft^2)(sec)	q" Heat Flux Btu/ft^{2}hr	Water Temp °F In-let	Water Temp °F Out-let	Start of local boil-ing in.[a]	Pressure Drop in.H$_2$O[b] 1	2	3	4	5	6	7	8	9
39	148.96	232.9	107,700	247.2	319.8	48.0	2.93	4.60	6.30	7.92	8.66	9.36	10.14	10.55	11.13
40	148.96	232.9	122,300	236.3	318.7	49.0	2.92	4.62	6.30	7.98	8.66	9.36	10.14	10.49	10.94
41	148.96	232.9	132,700	220.9	310.3	48.0	2.87	4.47	6.14	7.89	8.60	9.32	10.02	10.37	10.82
42	148.96	232.1	168,700	186.6	300.8	47.5	3.02	4.66	6.28	7.92	8.93	9.65	10.14	10.57	11.21
43	148.95	232.1	210,200	146.4	288.7	48.0	3.04	4.60	6.24	7.86	8.99	9.46	10.20	10.94	11.78
44	148.95	232.1	234,200	126.9	285.5	49.0	3.12	4.62	6.20	7.80	9.05	9.48	9.98	10.74	11.60
45	148.95	232.1	256,200	105.8	279.3	48.0	3.22	4.66	6.20	7.82	9.15	9.34	9.98	10.98	12.11
46	148.95	232.9	272,800	88.7	272.5	48.0	3.27	4.64	6.12	7.78	8.93	9.32	9.98	11.21	12.50
47	198.96	232.1	149,200	227.0	328.0	54.5	2.93	4.56	6.24	7.96	8.72	9.44	10.18	10.55	11.16
48	198.96	232.1	174,100	207.1	325.0	54.0	2.98	4.62	6.26	7.92	8.74	9.36	10.04	10.53	11.13
49	198.96	232.1	206,500	176.0	315.8	55.0	3.00	4.54	6.20	7.82	8.68	9.42	10.04	10.35	10.74
50	198.98	232.1	241,300	135.9	299.3	54.0	3.10	4.60	6.18	7.78	8.62	9.38	10.06	10.32	10.72
51	248.94	232.1	93,700	303.8	367.2	60.2	2.91	4.58	6.30	8.00	8.81	9.67	10.34	10.49	10.78
52	248.94	232.1	116,100	285.9	364.5	52.2	2.94	4.64	6.30	8.01	8.64	9.46	10.18	10.51	10.94

TABLE II (Continued)

Run No.	P Pres- sure psia	G Velocity lb/(ft²)(sec)	q" Heat Flux Btu/ ft²hr	Water Temp °F In- let	Out- let	Start[a] of local boil- ing in.	Pressure Drop[b] in. H₂O 1	2	3	4	5	6	7	8	9
53	248.93	232.1	124,800	266.2	350.7	54.0	2.94	4.62	6.32	7.98	8.70	9.38	10.27	10.53	11.09
54	248.94	232.1	167,500	235.4	345.4	59.0	2.91	4.52	6.22	7.88	8.66	9.48	10.06	10.35	10.78
55	248.93	232.1	190,700	206.6	335.7	60.0	2.98	4.62	6.25	7.92	8.68	9.52	10.22	10.53	11.10
56	248.94	232.1	205,600	186.6	325.8	59.0	2.94	4.58	6.24	7.84	8.68	9.48	10.28	10.53	11.00
57	248.94	232.1	269,500	121.3	303.7	58.0	3.10	4.58	6.08	7.66	8.42	9.36	9.95	10.30	10.92
58	48.75	270.3	114,000	176.4	240.2	48.0	3.70	6.01	8.27	10.49	11.45	12.54	13.49	14.31	15.01
59	48.81	270.3	151,700	145.8	230.7	49.5	3.72	5.97	8.11	10.32	11.58	12.50	13.63	14.27	14.92
60	48.80	270.3	215,200	84.2	204.7	48.5	4.08	6.16	8.21	10.34	11.56	12.50	13.40	14.45	15.64
61	98.76	270.3	96,400	245.2	299.1	48.0	3.70	5.95	8.37	10.57	11.47	12.40	13.44	13.67	14.37
62	98.75	270.3	124.400	216.5	286.1	49.0	3.70	5.95	8.33	10.53	11.50	12.46	13.42	13.98	14.66
63	98.75	270.3	133,500	202.5	277.2	49.0	3.69	5.95	8.29	10.51	11.43	12.46	13.46	14.06	14.68
64	98.76	270.3	149,200	197.5	281.1	53.0	3.72	6.01	8.33	10.47	11.64	12.42	13.46	13.96	14.59
65	98.76	270.3	165,800	178.9	271.7	56.5	3.70	5.99	8.27	10.32	11.68	12.60	13.46	14.10	14.86
66	98.76	270.3	221,800	124.3	248.5	52.5	3.86	5.97	8.19	10.30	11.56	12.48	13.07	13.69	14.47

TABLE II (Continued)

Run No.	P Pressure psia	G Velocity lb/(ft²)(sec)	q" Heat Flux Btu/ft²hr	Water Temp °F Inlet	Outlet	Start of local boiling in.	Pressure Drop in. H_2O 1	2	3	4	5	6	7	8	9
67	98.75	270.3	282,000	78.6	236.4	51.0	4.13	6.20	8.23	10.35	11.82	12.66	13.36	14.41	15.64
68	148.76	270.3	125,500	247.2	317.6	48.0	3.69	5.89	8.31	10.37	11.39	12.28	13.42	13.77	14.53
69	148.76	270.3	148,400	236.3	219.4	54.0	3.67	5.95	8.23	10.35	11.43	12.30	13.26	13.75	14.57
70	148.76	270.3	186,700	200.0	304.5	54.0	3.67	5.87	8.21	10.28	11.49	12.36	13.24	13.63	14.43
71	198.82	270.3	139,700	264.0	342.2	49.5	3.55	5.81	7.98	10.32	10.92	12.11	13.08	13.83	14.78
72	198.84	269.9	169,100	237.4	335.9	55.0	3.55	5.75	7.94	10.12	11.17	12.09	13.03	13.49	14.43
73	198.82	269.9	194,900	216.6	330.0	54.1	3.53	5.75	7.92	10.19	11.29	12.15	13.22	13.94	15.19
74	198.82	269.9	195,300	238.4	352.1	53.0	3.51	5.66	7.80	10.02	11.12	11.99	12.89	13.52	14.45
75	198.82	269.9	228,000	186.6	319.4	49.0	3.71	5.87	7.98	10.16	11.47	12.23	13.03	13.57	14.41
76	198.42	269.9	245,000	166.5	309.2	49.0	3.71	5.85	7.90	10.12	11.43	12.15	12.95	13.38	14.06
77	198.83	269.9	264,500	149.9	303.9	49.3	3.72	3.55	7.96	10.10	11.39	12.25	13.04	13.49	14.22
78	248.80	269.9	145,100	281.0	365.5	64.5	3.57	5.85	8.01	10.32	11.13	12.30	13.42	13.83	14.25
79	284.81	269.9	181,600	246.3	352.0	61.9	3.51	5.66	7.85	10.14	11.10	12.21	13.07	13.57	14.20
80	248.80	269.9	208,100	222.6	343.8	62.0	3.55	5.75	7.86	10.14	11.12	12.27	13.07	13.59	14.08

TABLE II (Continued)

Run No.	P Pressure psia	G Velocity $lb/(ft^2)$ (sec)	q" Heat Flux Btu/ ft^2hr	Water Temp °F Inlet	Outlet	Start [a] of local boiling in.	Pressure Drop [b] in. H_2O								
							1	2	3	4	5	6	7	8	9
81	248.80	269.9	245,400	191.6	334.5	60.0	3.69	5.89	7.98	10.20	11.25	12.30	13.24	13.65	14.24
82	248.81	269.9	277,800	156.5	318.2	60.0	3.74	5.85	7.84	10.12	11.10	12.15	13.05	13.34	13.83
83	49.37	307.9	96,400	205.5	254.5	54.0	4.09	7.12	9.85	12.66	14.06	15.25	16.46	16.71	17.67
84	50.35	307.9	131,600	177.5	244.6	54.0	4.25	7.18	10.06	12.83	14.59	15.60	16.80	17.57	18.49
85	48.67	307.9	163,300	145.7	228.8	53.0	4.50	7.37	10.00	12.85	14.29	15.78	16.93	17.63	18.35
86	48.68	307.9	234,200	83.7	202.9	53.0	4.89	7.61	10.32	12.75	14.22	15.58	16.59	17.37	18.17
87	98.70	307.9	122,300	247.2	309.4	54.5	4.08	7.02	9.83	12.48	13.75	14.78	16.30	16.85	18.08
88	97.69	307.9	161,700	216.4	298.7	54.0	4.06	6.96	9.75	12.48	13.88	14.84	16.34	16.93	18.14
89	98.68	307.9	174,500	202.5	291.3	54.0	4.33	7.25	10.16	12.85	14.37	15.25	16.71	17.26	18.50
90	98.68	307.9	217,600	178.4	289.1	50.0	4.33	7.25	9.96	12.83	14.33	15.42	16.67	17.76	18.70
91	148.72	307.9	157,500	250.2	330.4	55.1	4.29	7.22	10.00	12.68	14.08	14.94	16.61	17.24	18.51
92	148.74	307.9	176,100	253.3	325.0	54.2	4.13	7.04	9.75	12.59	14.04	14.84	16.36	16.95	18.17
93	148.64	307.9	198,600	216.5	317.5	49.0	4.29	7.18	9.79	12.68	14.31	15.23	16.40	17.12	18.29
94	148.89	307.9	215,600	202.5	312.2	49.5	4.27	7.04	9.75	12.46	14.16	15.05	16.40	16.95	18.06

TABLE II (Continued)

Run No.	P Pressure psia	G Velocity lb/(ft^2)(sec)	q" Heat Flux Btu/ft^{2}hr	Water Temp °F In-let	Out-let	Start of local boil-ing in. [a]	Pressure Drop [b] in. H_2O								
							1	2	3	4	5	6	7	8	9
95	148.64	307.9	246,700	176.4	301.9	49.5	4.35	7.20	9.77	12.60	14.39	15.21	16.34	16.95	17.92
96	198.88	307.9	194,900	245.2	344.3	54.0	4.31	7.16	9.94	12.50	13.84	15.05	16.65	17.32	18.47
97	198.56	307.9	207,800	231.4	336.9	48.0	4.41	7.23	9.93	12.68	14.31	15.19	16.40	17.18	18.37
98	198.56	307.9	236,300	216.0	336.2	49.1	4.41	7.22	9.95	12.66	14.61	15.23	16.48	17.37	18.53
99	198.88	307.9	244,600	202.5	327.0	54.7	4.35	7.14	9.77	12.46	13.79	14.98	16.30	16.93	17.98
100	248.67	306.6	199,400	260.2	362.4	53.0	4.29	7.20	9.91	12.69	13.92	15.35	16.50	17.24	18.33
101	248.67	307.9	241,300	226.4	349.2	54.0	4.29	7.20	9.83	12.66	14.02	15.17	16.42	16.87	17.69
102	48.74	346.7	110,900	202.5	252.8	49.5	5.15	8.79	12.38	15.87	17.63	19.25	20.85	21.61	22.52
103	48.74	346.7	157,500	175.4	246.8	48.0	5.21	8.79	12.30	15.70	17.57	19.25	20.85	21.64	22.78
104	48.51	346.7	165,800	145.7	221.9	51.0	5.46	9.07	12.50	15.87	17.67	19.38	21.06	22.25	23.61
105	48.74	346.7	221,900	127.8	228.3	49.5	5.50	8.99	12.42	15.68	17.63	19.07	20.83	22.13	23.81
106	98.50	346.7	167,800	218.9	295.0	54.0	5.19	8.76	12.32	15.58	17.51	18.88	20.40	21.29	22.37
107	98.52	346.7	190,700	200.0	286.5	55.0	5.03	8.48	12.11	15.50	17.26	18.64	20.07	20.85	22.05
108	98.51	346.7	215,600	177.4	275.1	51.0	5.23	8.77	12.28	15.62	17.59	18.90	20.49	21.08	22.00

TABLE II (Continued)

Run No.	P Pressure psia	G Velocity lb/(ft²)(sec)	q" Heat Flux Btu/ft²hr	Water Temp °F Inlet	Outlet	Start of local boiling in.	Pressure Drop in.H₂O 1	2	3	4	5	6	7	8	9
109	98.52	346.7	257,000	146.3	262.8	53.0	5.38	8.81	12.11	15.56	17.63	18.97	21.02	22.41	24.39
110	98.53	346.7	299,300	97.2	232.8	49.5	5.81	9.13	12.25	15.62	17.16	18.84	20.42	22.85	25.78
111	148.48	346.7	215,600	221.4	319.1	53.0	5.32	8.99	12.64	15.95	17.80	19.23	20.87	21.51	22.72
112	148.49	346.7	246,700	199.5	311.3	48.5	5.15	8.66	12.25	15.64	17.67	18.97	20.51	21.27	22.39
113	148.49	346.7	282,800	176.4	304.6	49.5	5.23	8.70	11.95	15.48	17.94	18.76	20.26	21.12	22.50
114	148.48	346.7	306,800	163.4	302.5	49.5	5.30	8.81	12.11	15.60	18.17	18.95	20.26	21.41	22.78
115	198.49	346.7	249,600	228.4	341.5	48.0	5.13	8.74	12.03	15.42	17.59	18.58	20.30	21.29	22.58
116	198.49	346.7	281,500	211.5	339.1	48.0	5.03	8.54	11.82	15.35	17.69	18.53	20.12	21.26	22.60
117	198.49	346.7	311,800	193.0	334.3	48.0	5.21	8.66	11.89	15.42	17.88	18.64	20.12	21.26	22.58
118	248.48	246.7	286,000	227.5	357.2	49.5	5.11	8.62	12.03	15.37	17.36	18.45	20.40	21.66	23.32
119	248.43	346.7	315,000	208.5	351.3	29.5	5.21	8.70	12.71	15.58	16.56	18.64	20.94	22.58	24.32

a. Start of local boiling measured from (0) pressure tap

b. All pressure drop data were measured with respect to (0) pressure tap

CHAPTER VII

DISCUSSION

The results of this experimental study may be discussed in terms
of nonboiling pressure drop, determination of $(\Delta t)_{sat}$, and local boil-
ing pressure drop. A comparison of the ratio of friction factors with
and without heat transfer from previous studies (4),(5), to those ob-
tained in the present investigation is shown in Figure 22. The data of
Kreith and Summerfield (4) cover a range of Reynolds numbers of 100,000
to 250,000 while for the present investigation the range is 10,000 to
30,000. The Reynolds numbers in both cases were computed at the average
bulk temperature of the fluid. The curve in Figure 22 representing the
present investigation is based on the computation method, Chapter V.
The maximum error of the data from the predicted values is ± 5 per cent
and the maximum error of the data from that predicted by the equation
from reference (4) is ± 7 per cent. (18). The line with a slope of
0.60 represents both friction and momentum pressure drop. The nonboil-
ing frictional pressure drop predicted by the equations of other investi-
gators was lower than similar data reported in this thesis. (4), (5).

Nonboiling frictional pressure drop may be analyzed in another way
as discussed in Chapter II. (15). Equation (II-10) for the pressure
drop may be solved for the friction factor by comparing it with Equation
(VI-1). The resulting expression is
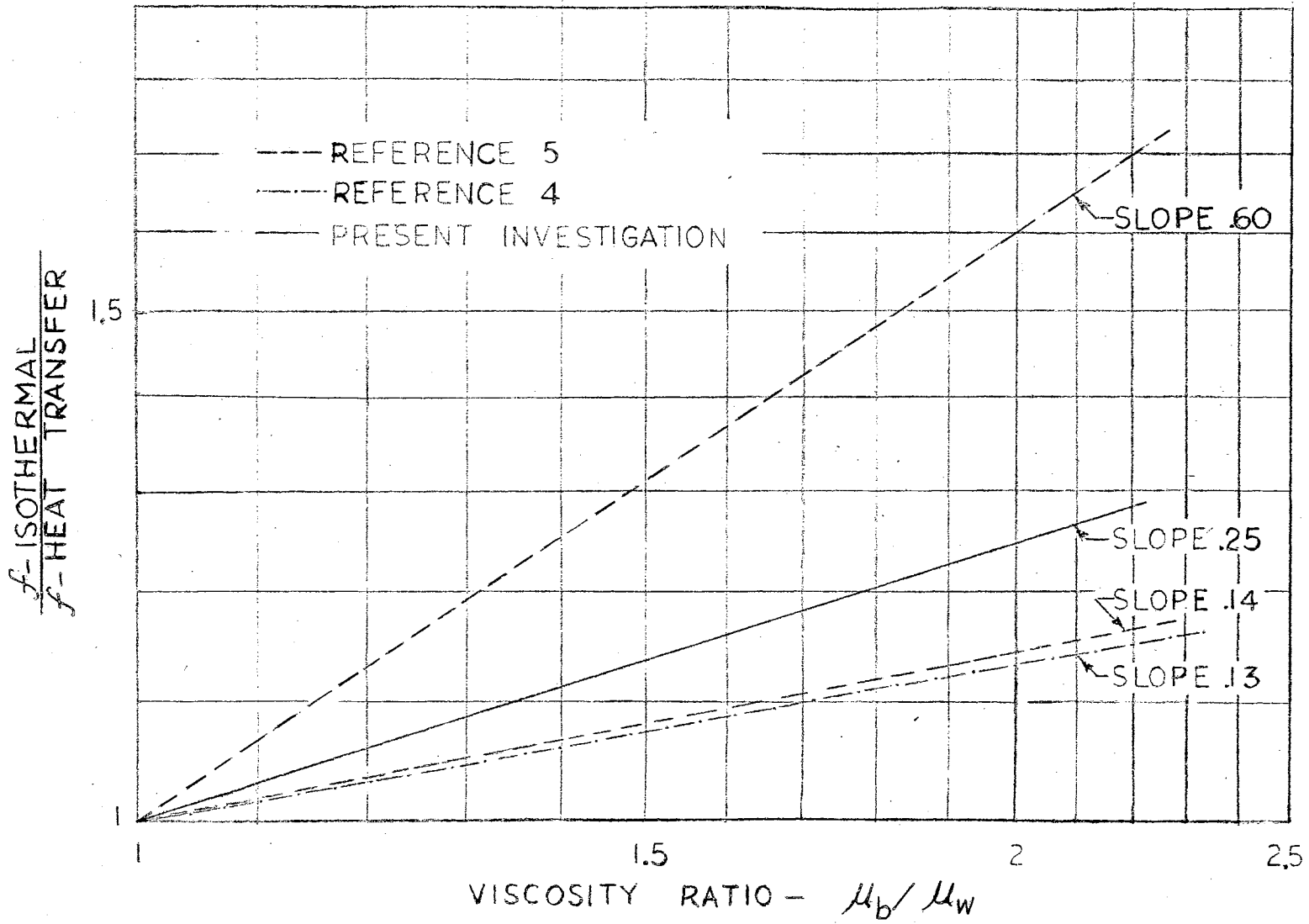
Figure 22. Comparison of Nonboiling Friction Factor Equations

$$f = 0.164 \; \frac{1}{(GD)^{0.175}} \; (\mu)^{0.175} . \qquad \text{(VII-1)}$$

In Figure 23, variation of friction factor with Reynolds number is shown for the above equation and for the present investigation. The range of Reynolds numbers for the equation given by Buchberg, Romie, Lipkis, and Greenfield (15) is not reported so the friction factor has been evaluated for the same Reynolds number as used in this research. It may be noted that this method will predict pressure drops that are about 10 per cent higher than for the present data. The nonboiling pressure drop data were reasonable since some variation in test conditions of the various investigations certainly existed.

The integration of Equation (II-14) presented by Rohsenow and Clark (5) is a method to take into account the variation of fluid properties as the fluid is heated. It was replaced by a stepwise method based on average densities and average wall friction factors in the solution presented in Chapter V. In the stepwise solution the size of the increments could be varied; thus, the integrated solution could be approached as closely as desired.

The quantity, Δt_{sat}, has been used in one of the methods for determining the start of local boiling. The Jens and Lottes (1) equation has been used by several authors (6), (8) and is recommended.

The present apparatus did not have provision for the removal of entrained gases; therefore, the experimental data are presented for gassed distilled water. It has been noted that the presence of nitrogen up to 110 cubic centimeters per liter at a pressure of 500 psia had no significant effect on heating-tube pressure loss for Δt_{sub} above 36°F. An
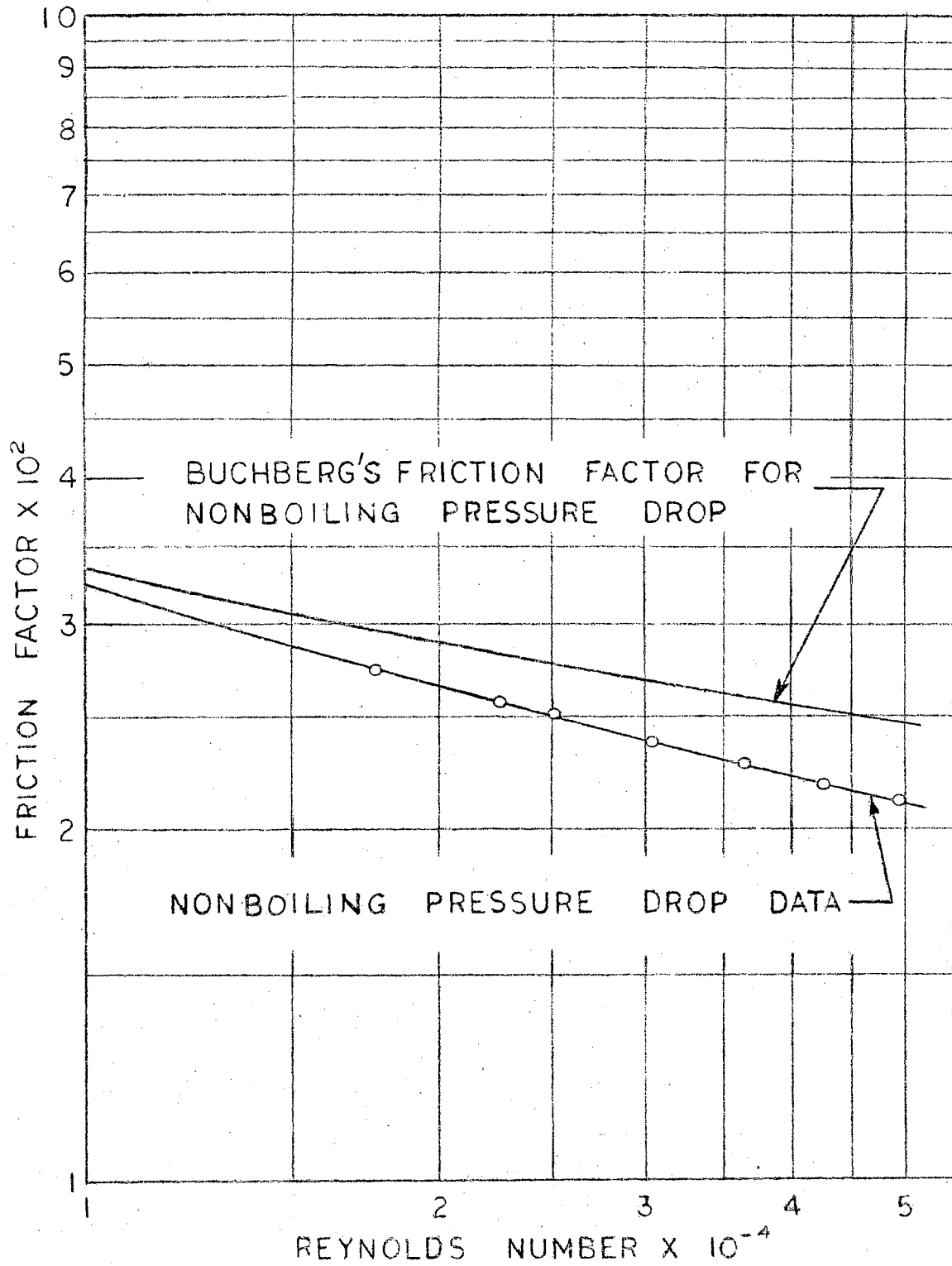
Figure 23. Comparison of Friction Factors for Nonboiling Heat
Transfer

increase in pressure loss of the order of 10 per cent was observed for Δt_{sub} of $36^{\circ}F$. (15).

An examination of Figure 1 and the examples of pressure profiles (Appendix I) show that the curves have a similar shape in the local boiling region. No analytical studies on the mechanism of local boiling pressure drop have been reported in the literature. The pressure plateau may be explained qualitatively in terms of bubble formation. At the first bubble formation, an increase in velocity occurs, and the static pressure decreases, due to increased frictional drag and change in fluid momentum. As the bubbles form they move downstream where more bubbles are forming until a point is reached where a rapid absorption of bubbles occurs. In the region where vapor absorption is high, a partial-pressure recovery is noted. In this area the bubbles form at an increased rate and a gradual increase in bubble absorption causes the static pressure to decrease. The pressure plateaus may eventually give a clue to the mechanism of local boiling pressure drop.

Reynolds' correlation equation is shown in Figure 24. An examination of the correlation equation presented from the present study shows the Reynolds' correlation equation does not take into account adequately the pressure change for the first half of the local boiling region. Reynolds' correlation has the advantage in that it is easier to calculate than the present correlation and is recommended for use for the last half of the local boiling length.

Equation (VI-2) for pressure gradient during local boiling is empirical but the variables contained in the equation are the important ones to be considered. Upon integrating Equation (VI-2) the following expression for pressure drop is obtained:
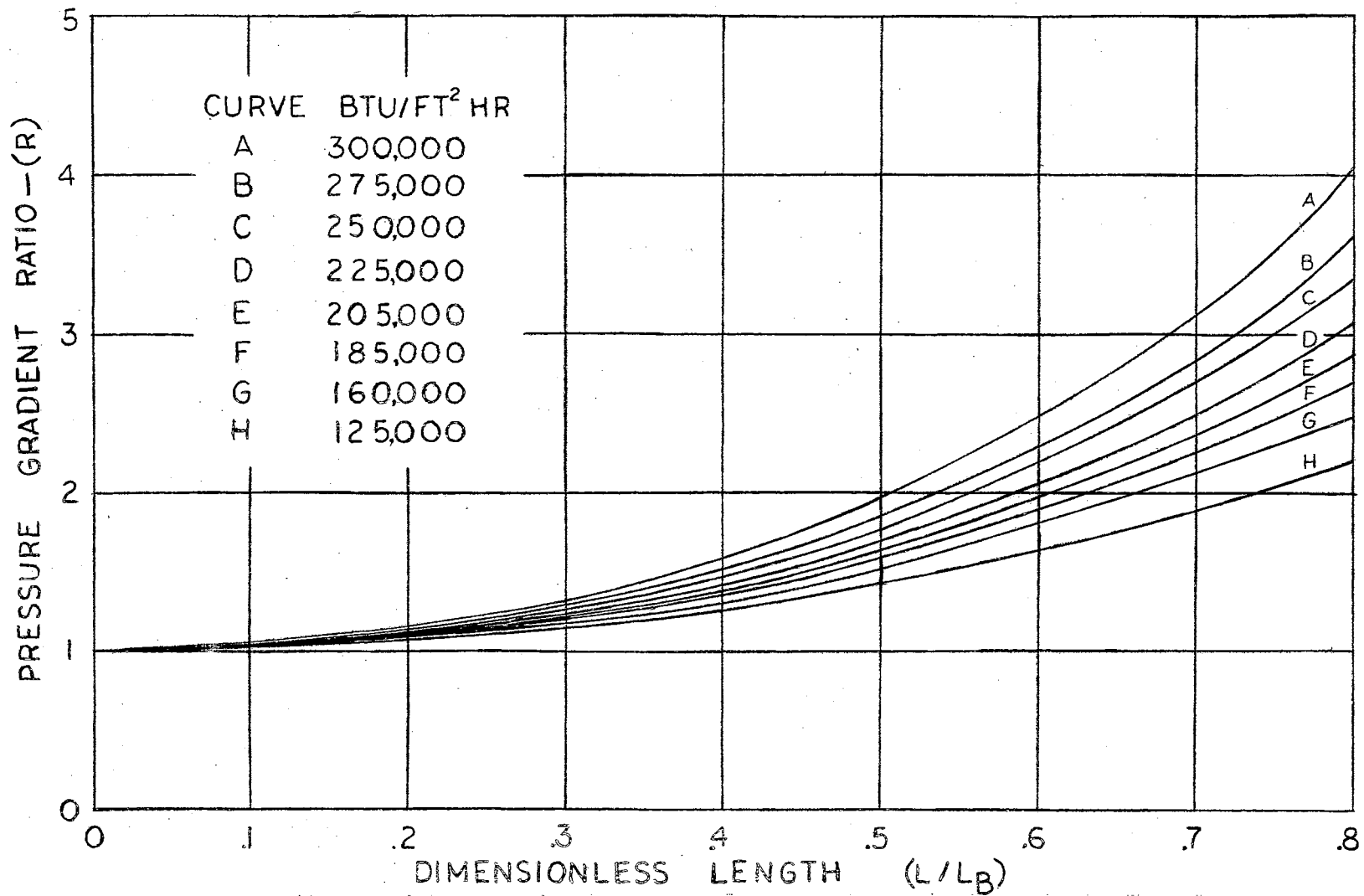
Figure 24. Graph of Local Boiling Pressure Drop Correlation Equation, from Reynolds (8)

$$\Delta P_{L.B.} = \left(\frac{dP}{dL}\right)_{N.B.} \cdot \left(\frac{G \, D \, C_p \, (\Delta t_{sub})_o}{4 \, q''}\right) \left[L/L_B \right.$$

$$+ \left\{ e^{0.2 \, (1 - p/200)} \right\} \left\{ \frac{q''}{40,000} - 2 \right\}$$

$$\left\{ 0.04332 \, (L/L_B) + 1.25293 \, (L/L_B)^2 \right.$$

$$\left. - 7.27288 \, (L/L_B)^3 + 9.30486 \, (L/L_B)^4 \right\} \left. \right] \quad \text{(VII-2)}$$

Study of the pressure-drop equation shows that it correlates the data of the present study within $\pm$ 25 per cent. Moreover it correlates the data of Reynolds (8) within $\pm$ 40 per cent.

CHAPTER VIII

CONCLUSIONS AND RECOMMENDATIONS

From an analysis of the experimental pressure drop data for non-boiling and local boiling and an examination of data and correlations presented by other investigators, the following specific conclusions can be drawn:

1. The local boiling pressure drop data may be correlated within plus or minus twenty-five per cent by the empirical equation relating significant variables as follows:

$$
\Delta P_{L.B.} = \left(\frac{dP}{dL}\right)_{N.B.} \left(\frac{G\ D\ C_p\ (\Delta t_{sub})_o}{4\ q''}\right) \Bigg[\ L/L_B
$$
$$
+ \left\{e^{0.2}\ (1 - p/200)\right\}\left\{\frac{q''}{40,000} - 2\right\}
$$
$$
\Bigg\{ 0.04332\ (L/L_B) + 1.25293\ (L/L_B)^2
$$
$$
- 7.27288\ (L/L_B)^3 + 9.30486\ (L/L_B)^4\Bigg\}\Bigg] \qquad (VII-2)
$$

It is recommended that the correlation equation be used for the first half of the local boiling length.

2. Within the limits of accuracy of the data, the pressure gradient ratio was found to be independent of flow rate.

3. The effect of pressure on the pressure gradient ratio may be

represented by a multiplier of the type, $e^{K(P/P_O - 1)}$, in which $K = 0.2$ and P_O is the reference pressure, 200 psia. In order to take into account the effect of system pressure, $(R - 1)$ was multiplied by the pressure term.

4. Reynolds' correlation equation is recommended for correlating data for the last one-half of the local boiling length.

5. Pressure drop during nonboiling heat transfer to the fluid may be computed by using the proper friction factor based on the fluid viscosity at the wall temperature. The calculation is easily adapted to processing by a digital computer.

6. Isothermal pressure drop for the present study may be computed by using friction factors for smooth tubes as given by Moody.

As a result of the present investigation, the following recommendations can be made:

1. An analytical solution for local boiling pressure drop should be developed since no adequate analytical study has been reported in the literature.

2. Photographic study and density measurements should be considered as a means for clarifying experimentally the mechanism of local boiling. A more detailed knowledge of vapor formation and absorption will make clear its effect on local boiling pressure drop.

3. Extensive local boiling pressure drop data at considerably higher pressures than in the present investigation should be obtained to aid in establishing more precisely the constants used in the equation for pressure effect.

In summary it may be said that local boiling pressure drop is

imperfectly understood. The correlation equations presented so far for local boiling pressure drop data are empirical and still are of limited application. Few detailed local boiling pressure drop data have been reported in the literature. One of the purposes of the present investigation was to contribute extensive pressure drop data which have not been available up to now. It is hoped that some of the methods outlined and discussed in this thesis may point the way to further understanding and development in the prediction of local boiling pressure drop.

SELECTED BIBLIOGRAPHY

(1) Jens, W. H., P. A. Lottes, "Analysis of Heat Transfer, Burnout, Pressure Drop, and Density Data for High-Pressure Water," ANL-4627, (May 1, 1951).

(2) McAdams, W. H., J. N. Addoms, W. E. Kennel, "Heat Transfer at High Rates to Water With Surface Boiling," ANL-4916, (October 20, 1952).

(3) Mumm, J. F., "Heat Transfer to Boiling Water Forced Through a Uniformly Heated Tube," ANL-5276 (November, 1954).

(4) Kreith, Frank, Martin Summerfield, "Heat Transfer to Water at High Flux Densities With and Without Surface Boiling," Transactions of ASME, 71, 805-815, (October, 1949).

(5) Rohsenow, W. M., J. A. Clark, "Heat Transfer and Pressure Drop Data for High Heat Flux Densities to Water at High Subcritical Pressures," 1951 Heat Transfer and Fluid Mechanics Institute, Stanford University, (June, 1951).

(6) Weiss, D. H., "Pressure Drop in Two-Phase Flow," ANL-4916, (October 20, 1952).

(7) Leppert, G., "Two-Phase Pressure Drop," unpublished Ph.D. dissertation, Illinois Institute of Technology, (1953).

(8) Reynolds, J. B., "Local Boiling Pressure Drop," ANL-5178, (March 1954).

(9) Martinelli, R. C., D. B. Nelson, "Prediction of Pressure Drop During Forced-Circulation Boiling of Water," Transactions of ASME, 70, 695-702, (1948).

(10) Isbin, H. S., R. H. Moen, R. O. Wickey, D. H. Mosher, H. C. Larson, "Two-Phase Steam-Water Pressure Drops," Preprint 147, Nuclear Engineering and Science Conference, (March, 1958).

(11) Isbin, H. S., R. H. Moen, D. R. Mosher, "Two-Phase Pressure Drops," AECU-2994, (November, 1954).

(12) Gunther, F. C., "Photographic Study of Surface Boiling Heat Transfer to Water with Forced Convection," Transactions of ASME, Vol. 73, 115-123, (1951).

(13) Rohsenow, W. M., J. A. Clark, "A Study of the Mechanism of Boiling Heat Transfer," _Transactions of ASME_, Vol. 73 609-620, (1951).

(14) Zuber, N., "On the Stability of Boiling Heat Transfer," ASME-AICHE Heat Transfer Conference, 57-HT-4, (August, 1957).

(15) Buchberg, H., F. Romie, R. Lipkis, M. Greenfield, "Heat Transfer Pressure Drop, and Burnout Studies With and Without Surface Boiling for Deaerated and Gassed Water at Elevated Pressures in a Forced Flow System," 1951 Heat Transfer and Fluid Mechanics Institute, Stanford University, (June, 1951).

(16) Colburn, A. P., "Method of Correlating Forced Convection Heat Transfer Data and a Comparison with Fluid Friction," _Transactions of American Institute of Chemical Engineers_, 19, (1933).

(17) Moody, L. F., "Friction Factors for Pipe Flow," _Transactions of ASME_, 66, 671-684, (1944).

(18) Levengood, J. L., "Pressure Drop in a Tube with Forced Convection Heat Transfer in the Nonboiling Region." Master of Science Thesis, Oklahoma State University, 1959.

(19) Wellman, E. J., "A Survey of the Thermodynamic and Physical Properties of Water," M.S. Thesis, Purdue University, (1950).

(20) Keenan, J. H., and F. G. Keyes, _Thermodynamic Properties of Steam_, First Edition, John Wiley and Sons, Inc., New York, (1936).

(21) American Society for Metals, _Metals Handbook_, P. 314, (1948).

(22) Gess, L., and R.D. Irwin, _Flow Meter Engineering Handbook_, The Brown Instrument Co., Philadelphia, Pennsylvania, (1946).

APPENDIX A

REPRESENTATIVE PRESSURE PROFILES
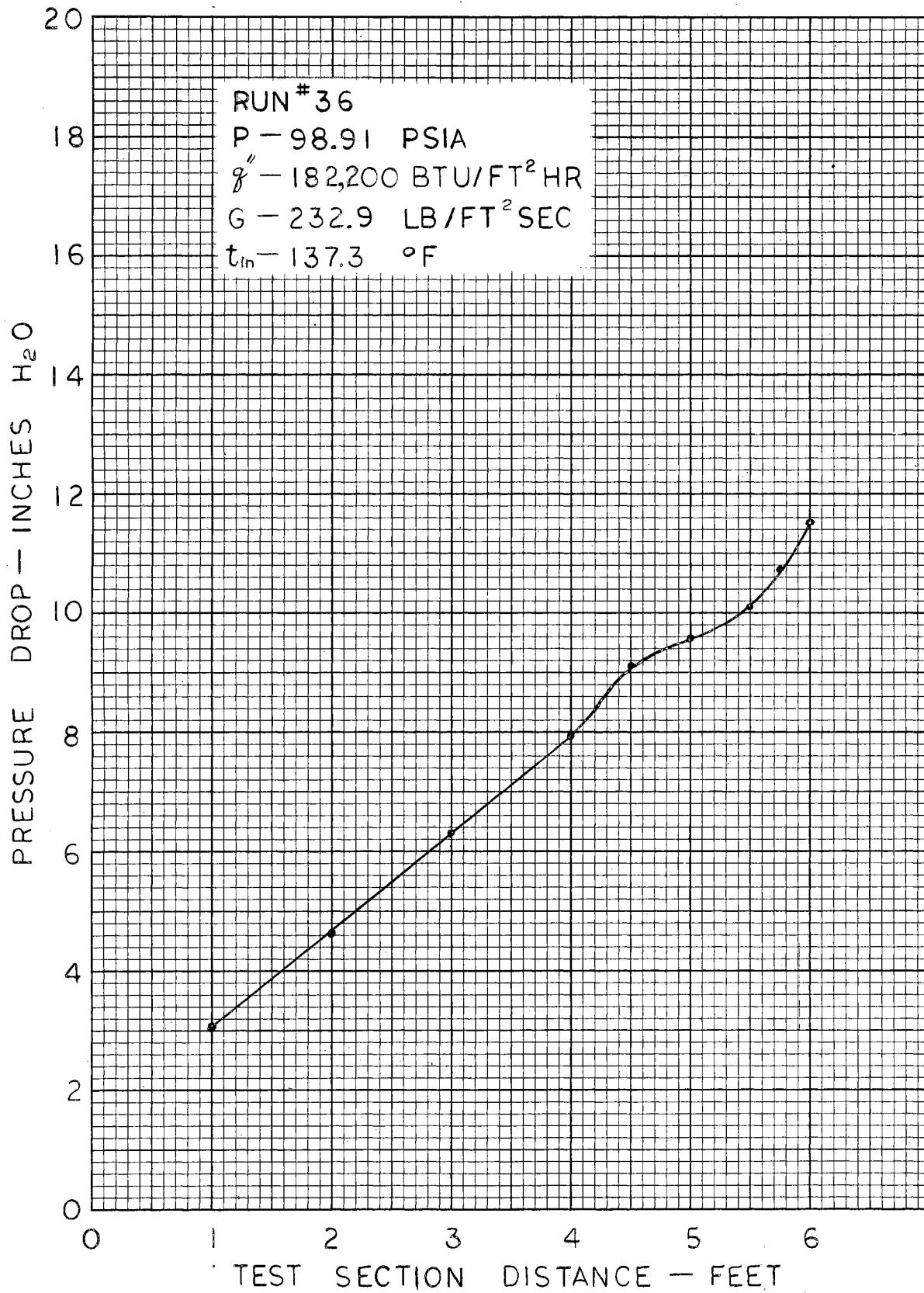
Figure 25(a). Experimental Pressure Profile

RUN #45
P — 148.95 PS.I.A
q'' — 256,200 BTU/FT^2 HR
G — 232.1 LB./FT^2 SEC
t_{in} — 105.8 °F
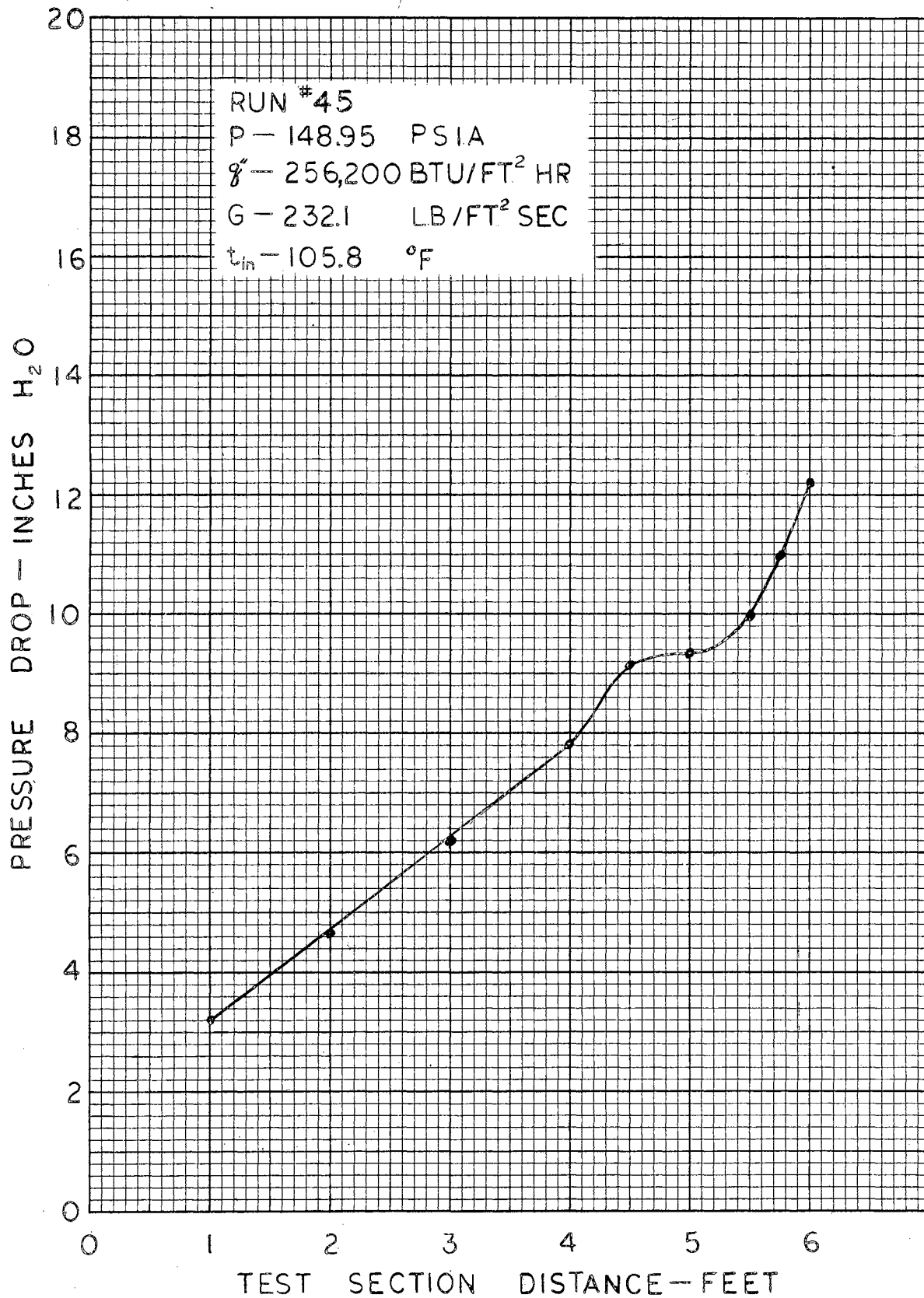
Figure 25(b). Experimental Pressure Profile
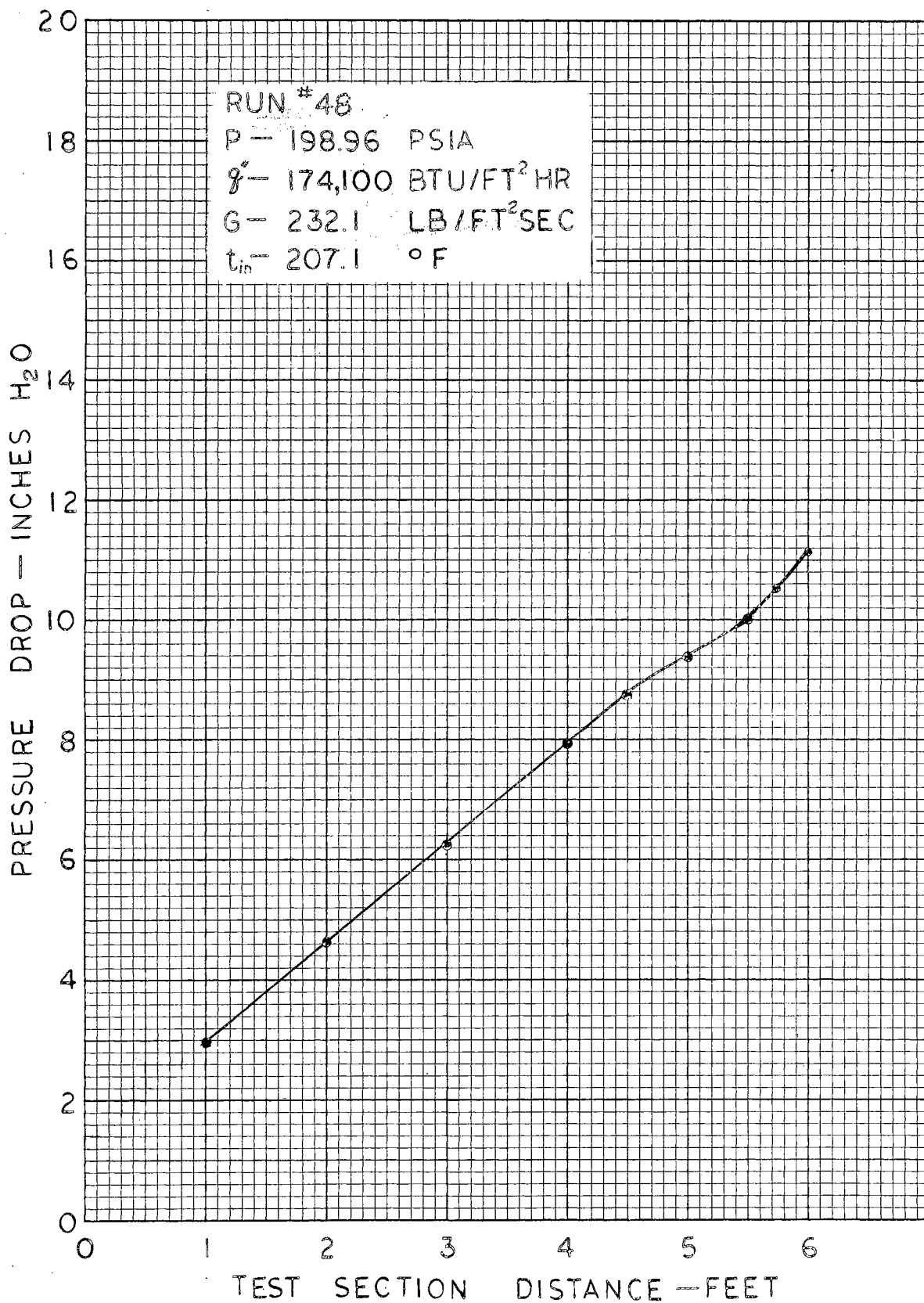
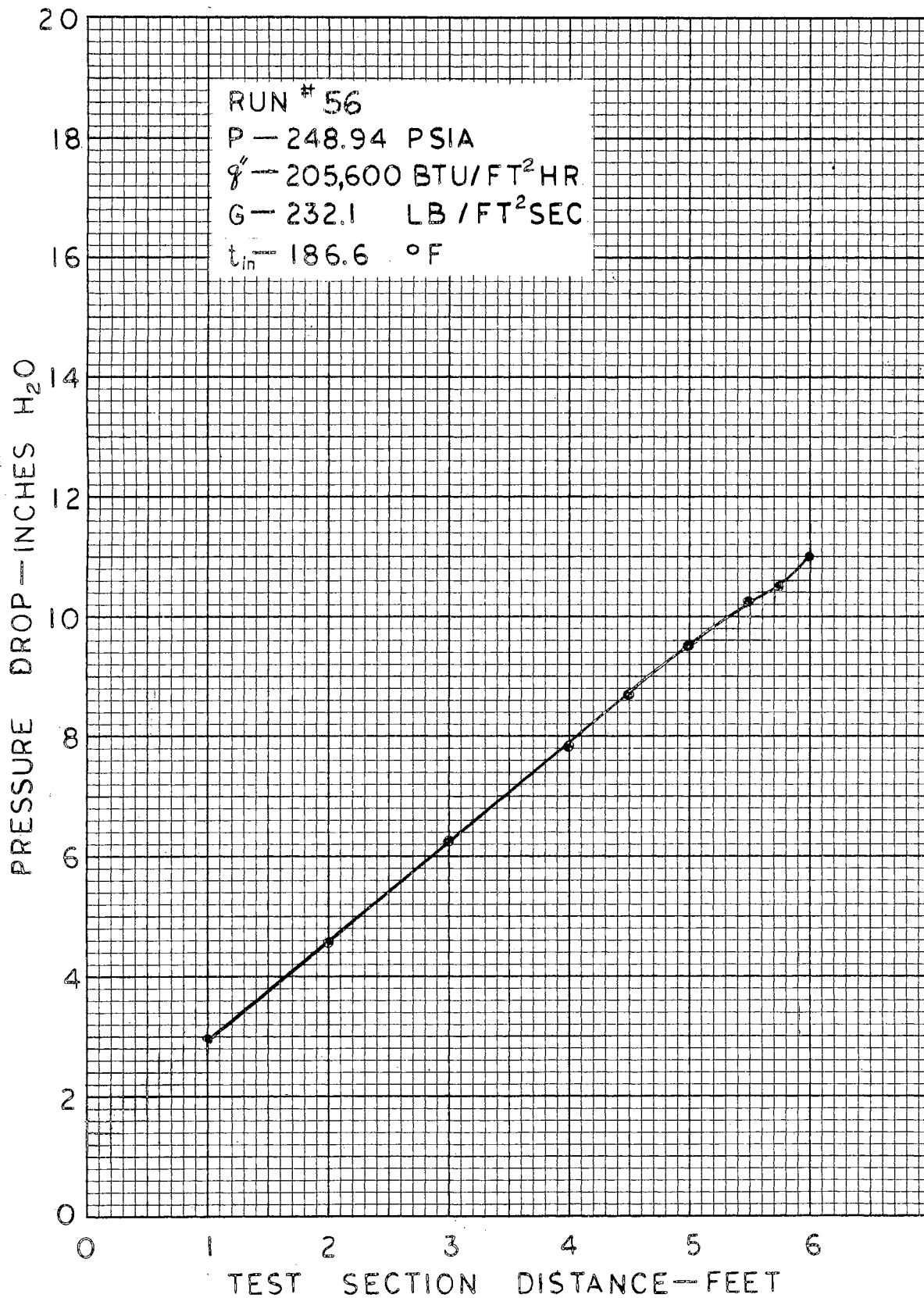Figure 25(c). Experimental Pressure Profile
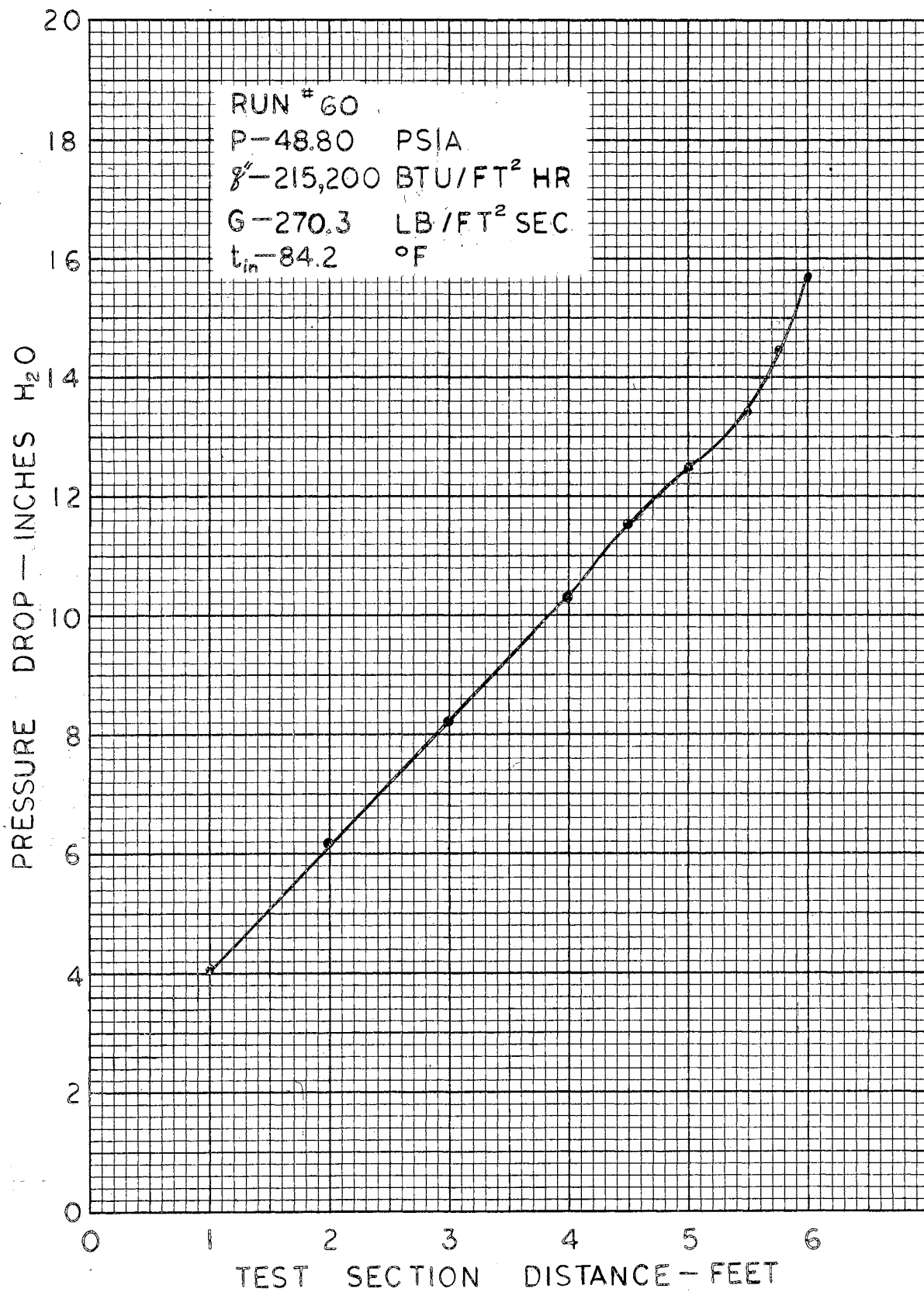
Figure 25(d). Experimental Pressure Profile

Figure 25(e). Experimental Pressure Profile

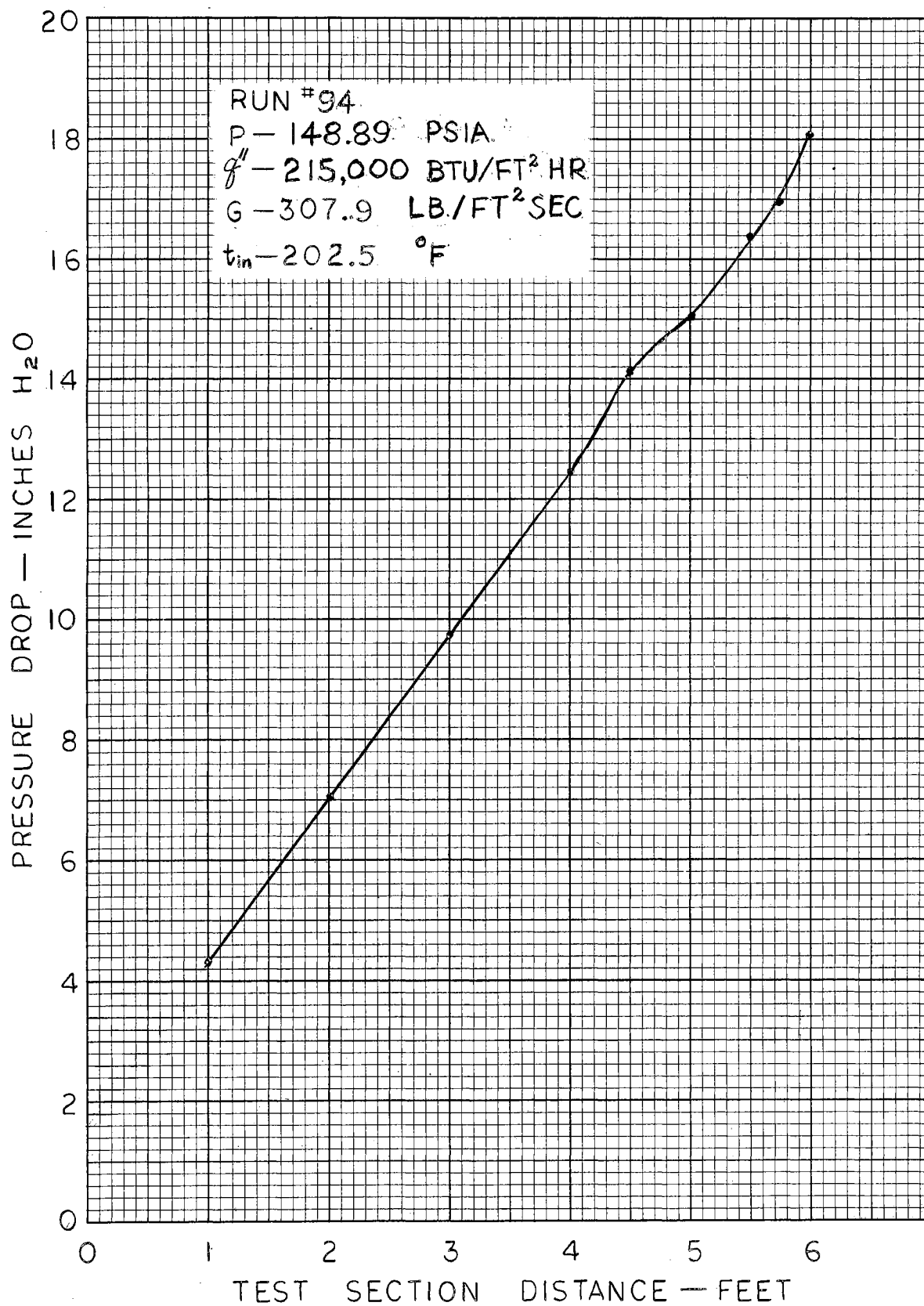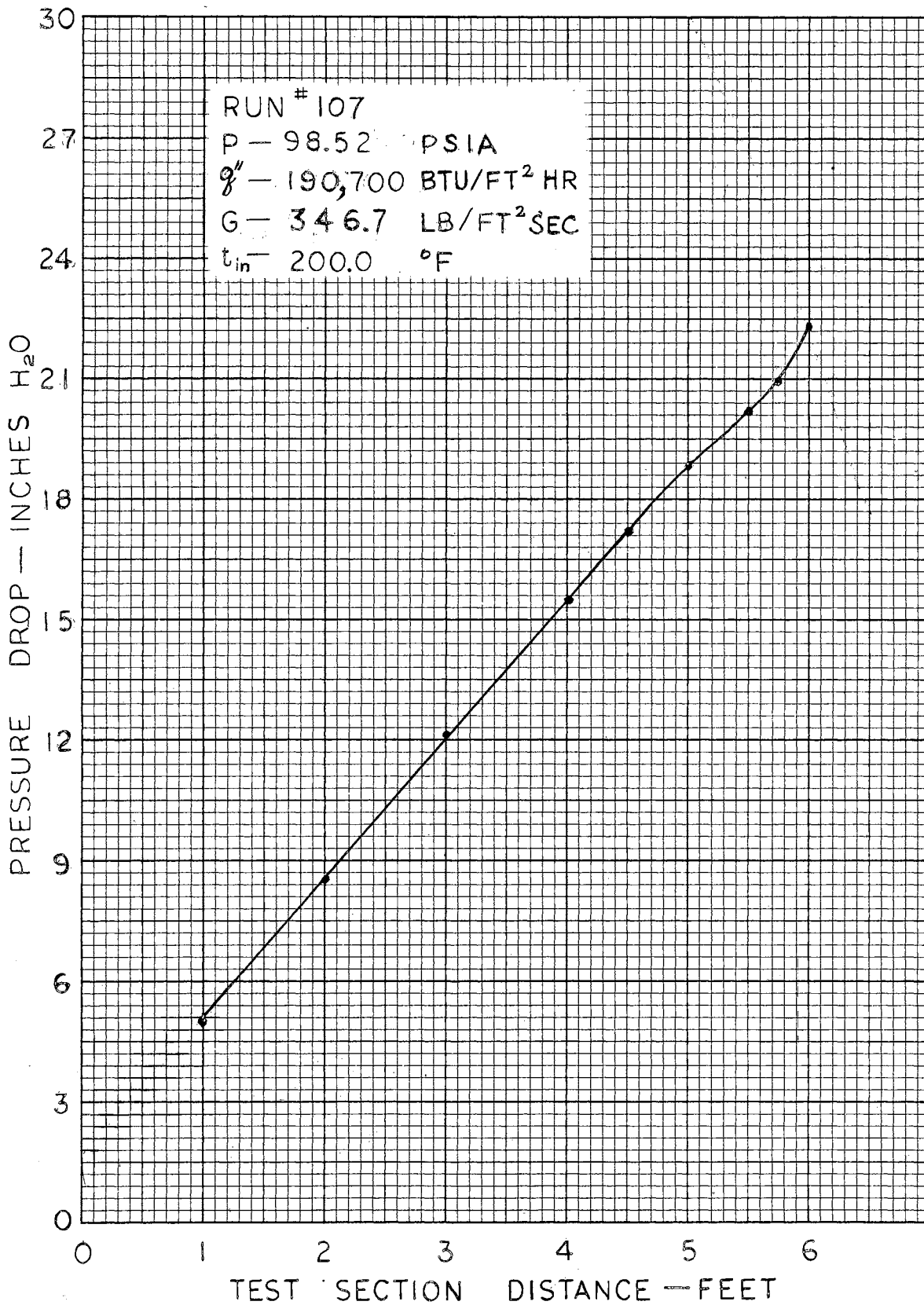Figure 25(f). Experimental Pressure Profile

Figure 25(g). Experimental Pressure Profile

APPENDIX B

PROPERTIES OF WATER

The properties of water were taken from references (19), (20).
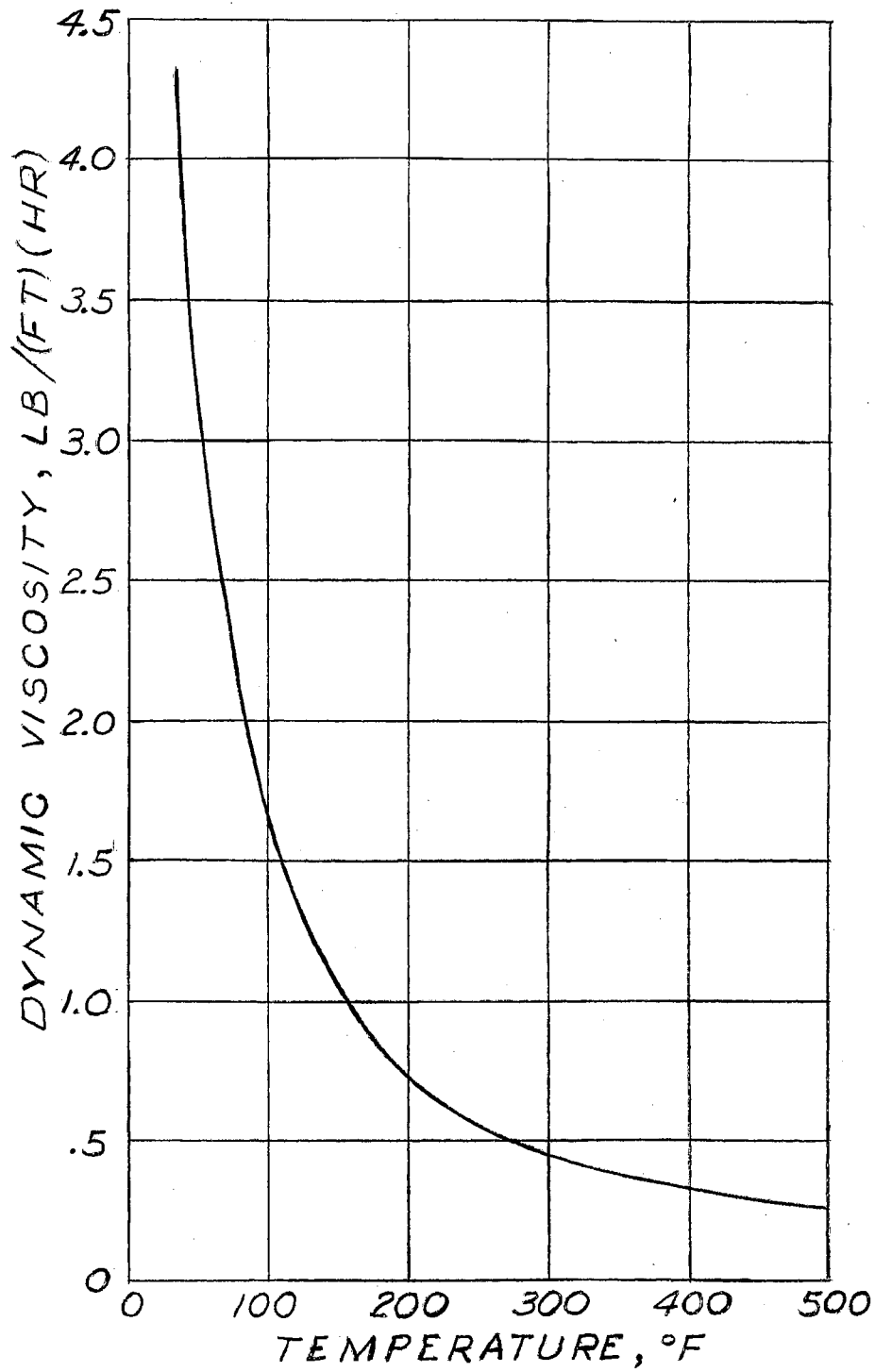
Figure 26. Dynamic Viscosity of Saturated Water
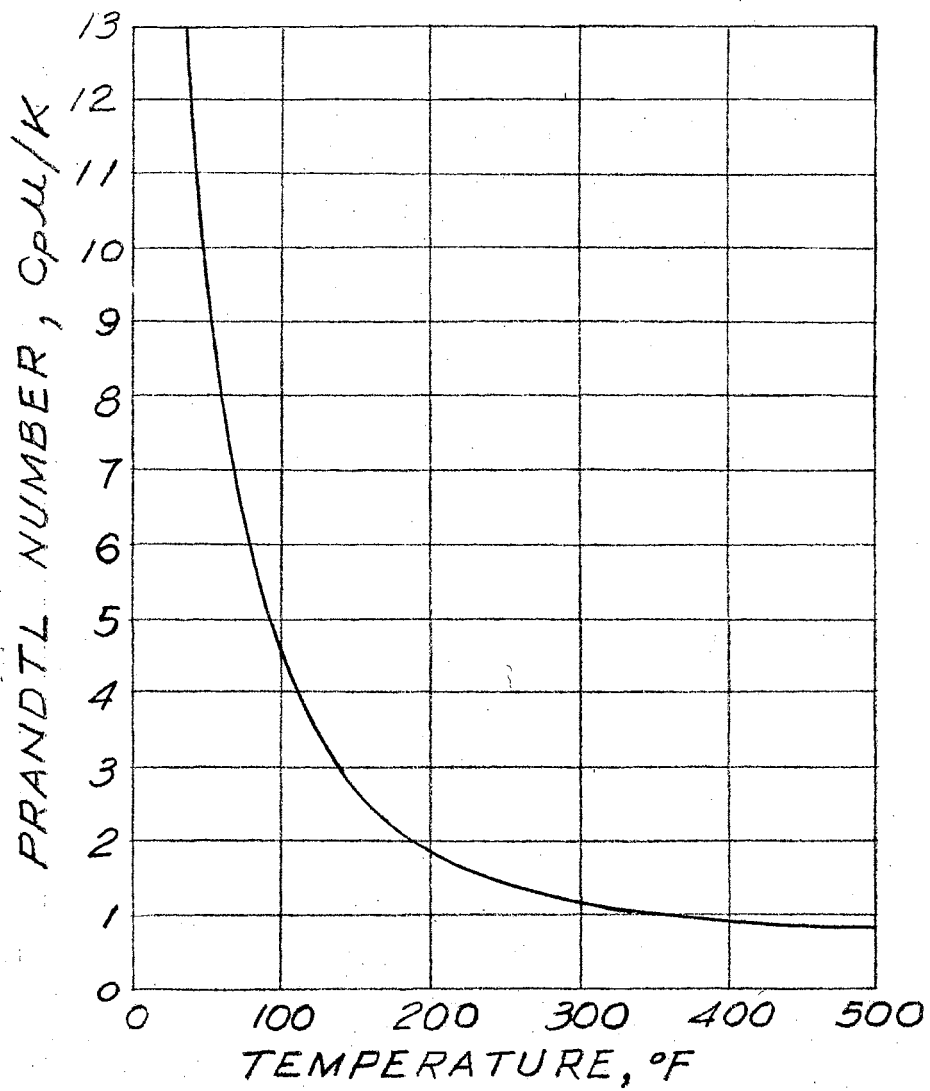
Figure 27

Variation of Prandtl Number with
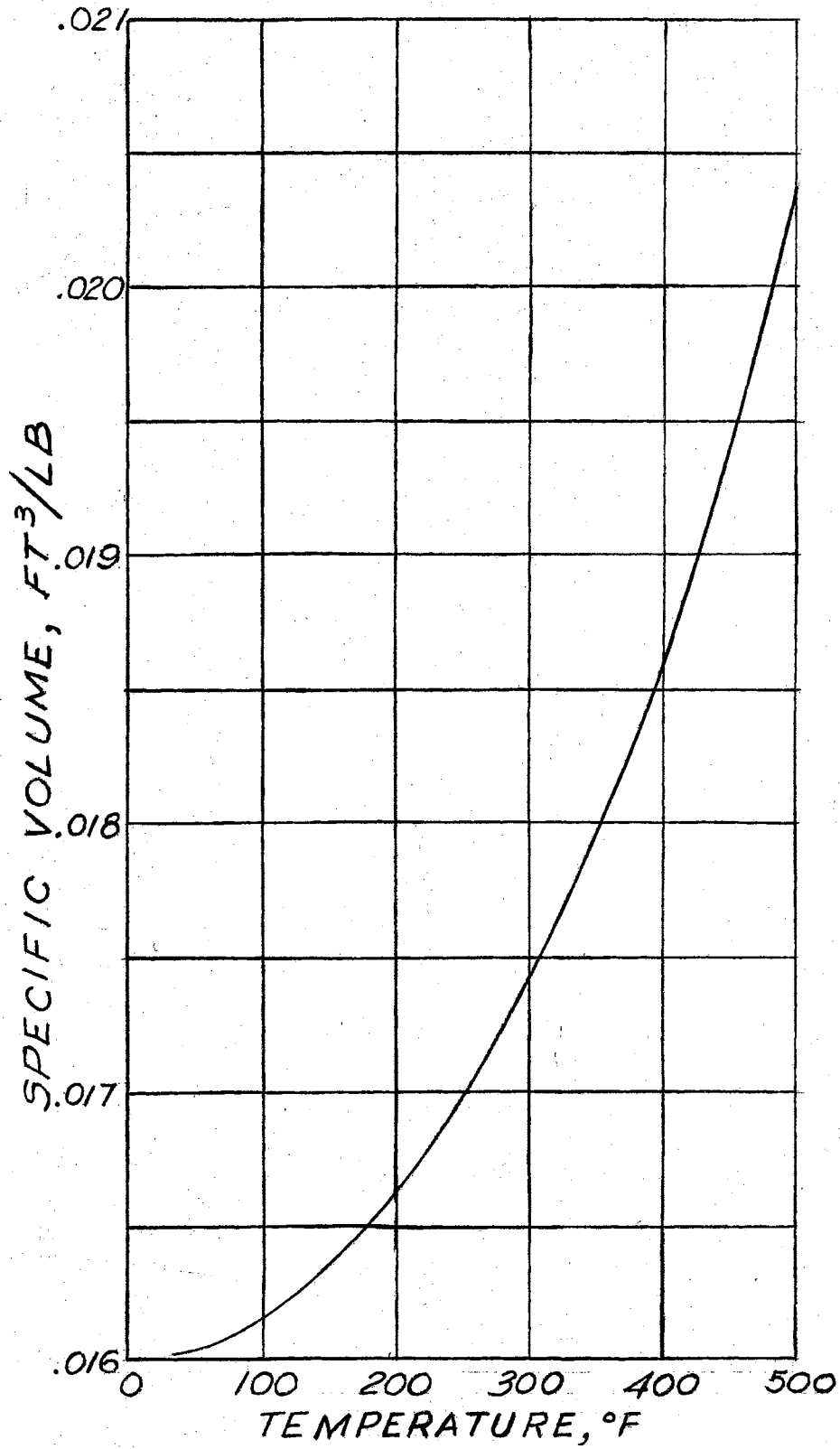Temperature for Saturated Water
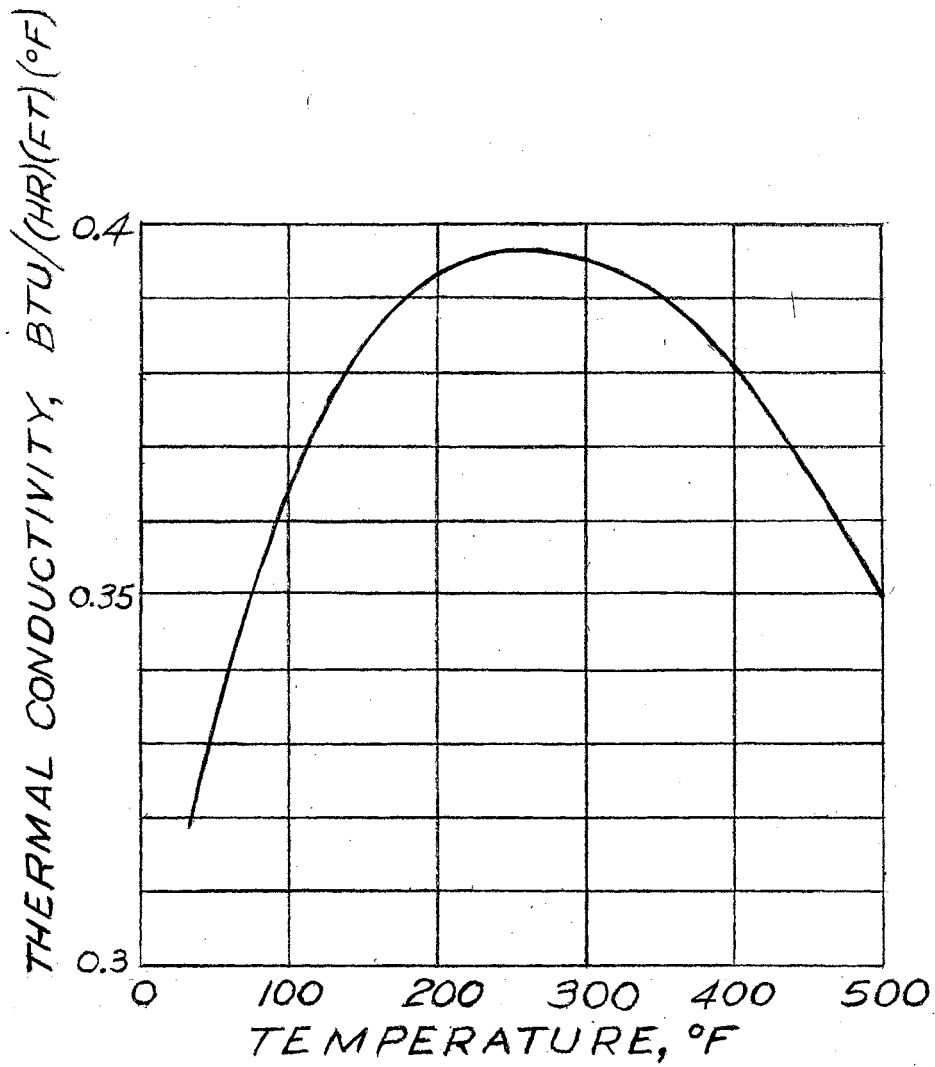
Figure 28

Thermal Conductivity of Saturated Water
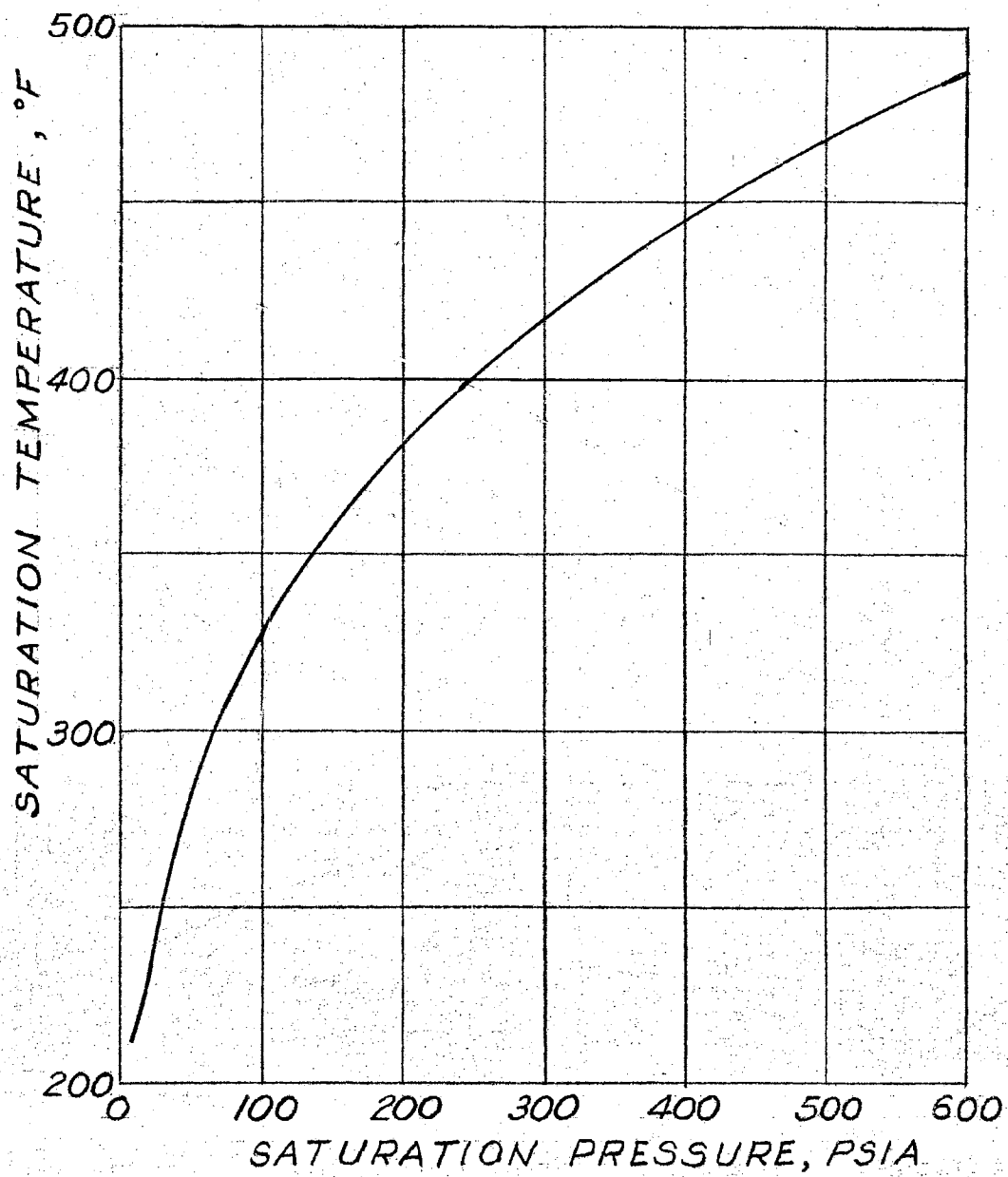
Figure 29. Specific Volume of Saturated Water

Figure 30

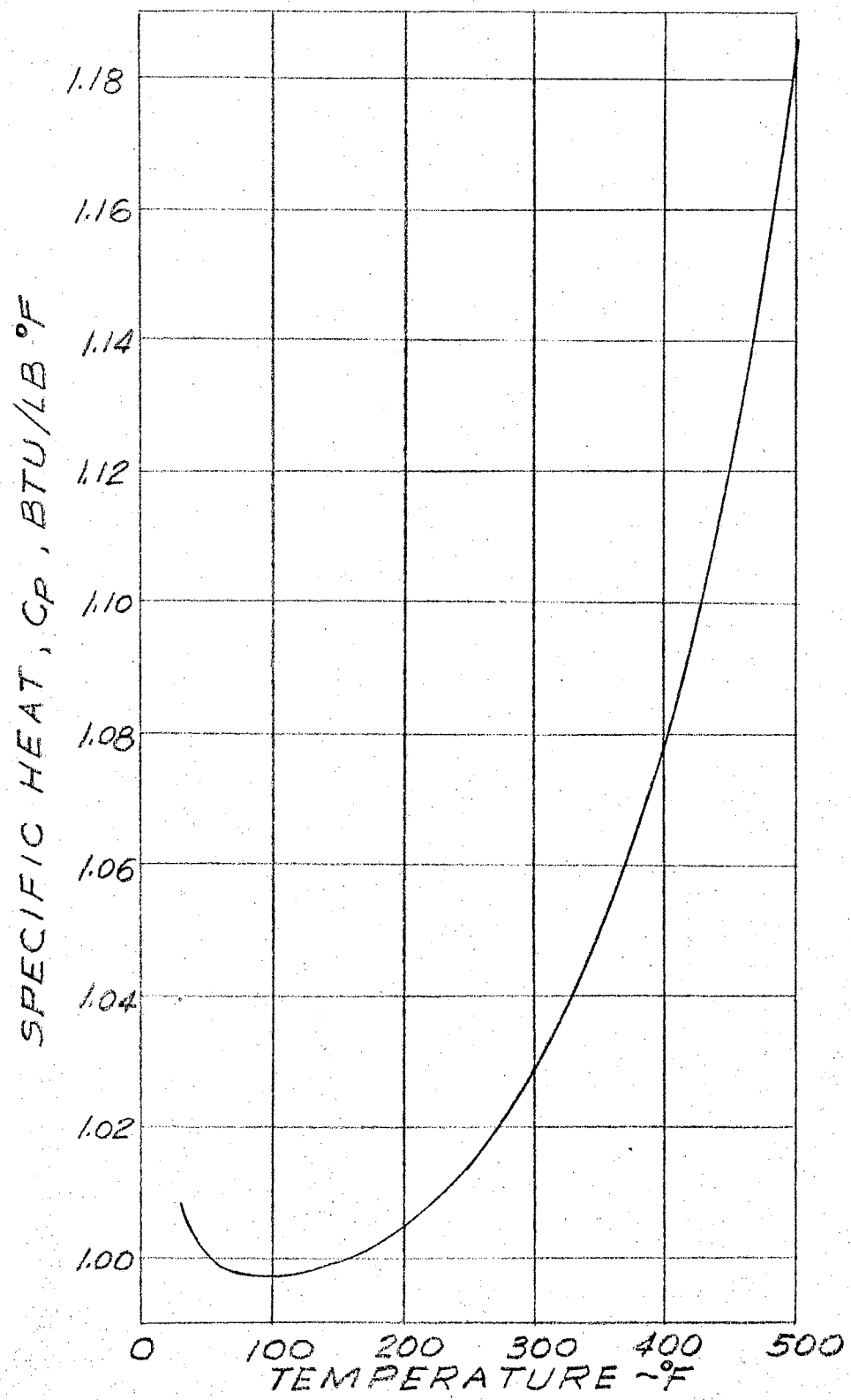Variation of Saturation Temperature with Saturation
Pressure for Water

Figure 31. Specific Heat of Saturated Water

APPENDIX C

ESTIMATE OF EXPERIMENTAL ERRORS

1. Lineal Measurements:

      variation of inside diameter is negligible

      heated length of test section is thought to be in error by no more than 0.002 inch.

2. Flow Rate:

      maximum error due to orifice plate calibration of $\pm$ 1 per cent.

3. Inlet Temperature:

      $\pm$ 1.5°F

4. Power Measurements:

      maximum error of test section power $\pm$ 0.5 per cent

5 Pressure Measurements:

      maximum error of system pressure measurement $\pm$ 1 per cent

      maximum error of manometer pressure measurements $\pm$ 0.2 inch H_2O

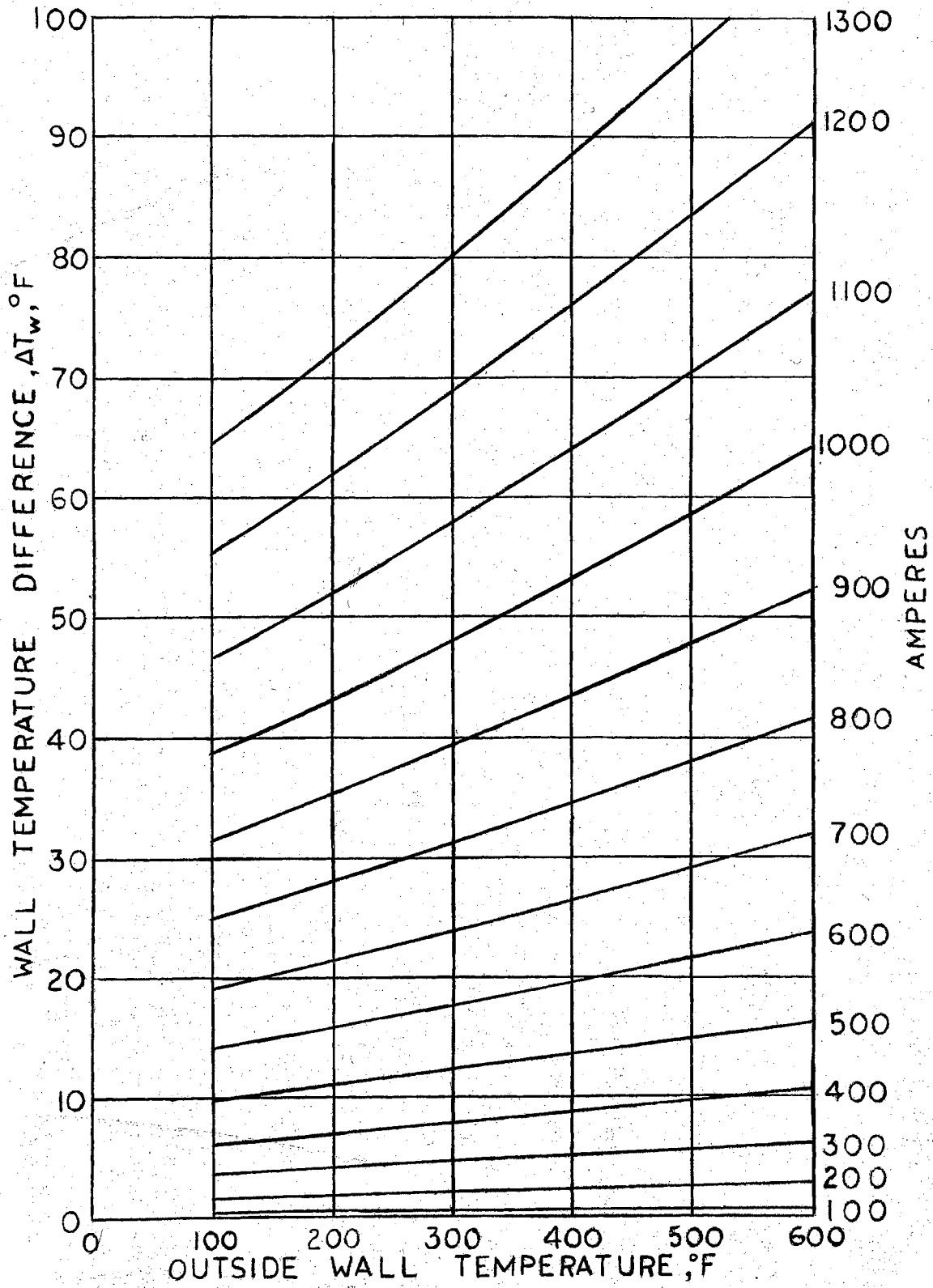APPENDIX D

SOLUTIONS OF THE KREITH-SUMMERFIELD EQUATION

Figure 32. Temperature Difference Across the Tube Wall

APPENDIX E

PROPERTIES OF AISI STAINLESS STEEL

The electrical resistivity and thermal conductivity values for AISI type 304 stainless steel tubing were taken from reference (21).
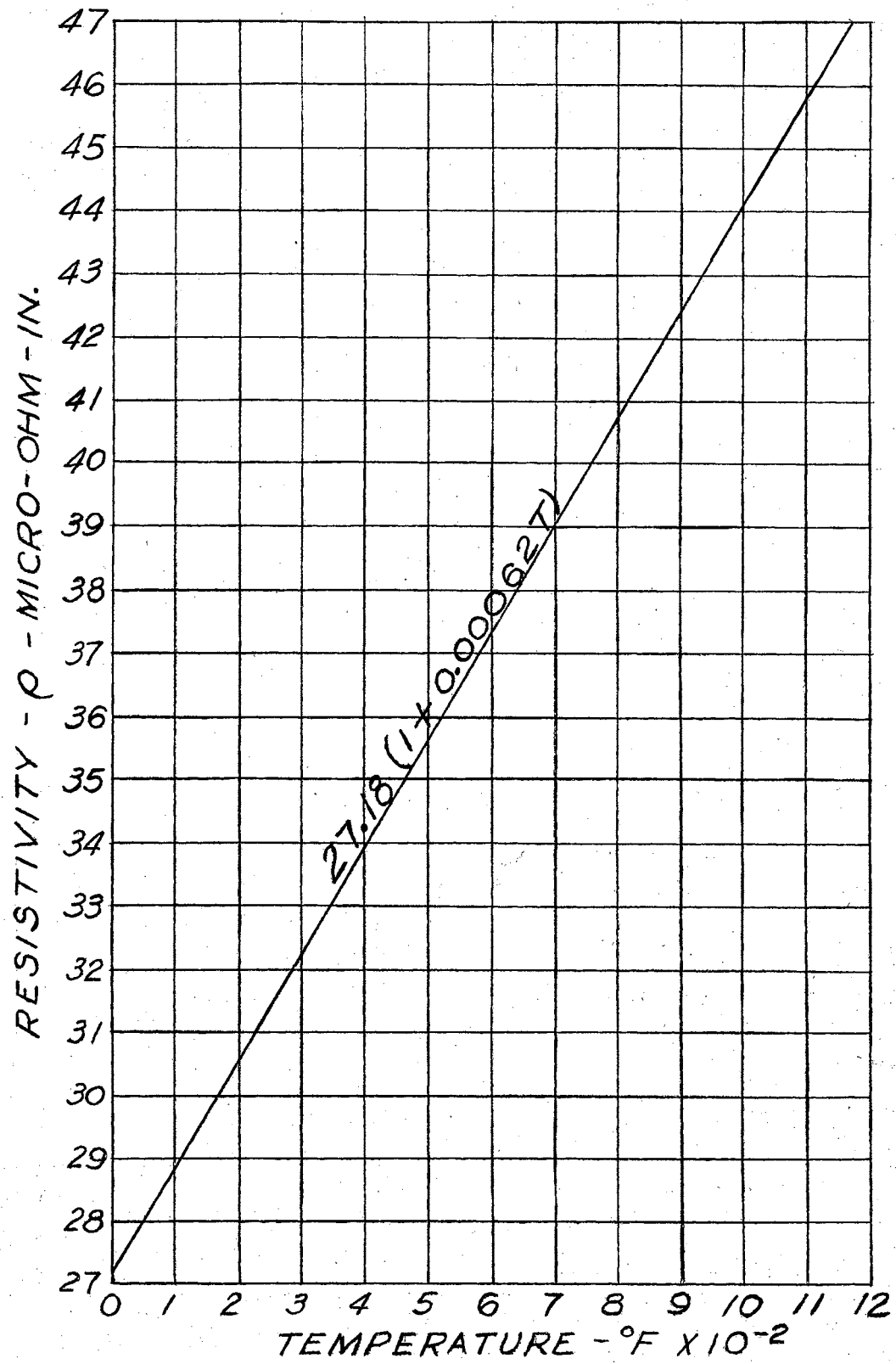
Figure 33. Electrical Resistivity of AISI Type 304 Stainless Steel
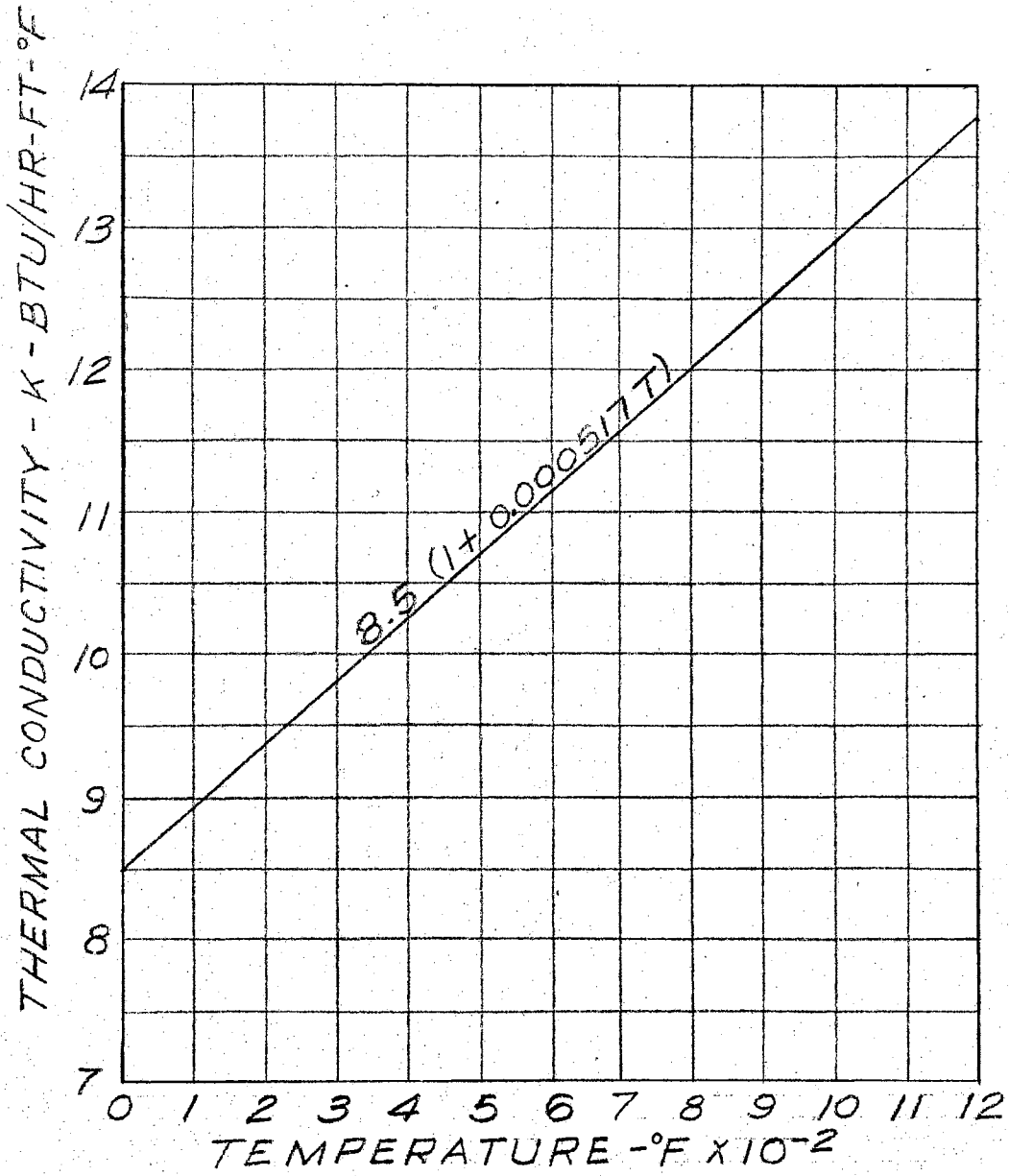
Figure 34

Thermal Conductivity of AISI
Type 304 Stainless Steel

APPENDIX F

ORIFICE CALIBRATION

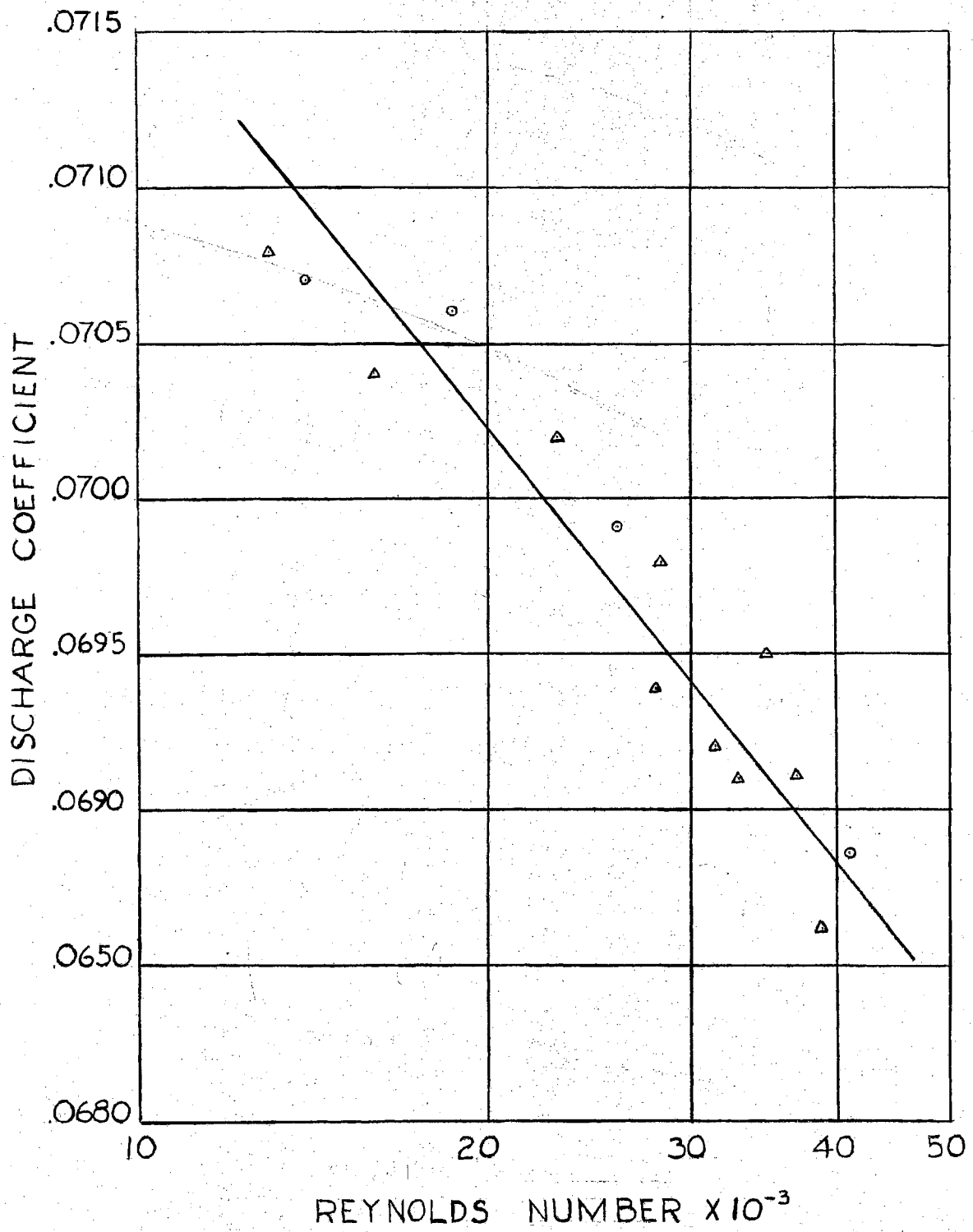The method of orifice calculation was taken from reference (22).

Figure 35. Orifice Calibration Curve
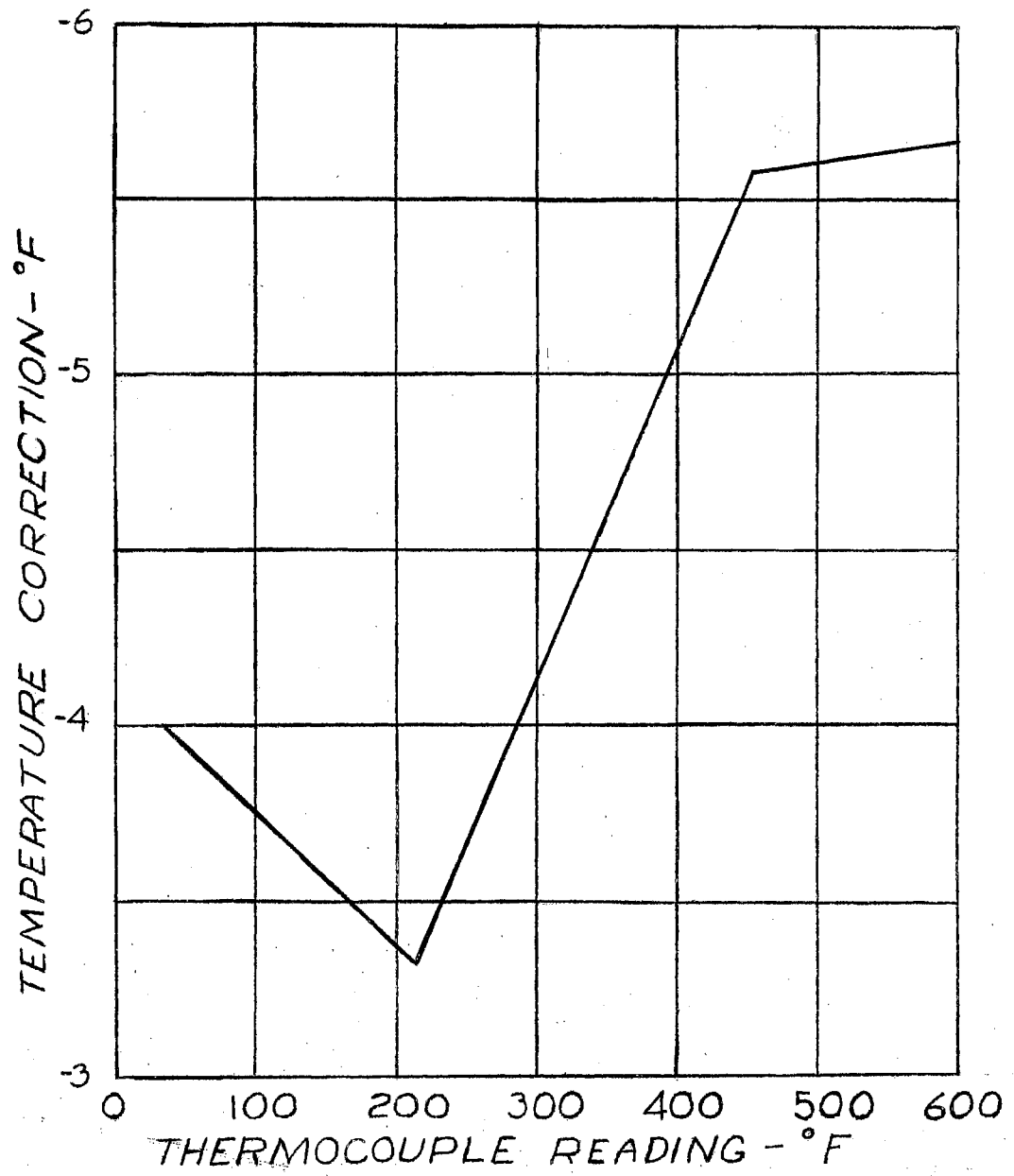
APPENDIX G

THERMOCOUPLE CALIBRATION

Figure 36

Temperature Measurement Calibration Curve

APPENDIX H

SYMBOLS

a   Parameter related to heat flux by the equation,
$(a = 4.6 \times 10^{-6} q'' + 1.2)$.

A   Area.

C' Coefficient defined by equation (II-8).

C_F Friction factor.

C_p Specific heat at constant pressure.

D   Diameter.

f   Fanning friction factor.

F   Frictional pressure drop.

g_c Gravitational constant.

G   Mass velocity.

G' Mass velocity.

h   Heat transfer film coefficient.

h   Enthalpy.

I   Electric current.

K   Thermal conductivity.

K   Constant defined by equation (VI-2).

l   Length.

L   Length of test section from start of local boiling to any point.

L_B Local boiling length.

108

$L/_{LB}$ Ratio of length of test section from start of local boiling to any point to local boiling length.

m Variable defined by equation (IV-3).

n Variable number of intervals.

N Total number of intervals.

P System pressure.

ΔP Pressure drop.

$\frac{dP}{dL}$ Pressure gradient.

q Heat transfer rate.

q" Heat flux.

r Radius.

R Ratio of pressure gradient in local boiling region to reference pressure gradient.

t Variable temperature.

t_b Bulk temperature.

Δt_b Change in bulk temperature.

t_{sat} Saturation temperature.

Δt_{sat} Temperature difference between wall and saturation temperature.

$\Delta t_{sat,tr}$ Wall superheat occurring at the transition point from nonboiling to local boiling.

Δt_{sub} Temperature difference between saturation and bulk temperature.

Δt_{tr} Difference in bulk temperature from inlet to point of local boiling.

t_w Inside wall temperature.

v Specific volume.

V Velocity.

W Flow rate.

x Variable distance.

Δx Wall thickness.

y Variable length of tube not in local boiling.

Z Reciprocal of local boiling length.

α Temperature coefficient of electrical resistivity.

β Temperature coefficient of thermal conductivity.

ρ Electrical resistivity.

ρ Fluid density.

μ Dynamic viscosity.

Dimensionless Groups

Pr   Prandtl number.

Re   Reynolds number.

Subscripts

av   Average conditions.

b   Bulk conditions.

B   Boiling conditions.

c   Cross sectional conditions.

f   Frictional conditions.

f   Film conditions.

f,M   Friction plus momentum conditions.

F   Frictional conditions.

i   Inlet conditions.

i   Inside wall conditions.

L.B.   Local boiling conditions.

m   Mean conditions.

N.B.   Nonboiling conditions.

o   Isothermal conditions.

o   Outside wall conditions.

o   Reference conditions.

s   Surface conditions.

tr   Transition point conditions.

T.S. Test section.

w   Wall conditions.

VITA

Gerald Eugene Tanger

Candidate for the Degree of

Doctor of Philosophy

Thesis: LOCAL BOILING PRESSURE DROP FOR FORCED CIRCULATION OF WATER

Major Field: Engineering

Biographical:

Born: The writer was born in Redfield, South Dakota, July 24, 1925, the son of Charles A. and Elsie M. Tanger.

Undergraduate Study: He graduated from Huron High School, Huron, South Dakota, in June, 1943. After serving in the Army he entered South Dakota School of Mines and Technology in September, 1946. He received a Bachelor of Science Degree in Physics, with honors, from that institution in June, 1950.

Graduate Study: In September, 1950, the writer entered the Graduate School of South Dakota School of Mines and Technology. He received the Master of Science Degree in Physics from that Institution in June, 1951. In September, 1951, he entered the Graduate School of Brown University where he continued his study toward the Doctor of Philosophy Degree. In September, 1957, he entered the Graduate School of Oklahoma State University, where he completed the requirements for a Doctor of Philosophy Degree in May, 1959.

Experience: The writer entered the United States Armed Forces in December, 1942. He served in the United States and in the Philippines prior to his honorable separation from the service as Technical Sergeant of the Field Artillery in May, 1946. While studying at the South Dakota School of Mines and Technology, he served as an Assistant Instructor from 1948 to 1950. While studying at Brown University he served as Instructor in Mechanical Engineering and carried on research in heat transfer and fluid flow. In 1955, he became an Associate Professor in Mechanical Engineering at the University of Mississippi. In May, 1956, the writer became a registered Professional Engineer in the state of Mississippi. During the summers of 1956, and 1957, he carried

on research in heat transfer at Boeing Airplane Company, Wichita, Kansas.

Publications: Boeing Research Documents, "Heat Transfer and Pressure Loss From Ducts for Subsonic Flow of Air", and "Gas Turbine Cycle Analysis".

Professional Organizations: The writer is a member of the following professional organizations: Society of Professional Engineers (Mississippi), American Society of Mechanical Engineers, American Society for Engineering Education, Sigma Tau, and Sigma Pi Sigma.